

LTR-CDME-05-180-NP, Revision 2

**Steam Generator Tube Alternate Repair Criteria
for the Portion of the Tube Within the Tubesheet
at Catawba 2**

December 2005

Author: */s/ Robert F. Keating*

Robert F. Keating

Major Component Replacements & Engineering

Verified: */s/ Gary W. Whiteman*

Gary W. Whiteman

Regulatory Compliance and Plant Licensing

Westinghouse Electric Company LLC

P.O. Box 355

Pittsburgh, PA 15230-0355

© 2005 Westinghouse Electric Company LLC

All Rights Reserved

Official Record Electronically Approved in EDMS

This page intentionally blank.

Abstract

Nondestructive examination indications of primary water stress corrosion cracking were found in the Westinghouse Model D5 Alloy 600 thermally treated steam generator tubes at the Catawba 2 nuclear power plant in the fall of 2004. Most of the indications were located in the tube-to-tubesheet welds with a few of the indications being reported as extending into the parent tube. In addition, a small number of tubes were reported with indications about 3/4 inch above the bottom of the tube within a region referred to as the tack-expansion, and multiple indications were reported in one tube at internal bulge locations in the upper third of the tubesheet. The tube end weld indications were dominantly axial in orientation and almost all of the indications were concentrated in one steam generator. Circumferential cracks were also reported at internal bulge locations in two of the Alloy 600 thermally treated steam generator tubes at the Vogtle 1 plant site in the spring of 2005. Based on interpretations of requirements published by the NRC staff in GL 2004-01 and IN 2005-9, Duke Power requested that an alternate repair criterion be developed for the tubesheet regions of the steam generator tubes at the Catawba 2 power plant. An evaluation was performed that considered the requirements of the ASME Code, Regulatory Guides, NRC Generic Letters, NRC Information Notices, the Code of Federal Regulations, NEI 97-06, and additional industry requirements. The conclusion of the technical evaluation is that: 1) the structural integrity of the primary-to-secondary pressure boundary is unaffected by tube degradation of any magnitude below a tube location-specific depth ranging from 2.3 to 8.6 inches (depending on the tube leg), designated as H*, and, 2) that the accident condition leak rate integrity can be bounded by the normal operation leak rate from degradation at or below about 11 inches, designated as B*, from the top of the 21 inch thick tubesheet, including degradation of the tube end welds. These results follow from analyses demonstrating that the tube-to-tubesheet hydraulic joints make it extremely unlikely that any operating or faulted condition loads are transmitted below the H* elevation, and the contact pressure dependent leak rate resistance increases below the B* elevation within the tubesheet. Internal tube bulges within the tubesheet are created in a number of tubes as an artifact of the manufacturing process. The possibility of additional degradation at such locations exists based on the already reported degradation at Catawba 2 and Vogtle 1. The determination of the required engagement depth was based on the use of finite element model structural analyses and a steam line break to normal operation comparative leak rate evaluation. It was also concluded that the evaluation of the conditions on the hot leg would always bound those for the cold leg with regard to leak rate performance. The cold leg requirements are greater than the hot leg requirements with regard to pullout resistance (the above numbers bound both). However, the structural length is still less than that needed to restrict leakage to be the same during accident conditions, and the inspection criteria for the cold leg is bounded by that for the hot leg. Application of the structural analysis and leak rate evaluation results to eliminate inspection and/or repair of tube indications in the region of the tube below the H* or B* elevation is interpreted to constitute a redefinition of the primary-to-secondary pressure boundary relative to the original design of the SG and requires the approval of the NRC staff through a license amendment.

This page intentionally blank.

Table of Contents

1.0	Introduction	11
2.0	Summary Discussion	16
3.0	Historical Background Regarding Tube Indications in the Tubesheet	19
4.0	Design Requirements for the Tube-to-Tubesheet Joint Region	21
5.0	Operating Conditions	23
5.1	Bounding Operating Conditions	23
5.2	Faulted Conditions	23
6.0	Steam Generator Tube Leakage and Pullout Test Program Discussion	25
6.1	Tube Pullout Resistance Programs.....	26
6.1.1	Model F Tube Pullout Test Program and Results.....	26
6.1.2	Model D5 Tube Pullout Test Program and Results.....	26
6.2	Leak Rate Testing Programs	27
6.2.1	Model F Tube Joint Leakage Resistance Program	28
6.2.2	Model F Leakage Resistance Tests.....	30
6.2.3	Model D5 Tube Joint Leakage Resistance Program.....	31
6.2.4	Model D5 Leakage Resistance Tests.....	33
6.3	Loss Coefficient on Contact Pressure Regression.....	33
7.0	Structural Analysis of Tube-to-Tubesheet Joint.....	48
7.1	Evaluation of Tubesheet Deflection Effects for Tube-to-Tubesheet Contact Pressure.....	49
7.1.1	Material Properties and Tubesheet Equivalent Properties.....	49
7.1.2	Finite Element Model	52
7.1.3	Tubesheet Rotation Effects.....	53
7.1.4	Catawba 2 Contact Pressures.....	56
7.2	Determination of Required Engagement Length of the Tube in the Tubesheet.....	58
8.0	Leak Rate Analysis of Cracked Tube-to-Tubesheet Joints	77
8.1	The Bellwether Principle for Normal Operation to Steam Line Break Leak Rates	77
8.2	Ligament Tearing Discussion.....	81
9.0	Determination of the B* Distance	86
9.1	Background Information	87
9.2	Flow Through a Crevice (Darcy's Equation)	88
9.3	Tube-to-Tubesheet Contact Pressure Variation	89
9.4	Determination of the B* Distance.....	90
9.5	Sensitivity of the B* Calculation	92
9.6	Conclusions Relative to B*	93
10.0	Discussion of NRC Staff One Cycle Approval B* Braidwood Unit 2.....	106
10.1	Joint Structural Integrity Discussion	106
10.1.1	Discussion of Interference Loads	107

10.1.2 Flexibility Discussion	109
10.1.3 Analysis	111
10.1.4 Conclusions	113
10.2 Joint Leakage Integrity Discussion	113
11.0 Conclusions	118
12.0 References	122

List of Tables

Table 6-1. Model F Leak Test Program Matrix	35
Table 6-2. Model D5 Leak Test Program Matrix	36
Table 6-3. Model F Leak Rate Testing Data.....	37
Table 6-4. Model D5 Experimental Loss Coefficients	38
Table 6-4. Model D5 Experimental Loss Coefficients (Cont.).....	39
Table 6-5. Model F Small Displacement Pullout Test Data	40
Table 6-6. Model F 0.25 Inch Displacement Data at 600°F	40
Table 6-7. Model D5 0.25 Inch Displacement Pullout Test Data.....	41
Table 7-1. Summary of Material Properties Alloy 600 Tube Material.....	63
Table 7-2. Summary of Material Properties for SA-508 Class 2a Tubesheet Material	63
Table 7-3. Summary of Material Properties SA-533 Grade A Class 2 Shell Material	63
Table 7-4. Summary of Material Properties SA-216 Grade WCC Channelhead Material	64
Table 7-5. Equivalent Solid Plate Elasticity Coefficients for D5 Perforated TS SA-508 Class 2a Tubesheet Material (10^6 psi)	64
Table 7-6. Tube/Tubesheet Maximum & Minimum Contact Pressures & H* for Catawba Unit 2 Steam Generators	65
Table 7-7. Cumulative Forces Resisting Pull Out from the TTS Catawba 2 Hot Leg Normal Conditions T_{ave} Coastdown with 0% Plugging	66
Table 7-8. Cumulative Forces Resisting Pull Out from the TTS Catawba 2 Hot Leg Normal Conditions T_{ave} Coastdown with 10% Plugging	67
Table 7-9. Cumulative Forces Resisting Pull Out from the TTS Catawba 2 Faulted (SLB) Conditions	68
Table 7-10. Cumulative Forces Resisting Pull Out from the TTS Catawba 2 FLB Conditions Coastdown with 0% Plugging	69
Table 7-11. Cumulative Forces Resisting Pull Out for FLB Conditions T_{ave} Coastdown with 10% Plugging.....	70
Table 7-12. Summary of H* Calculations for Catawba Unit 2.....	71
Table 7-13. H* Summary Table.....	71
Table 9-1. First Order Equation Coefficients for the Variation of Contact Pressures Through Tubesheet.....	95
Table 10-1. Radial Flexibilities Times Elastic Modulus (in./psi).....	115
Table 10-2. Example Contact Pressure Influence Factors for Models F & D5 SG Tubes at 600°F	115

List of Figures

Figure 1-1. Distribution of Indications in SG A at Catawba 2.....	14
Figure 1-2. Distribution of Indications in SG B at Catawba 2.....	14
Figure 1-3. Distribution of Indications in SG D at Catawba 2.....	15
Figure 2-1. As-Fabricated & As-Analyzed Tube-to-Tubesheet Welds.....	18
Figure 6-1. Example Leakage Test Schematic.....	42
Figure 6-2. Example Tube Hydraulic Expansion Process Schematic.....	43
Figure 6-3. Example Tube Joint Leakage Test Configuration.....	44
Figure 6-4. Schematic for the Test Autoclave Systems for Leak Rate Testing	45
Figure 6-5. Example Tube Joint Sample Pullout Test Configuration.....	46
Figure 6-6. Loss Coefficient Values for Model F & D5 Leak Rate Analysis.....	47
Figure 7-1. Definition of H* Zones	72
Figure 7-2. Finite Element Model of Model D5-3 Tubesheet Region.....	73
Figure 7-3. Contact Pressures for Normal Condition (10% SGTP) at Catawba 2.....	74
Figure 7-4. Contact Pressures for Normal Condition (0% SGTP) at Catawba Unit 2.....	74
Figure 7-5. Contact Pressures for SLB Faulted Condition at Catawba 2.....	75
Figure 7-6. Contact Pressures for FLB Condition at Catawba 2 T _{ave} Coastdown 0% Plugging.....	75
Figure 7-7. Contact Pressures for FLB Condition at Catawba 2 T _{ave} Coastdown 10% Plugging....	76
Figure 8-1. Change in contact pressure at 21.0 inches below the TTS.....	83
Figure 8-2. Change in contact pressure at 16.9 inches below the TTS.....	83
Figure 8-3. Change in contact pressure at 12.6 inches below the TTS.....	84
Figure 8-4. Change in contact pressure at 10.5 inches below the TTS.....	84
Figure 8-5. Change in contact pressure at 8.25 inches below the TTS.....	85
Figure 8-6. Change in contact pressure at 6.0 inches below the TTS.....	85
Figure 9-1. Determination of H*.....	96
Figure 9-2. Determination of B*.....	97
Figure 9-3. Concepts for the Determination of B*	98
Figure 9-4. Determination of B* Parameters.....	98
Figure 9-5. First Order Linear Representation of Contact Pressure.....	99
Figure 9-6. Contact Pressure During Normal Operation	99
Figure 9-7. Contact Pressure During SLB, 2560 psi at 297°F	100
Figure 9-8. NOp Contact Pressure vs. Depth Coefficients by Radius	100
Figure 9-9. SLB Contact Pressure vs. Depth Coefficients by Radius.....	101

Figure 9-10. Contact Pressure Coefficients for NOP & SLB.....	101
Figure 9-11. Elevation Below the TTS for Invariant Contact Pressure	102
Figure 9-12. TTS Pc for NOP & SLB Conditions	102
Figure 9-13. Viscosity of Water as a Function of Pressure.....	103
Figure 9-14. Viscosity of Water at 2560 psi as a Function of Temperature	103
Figure 9-15. B* Depths for No Change in Resistance	104
Figure 9-16. B* Depths for Catawba 2 SGs for No Change in Leak Rate.....	104
Figure 9-17. Graphical Determination of B* Depth from Flow Resistance	105
Figure 9-18. Approximate Determination of B* Depth from Contact Pressure	105
Figure 10-1. Geometry of the Tube-to-Tubesheet Interface	116
Figure 10-2. Model for Initial Contact Pressure	116
Figure 10-3. Determination of Contact Pressure, Normal or Accident Operation.....	117
Figure 11-1. Comparison of Hot Leg H* and B* Results.....	121
Figure 11-2. Comparison of Cold Leg H* and B* Results	121

This page intentionally blank.

**Steam Generator Tube Alternate Repair Criteria
for the Portion of the Tube Within the Tubesheet
at Catawba 2**

1.0 Introduction

Indications of cracking were reported from the nondestructive, eddy current examination of the steam generator (SG) tubes during the fall 2004 outage at the Catawba 2 nuclear power plant operated by the Duke Power Company, References 1, 2, and 3. The tube indications at Catawba were reported about 7.6 inches from the top of the tubesheet in one tube, and just above the tube-to-tubesheet welds in a region of the tube known as the tack expansion (TE) in several other tubes. Finally, indications were also reported in the tube-end welds (TEWs), also known as tube-to-tubesheet welds, joining the tube to the tubesheet, with a small number of those indications extending into the tube material. The spatial distribution of indications by row and column number is shown on Figure 1-1 for SG A, Figure 1-2 for SG B, and Figure 1-3 for SG D at Catawba 2; there were no indications in SG C. The Catawba 2 plant has Westinghouse designed, Model D5 SGs fabricated with Alloy 600TT (thermally treated) tubes. It was subsequently noted that an indication was reported in each of two SG tubes at the Vogtle Unit 1 plant operated by the Southern Nuclear Operating Company (Reference 4). The Vogtle SGs are of the Westinghouse Model F design with slightly smaller, diameter and thickness, A600TT tubes. It has been concluded from these observations that there is the potential for additional tube indications similar to those already reported at Catawba 2 within the tubesheet region to be reported during future inspections.

Note: No indications were found during the planned inspections of the Braidwood 2 SG tubes in April 2005, a somewhat similar inspection of the tubes in two Model F SGs at Wolf Creek in April 2005, or an inspection of the Model D5 tubes at Comanche Peak 2 in the spring of 2005. Nor during similar inspections of the Model D5 tubes at Byron 2 and Model F tubes at Vogtle 1 in the fall of 2005.

The SGs at the four Model D5 plant sites were fabricated in the 1978 to 1980 timeframe using similar manufacturing processes with a few exceptions. For example, the fabrication technique used for the installation of the SG tubes at Braidwood 2 would be expected to lead to a much lower likelihood for crack-like indications to be present in the region known as the tack expansion relative to Catawba 2 because a different process for effecting the tack expansions was adopted prior to the time of the fabrication of the Braidwood 2 SGs.

The findings in the Catawba 2 and Vogtle 1 SG tubes present three distinct issues with regard to future inspections of A600TT SG tubes which have been hydraulically expanded into the tubesheet:

- 1) indications in internal bulges within the tubesheet,
- 2) indications at the elevation of the tack expansion transition, and
- 3) indications in the tube-to-tubesheet welds, including some extending into the tube.

The scope of this document is to:

- a) address the applicable requirements, including the original design basis, Reference 6, and regulatory issues, Reference 8, and,
- b) provide analysis support for technical arguments to ignore tube degradation within the tubesheet of any extent below a specified depth or depths as a function of tube location, i.e., the depths specified in Section 7.0 of this report.

An evaluation was performed that considered the requirements of the ASME Code, Regulatory Guides, NRC Generic Letters, NRC Information Notices, the Code of Federal Regulations, NEI 97-06, and additional industry requirements. The conclusion of the technical evaluation is that:

- 1) the structural integrity of the primary-to-secondary pressure boundary is unaffected by tube degradation of any magnitude below a tube location-specific depth ranging from 2.3 and 3.5 to 8.1 and 8.6 inches on the hot and cold legs respectively, criteria which are designated as H*, and,
- 2) the accident condition leak rate integrity can be bounded by the normal operation leak rate from degradation at or below about 11 inches, a criterion designated as B*, from the top of the 21 inch thick tubesheet, including degradation of the tube end welds.

These results follow from analyses demonstrating that the tube-to-tubesheet hydraulic joints make it extremely unlikely that any operating or faulted condition loads are transmitted below the H* elevation, and the tube-to-tubesheet contact leak rate resistance increases below the B* elevation within the tubesheet. Internal tube bulges within the tubesheet are created in a number of tubes as an artifact of the manufacturing process. The determination of the required engagement depth was based on the use of finite element model structural analyses and of a bounding leak rate evaluation based on the change in contact pressure between the tube and the tubesheet between normal operation and postulated accident conditions. The results support a license amendment to ignore tube degradation in the region of the tube below the H* or B* elevation, whichever is lower. Such an amendment is interpreted to constitute a redefinition of the primary-to-secondary pressure boundary relative to the original design of the SG and requires the approval of the NRC staff through a license amendment. Potential degradation regions would be limited to about the bottom 10 inches of the tube in the nominally 21.26 inch thick tubesheet, which is well below the mid-plane of the tubesheet. As described in Section 12.0 of this report, the potential leakage due to degradation below 11 inches from the TTS would clearly be below the accident analysis leakage assumption..

A similar type of Technical Specification change was approved, on a one-time basis, to limit inspections of the Braidwood 2 and Wolf Creek SGs during the spring 2005 inspection campaigns, for example see Reference 9. Subsequent approvals were also obtained for use at Byron 2 and Vogtle 2 for their fall 2005 inspection campaigns, Reference 10 for example. This report was prepared to justify the specialized probe exclusion zone to the portion of the tube below about 11 inches from the top of the tubesheet and to provide the necessary information for a detailed NRC

staff review of the technical basis for that request. The major difference between the evaluation done for the Catawba 2 SGs and prior applications is the identification of tube location-specific depths for the inspection instead of simply using a bounding, but arbitrary, value of 17 inches from the top of the tubesheet.

The development of the H* criteria involved consideration of the performance criteria for the operation of the SG tubes as delineated in NEI 97-06, Revision 2, Reference 11. The bases for the performance criteria are the demonstration of both structural and leakage integrity during normal operation and postulated accident conditions. The structural model was based on standard analysis techniques and finite element models as used for the original design of the SGs and documented in numerous submittals for the application of criteria to deal with tube indications within the tubesheet of other models of Westinghouse designed SGs with tube-to-tubesheet joints fabricated by other techniques, e.g., explosive expansion.

All full depth expanded tube-to-tubesheet joints in Westinghouse-designed SGs have a residual radial preload between the tube and the tubesheet. Early vintage SGs involved hard rolling which resulted in the largest magnitude of the residual interface pressure. Hard rolling was replaced by explosive expansion which resulted in a reduced magnitude of the residual interface pressure. Finally, hydraulic expansion replaced explosive expansion for the installation of SG tubes, resulting in a further reduction in the residual interface pressure. In general, it was found that the leak rate through the joints in hard rolled tubes, if any, is insignificant. Testing demonstrated that the leak rate resistance of explosively expanded tubes was not as great and prediction methods based on empirical data to support theoretical models were developed to deal with the potential for leakage. The same approach was followed to develop a prediction methodology for hydraulically expanded tubes. However, the model has been under review since its inception, with the intent of verifying its accuracy because it involved analytically combining the results from independent tests of leak rate through cracks with the leak rate through the tube-to-tubesheet crevice. The leak rate model associated with the initial development of H* to meet structural performance criteria is such a model; technical acceptance could be time consuming since it has not been previously reviewed by the NRC staff. An alternative approach was developed for application at Catawba 2 from engineering expectations of the relative leak rate between normal operation and postulated accident conditions based on a first principles engineering approach.

A summary of the evaluation is provided in Section 2.0 of this report. The historical background and design requirements for the tube-to-tubesheet joint are discussed in Sections 3.0 and 4.0 respectively. Section 5.0 addresses plant operating conditions at Catawba 2. Section 6.0 discusses the tube pullout and leakage test programs that are applicable to the Model D5 SGs at Catawba 2. A summary of the conclusions from the structural analysis of the joint is provided in Section 7.0, the leak rate analysis in Section 8.0, determination of the requisite inspection depth based on leak rate considerations is in Section 9.0, a review of the qualitative arguments used by the NRC Staff for the tube joint inspection length approved for other plants is discussed in Section 10.0, finally, the conclusions from the structural and leak rate evaluations are contained in Section 11.0.

SG - 2A +Point Indications Within the Tubesheet

Catawba EOC13 DDP D5

E 1 INDICATION WITHIN 0.25" OF HOT LEG TUBE END
66 PLUGGED TUBE

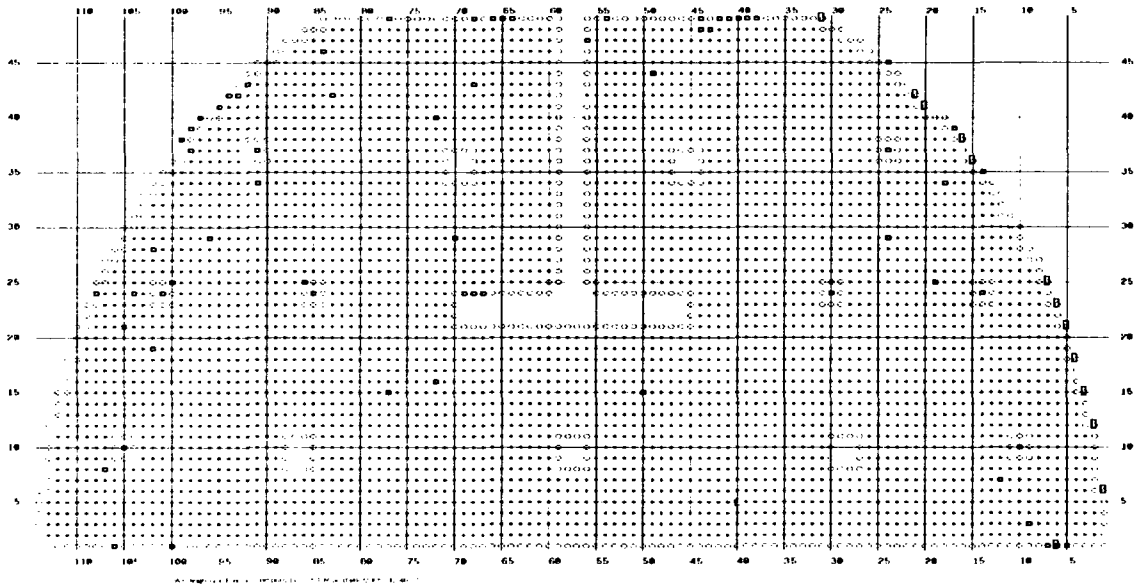


Figure 1-1. Distribution of Indications in SG A at Catawba 2

SG - 2B +Point Indications Within the Tubesheet

Catawba EOC13 DDP D5

Z 1 MULTIPLE INDICATIONS AT APPROXIMATELY 7" BELOW HOT LEG TOP OF TUBESHEET
L 192 INDICATION WITHIN 0.25" OF HOT LEG TUBE END
W 1 INDICATIONS WITHIN 0.25" AND BETWEEN 0.26" AND 0.00" OF HOT LEG TUBE END
B 9 INDICATION BETWEEN 0.26" AND 0.00" OF HOT LEG TUBE END
58 PLUGGED TUBE

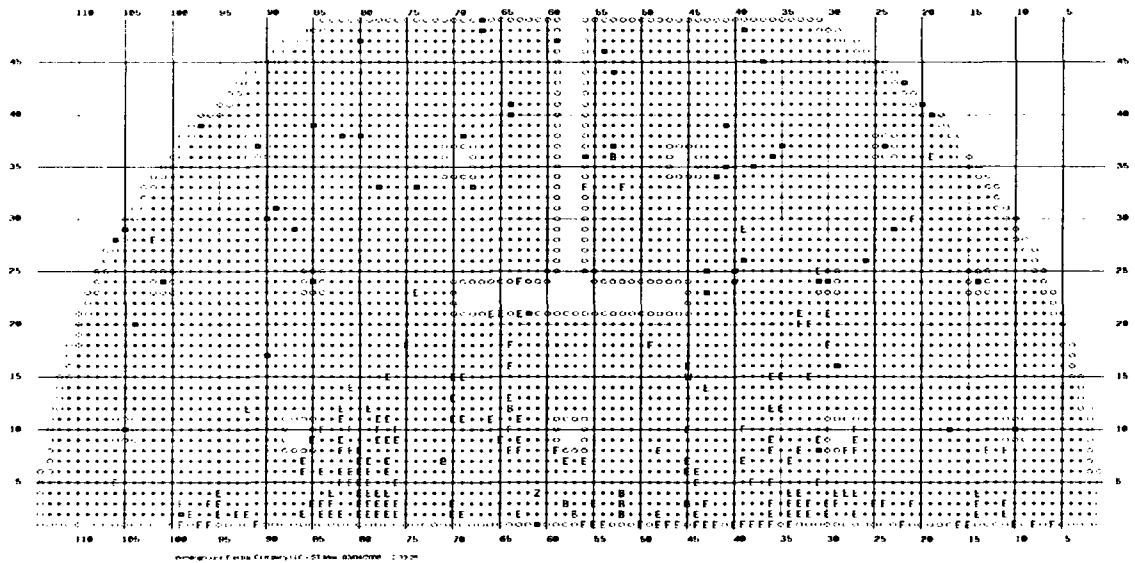


Figure 1-2. Distribution of Indications in SG B at Catawba 2

SG - 2D +Point Indications Within the Tubesheet

Catawba EOC13 DDP D5

E 7 INDICATION WITHIN 0.25" OF
HOT LEG TUBE END
■ 85 PLUGGED TUBE

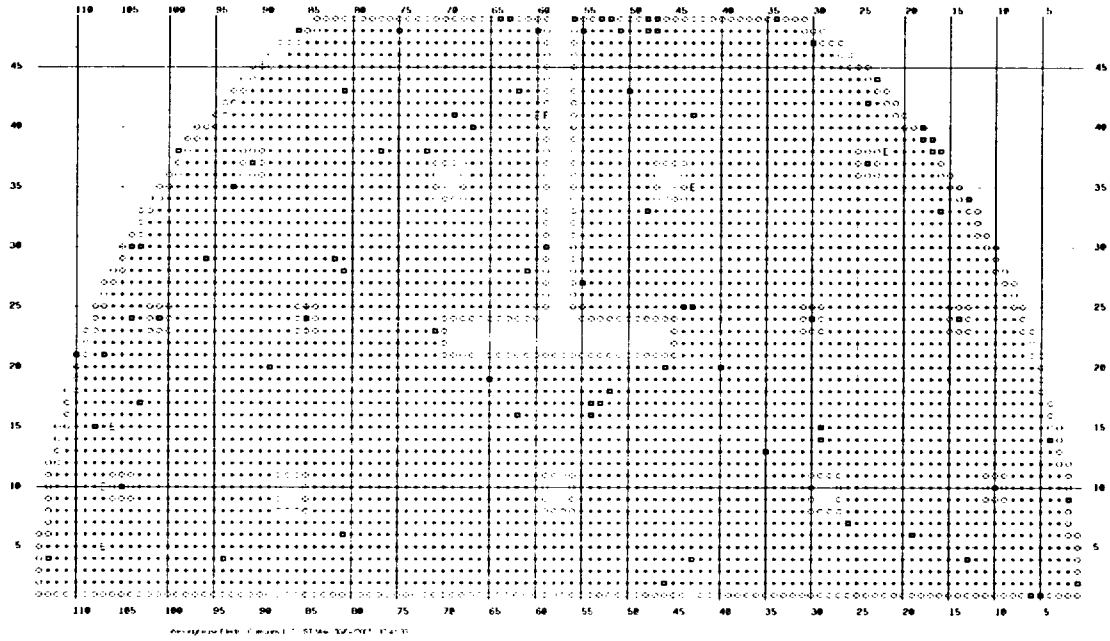


Figure 1-3. Distribution of Indications in SG D at Catawba 2

2.0 Summary Discussion

Evaluations were performed to assess the need for addressing degradation in the region of the SG tubes below a specified distance within the tubesheet at the Catawba 2 power plant. The conclusions from the evaluation are that a redefinition of the pressure boundary can be effected while still assuring that the structural and leak rate performance criteria would be met during both normal operation and limiting postulated accident conditions.

The result of effecting such a redefinition would be the elimination of repairing tubes for degradation below a depth on the order of 11¹ inches from the top of the tubesheet, including the region of the tube referred to as the tack expansion or the tack expansion transition. In addition, consideration was given to the need to address the tube-to-tubesheet weld in spite of the fact that the weld is specifically not part of the tube in the sense of the plant technical specification, see Reference 2. It is concluded that there is no need to inspect the tube-to-tubesheet welds for degradation because the tube in these regions has been shown to meet structural and leak rate criteria regardless of the level of degradation. Furthermore, it can also be concluded that for some of the tubes, depending on radial location in the tubesheet, there is no need to address the region of the tube below the shifted neutral plane of the tubesheet with regard to contact pressure,² roughly 8.3 inches below the top. The results from the evaluations performed as described herein demonstrate that the inspection of the tube within about 10 inches of the tube-to-tubesheet weld and of the weld is not necessary for structural adequacy of the SG during normal operation or during postulated faulted conditions, nor for the complying with leak rate limits during postulated faulted events. This conclusion applies to both the hot and cold legs of the SG tubes.

In summary:

- The structural integrity requirements of NEI 97-06, Reference 11, are met by sound tube engagement lengths ranging from 3.45 to 8.61 inches from the top of the tubesheet, regardless of hot or cold leg considerations, thus the region of the tube below those elevations, including the tube-to-tubesheet weld is not needed for structural integrity during normal operation or accident conditions (see Table 7-13).
- NEI 97-06, Reference 11, defines the tube as extending from the tube-to-tubesheet weld at the tube inlet to the tube-to-tubesheet weld at the tube outlet, but specifically excludes the tube-to-tubesheet weld from the definition of the tube. The acceptance of the definition by the NRC staff was recorded in the Federal Register on March 2, 2005, Reference 13.
- The welds were originally designed and analyzed as primary pressure boundary in accordance with the requirements of Section III of the 1971 edition of the ASME Code,

¹ The value of 11 inches is based on leak rate considerations and corresponds to the worst location in the tubesheet. The value can be considerably less towards the periphery.

² The neutral plane of the tubesheet is shifted away from the center because of the tensile stress in the tubesheet and the internal pressure in the tube.

with selected sections of the Winter 1974 Addenda, References 6, 7 and 14. The analyses are documented in Reference 15 for the Catawba 2 SGs. The typical as-fabricated and the as-analyzed weld configurations are illustrated on Figure 2-1. The “stiff tube” representation was an analysis feature to maximize the stress in the weld.

- Section XI of the ASME Code, Reference 16 (1971) through 17 (2004), deals with the inservice inspection of nuclear power plant components. The ASME Code specifically recognizes that the SG tubes are under the purview of the NRC through the implementation of the requirements of the Technical Specifications as part of the plant operating license.

The hydraulically expanded tube-to-tubesheet joints in Model D5 SGs are not leak-tight without the tube end weld and considerations were also made with regard to the potential for primary-to-secondary leakage during postulated faulted conditions. However, the leak rate during postulated accident conditions would be expected to be less than that during normal operation for indications near the bottom of the tubesheet (including indications in the tube end welds) based on the observation that while the driving pressure increases by about a factor of almost two, the flow resistance increases because the tube-to-tubesheet contact pressure also increases. Depending on the depth within the tubesheet, the relative increase in resistance could easily be larger than that of the pressure potential. Therefore, the leak rate under normal operating conditions could exceed its allowed value before the accident condition leak rate would be expected to exceed its allowed value. This approach is termed an application of the “bellwether principle.” The evaluations were performed to specifically determine relative changes in the leak rate resistance as a function of tube location from the center of the tubesheet and degradation distance from the top of the tubesheet.. The assessment envelopes postulated circumferential cracking of the tube or the tube-to-tubesheet weld that is 100% deep by 360° in extent because it is based on the premise that the tube and weld are not present below the analyzed elevations.

Based on the information summarized above, no inspection of the tube-to-tubesheet welds, tack roll region or bulges below the distance determined to have the potential for safety significance as specified in Reference 5, i.e., the H* depths, would be necessary to assure compliance with the structural requirements for the SGs. In addition, the application of the bellwether principle with regard to potential leak during postulated accident conditions showed that inspection depths as a function of tube location established using the results from these analyses are conservative and justified.

The length determined for structural compliance purposes can bound the required length for leak

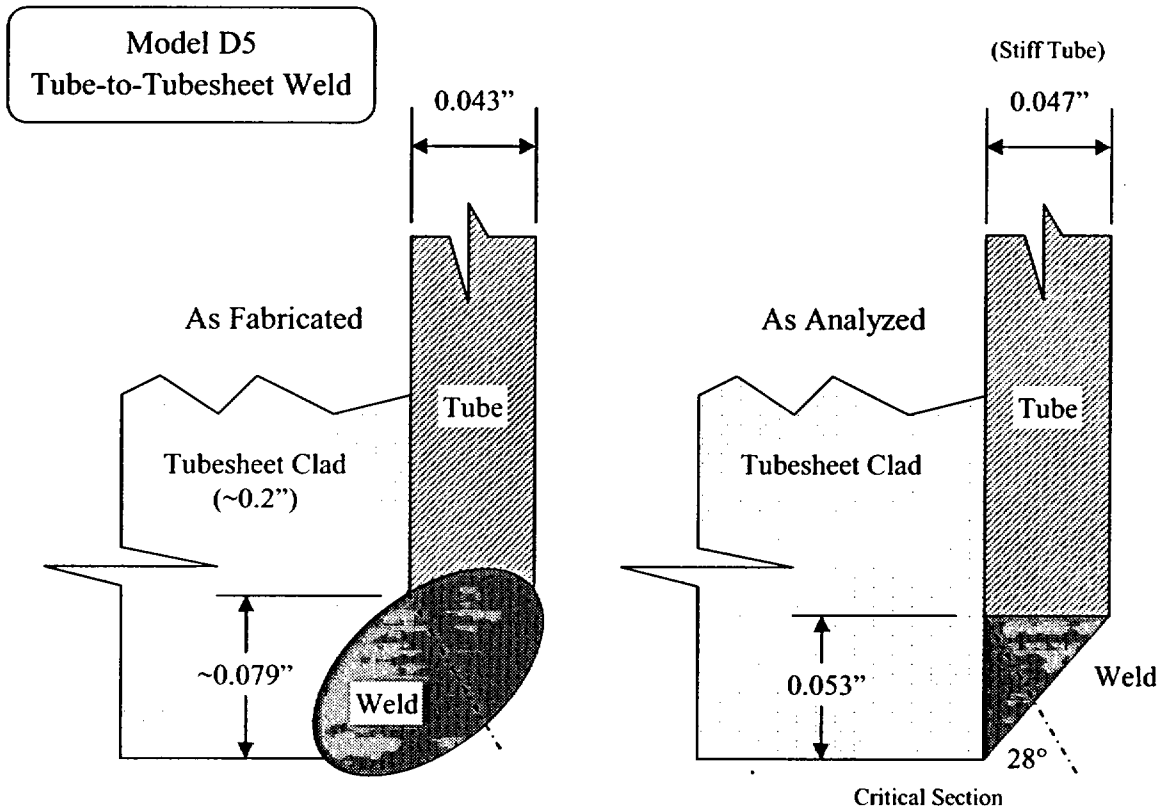


Figure 2-1. As-Fabricated & As-Analyzed Tube-to-Tubesheet Welds

3.0 Historical Background Regarding Tube Indications in the Tubesheet

There has been extensive experience associated with the operation of SGs wherein it was believed, based on NDE, that throughwall tube indications were present within the tubesheet. The installation of the SG tubes usually involves the development of a short interference fit, referred to as the tack expansion, at the bottom of the tubesheet. The tack expansion was usually effected by a hard rolling process through October of 1979 and thereafter, in most instances, by the Poisson expansion of a urethane plug inserted into the tube end and compressed in the axial direction. The rolling process by its very nature is considered to be more intensive with regard to metalworking at the inside surface of the tube and would be expected to lead to higher residual surface stresses. The rolling process was used during fabrication of the Catawba 2 SGs. The tube-to-tubesheet weld was then performed to create the ASME Code pressure boundary between the tube and the tubesheet.³

The development of the F* alternate repair criterion (ARC) in 1985-1986 for tubes hard rolled into the tubesheet was prompted by the desire to account for the inherent strength of the tube-to-tubesheet joint away from the weld and to allow tubes with degradation within the tubesheet to remain in service, Reference 18. The result of the development activity was the demonstration that the tube-to-tubesheet weld was superfluous with regard to the structural and leakage integrity of the rolled joint between the tube and the tubesheet. Once the plants were in operation, the structural and leakage resistance requirements for the joints were based on the plant Technical Specifications, and a means of demonstrating joint integrity that was acceptable to the NRC staff was delineated in Reference 12. License amendments were sought and granted for several plants with hard rolled tube-to-tubesheet joints to omit the inspection of the tube below a depth of about 1.5 inches from the top of the tubesheet. Similar criteria, designated as W*, were developed for explosively expanded tube-to-tubesheet joints in Westinghouse designed SGs in the 1991-1992 timeframe, Reference 19. The W* criteria were first applied to operating SGs in 1999 based on a generic evaluation for Model 51 SGs, Reference 20, and the subsequent safety evaluation by the NRC staff, Reference 21. However, the required engagement length to meet structural and leakage requirements was on the order of 4 to 6 inches because an explosively expanded joint does not have the same level of residual interference fit as that of a rolled joint. It is noted that the length of joint necessary to meet the structural requirements is not the same as, and is usually shorter than, that needed to meet the leakage integrity requirements.

The post-weld expansion of the tube into the tubesheet in the Catawba 2 SGs was effected by a hydraulic expansion of the tube instead of rolling or explosive expansion. The hydraulically formed joints do not exhibit the level of interference fit that is present in rolled or explosively expanded joints, however, when the thermal and internal pressure expansion of the tube is considered during normal operation and postulated accident conditions, appropriate conclusions regarding the need for the weld similar to those for the other two types of joint can be made. Evaluations were performed in 1996 of the effect of tube-to-tubesheet weld damage that occurred from an object in the bowl of a SG with tube-to-tubesheet joints similar to those in the Catawba 2

SGs, on the structural and leakage integrity of the joint, References 22 and 23. It was concluded in that evaluation that the strength of the tube-to-tubesheet joint is sufficient to prevent pullout in accordance with the requirements of the performance criteria of Reference 11 and that a significant number of tubes could be damaged without violating the performance criterion related to the primary-to-secondary leak rate during postulated accident conditions.

³ The actual weld is between the Alloy 600 tube and weld buttering, a.k.a. cladding, on the bottom of the carbon steel tubesheet.

4.0 Design Requirements for the Tube-to-Tubesheet Joint Region

This section provides a review of the applicable design and analysis requirements, including the ASME Code pre-service design requirements of Section III and the operational/maintenance requirements of Section XI. The following is the Westinghouse interpretation of the applicable analysis requirements and criteria for the condition of TEW cracking. Recommendations that include code requirements and the USNRC position as expressed in References 8 and 11. Reference 8 notes that:

“In accordance with Section III of the Code, the original design basis pressure boundary for the tube-to-tubesheet joint included the tube and tubesheet extending down to and including the tube-to-tubesheet weld. The criteria of Section III of the ASME Code constitute the “method of evaluation” for the design basis. These criteria provide a sufficient basis for evaluating the structural and leakage integrity of the original design basis joint. However, the criteria of Section III do not provide a sufficient basis by themselves for evaluating the structural and leakage integrity of a mechanical expansion joint consisting of a tube expanded against the tubesheet over some minimum embedment distance. If a licensee is redefining the design basis pressure boundary and is using a different method of evaluation to demonstrate the structural and leakage integrity of the revised pressure boundary, an analysis under 10 CFR 50.59 would determine whether a license amendment is required.”

The industry definition of Steam Generator tubing excludes the tube-end weld from the pressure boundary as noted in NEI 97-06 (Reference 11):

“Steam generator tubing refers to the entire length of the tube, including the tube wall and any repairs to it, between the tube-to-tube sheet weld at the tube inlet and the tube-to-tube sheet weld at the tube outlet. The tube-to-tube sheet weld is not considered part of the tube.”

The NRC has indicated its concurrence with this definition, see Reference 13 for example. In summary, from a non-technical viewpoint, no specific inspection of the tube-end welds would be required because:

1. The industry definition of the tube excludes the tube-end weld,
2. The ASME Code defers the judgment regarding the redefined pressure boundary to the licensing authority under 10CFR50.59,
3. The NRC has accepted this definition; therefore, by inference, may not consider cracked welds to be a safety issue on a level with that of cracked tubes, and
4. There is no qualified technique that can realistically be applied to determine if the tube-end welds are cracked.

However, based on the discussion of Information Notice 2005-09, Reference 2, it is clear that the NRC staff has concluded that “the findings at Catawba illustrate the importance of inspecting the parent tube adjacent to the weld and the weld itself for degradation.” The technical considerations documented herein obviate the need for consideration of any and all non-technical arguments.

5.0 Operating Conditions

Catawba 2 is a four-loop nuclear power plant with Westinghouse designed and fabricated Model D5 SGs; there are 4570 tubes in each SG. The design of these SGs includes Alloy 600 thermally treated (A600TT) tubing, full-depth hydraulically expanded tubesheet joints, and broached hole quatrefoil tube support plates constructed of stainless steel.

5.1 Bounding Operating Conditions

Values that bound the current Catawba 2 SG thermal and hydraulic parameters during normal operation are tabulated below (Note: these values assume a 10% SG tube plugging level.):

Parameter and Units		Bounding Operating Conditions ⁽¹⁾
Power – NSSS	MWt	3499
Reactor Vessel Outlet Temperature	°F	603.4
Reactor Coolant System Pressure	psig	2235
SG Steam Temperature	°F	516.2
SG Steam Pressure	psig	771
Feedline Break Pressure	psig	2560
Ratio of Normal to Accident Pressures		1.81
(1) Reference 24		

5.2 Faulted Conditions

In addition to the RG 1.121 criteria, it is necessary to satisfy the updated final safety analysis report (UFSAR) accident condition assumptions for primary-to-secondary leak rates. Calculated primary-to-secondary side leak rate during postulated events should: 1) not exceed the total charging pump capacity of the primary coolant system, and 2) be such that the off-site radiological dose consequences do not exceed Title 10 of the Code of Federal Regulations (10 CFR) Part 100 guidelines.

The accident condition primary-to-secondary leakage must be limited to acceptable values established by plant specific UFSAR evaluations. Pressure differentials associated with a postulated accident condition event can result in leakage from a throughwall crack through the interface between a hydraulically expanded tube in the tubesheet and the tube hole surface. Therefore, a steam generator leakage evaluation for faulted conditions is provided in this report. The accidents that are affected by primary-to-secondary leakage are those that include, in the activity release and off-site dose calculation, modeling of leakage and secondary steam release to

the environment. Steamline break (SLB) is the limiting condition; the reasons that the SLB is limiting are:

- 1) the SLB primary-to-secondary leak rate in the faulted loop is assumed to be greater than the operating leak rate because of the sustained increase in differential pressure, and
- 2) leakage in the faulted steam generator is assumed to be released directly to the environment.

For evaluating the radiological consequences due to a postulated SLB, the activity released from the affected SG (which is connected to the broken steam line) is released directly to the environment. The unaffected steam generators are assumed to continually discharge steam and entrained activity via the safety and relief valves up to the time when initiation of the RHR system can be accomplished. The radiological consequences evaluated, based on meteorological conditions, usually assume that all of this flow goes to the affected SG. With the analytically determined level of leakage, the resultant doses are expected to be well within the guideline values of 10 CFR 100.

6.0 Steam Generator Tube Leakage and Pullout Test Program Discussion

While the tube material and tube installation into the tubesheet technique are similar between the Westinghouse Model F and D5 SGs, there are also differences between the designs with regard to the tube size, thickness, number of tubes and tube pitch. Data are available with regard to pullout and leak rate testing for both SG geometries. The original testing of Reference 23 was performed to investigate postulated extreme effects on the tube-to-tubesheet weld from a loose part on the primary side of one Model F SG. These data were also used to support the model specific development of the required H^* length and to characterize the leak rate from throughwall tube indications within the tubesheet as a function of the contact pressure between the tube and the tubesheet, e.g., Reference 10 was originally written for the Vogtle 1 and 2 SGs. The testing also provides valuable information regarding the calculation of B^* once a relative SLB to NOP leak rate has been identified.⁴ Pullout and leak rate data were also available from similar testing performed using Model D5 specific geometry, References 25 and 26. The data from both sets of testing programs were combined to support the development of the inspection criteria delineated in this report.

- The results from strength tests were used to establish the joint lengths needed to meet the structural performance criteria during normal operation and postulated accident conditions, the required engagement length being designated as H^* . The inherent strength of the joint coupled with the results from a finite element model of the loading conditions is used to calculate the required H^* values subsequently described in Section 7.0.
- The results from leak rate tests were used to support the methodology to quantify the leak rate during postulated accident conditions as a function of the leak rate during normal operation. The required engagement length to meet a specific leak rate objective is designated as B^* . For example, it may be desired to determine the engagement length needed so that the leak rate expected during a postulated accident event is no more than twice that during normal operation. The calculation of the relative leak rates as a function of engagement length is described in Section 9.0 of this report.

Data from the test programs for the Model F SGs, Reference 23, directly supports the determination of both the H^* and B^* values for the SG tubes. The testing programs had two purposes:

- 1) To characterize the strength of the tube-to-tubesheet joints in Model F SGs during normal operation, e.g., 600°F, and under postulated accident conditions, and,
- 2) To characterize the leak resistance of the tube-to-tubesheet joints in Model F SGs during normal operation and under postulated accident conditions.

⁴ It is noted that the discussion in Section 9.0 shows that the B^* depths are not very sensitive to changes in the correlating parameters between the leak rate and contact pressure.

Similar testing was performed using specimens designed to simulate installed tubes in Model D5 SGs to develop parallel criteria for other plants. The independent testing programs that were conducted to characterize the joint strength and leak rate characteristics for Model F and Model D5 SGs are discussed separately in the following sections.

6.1 Tube Pullout Resistance Programs

To determine the resistance of the simulated Model F and D5 tube-to-tubesheet joints to pullout at temperatures ranging from ambient to 600°F.

6.1.1 Model F Tube Pullout Test Program and Results

Mechanical loading tests were performed on [

] ^{a,c,e}. All of the test results are listed in Table 6-5. The mechanical loading, [

] ^{a,c,e}
The objective was to develop input information for analytically determining tube-to-tubesheet contact pressure and axial pullout resistance (lb/inch). In this configuration, there is no contribution to tube-to-tubesheet contact pressure from tube internal pressurization. Internal pressurization also resists Poisson contraction associated with the axial load.

The data from the series of pullout tests are listed in Table 6-5 and in Table 6-6 for the 0.25 inch displacement data at 600°F. [

] ^{a,c,e} A comparison of the implied net contact pressure, “Net P,” from the tests can be made by looking at the values in the next to last column of Table 6-6. These include a correction factor to account for the increase in interface pressure due to the greater thermal expansion of the tube relative to the TS simulating collar. The last column converts the “Net P” into a “Net F / L” for force per unit inch of engagement for use in the H* calculations. The results exhibit a small degree of scatter, with an average net force of [

] ^{a,c,e} The use of a larger coefficient of friction results in calculating a lower value of the contact pressure. Subsequent use of the lower coefficient of friction results in calculating a larger required engagement length. A conservative value used for the pullout force in the H* calculations was the average minus three standard deviations, or [

] ^{a,c,e}.

6.1.2 Model D5 Tube Pullout Test Program and Results

The Model D5 pullout test samples were fabricated with the same processes as used for the leakage tests, refer to Figure 6-5, and described later in this section. The tube expansion tool used

in the program was a factory device, modified to achieve an expansion ranging of from three to seven inches.

Model D5 hydraulic expansion joints with nominal axial lengths of [

] ^{a,c,e} The conduct of the tests was similar to those using Model F tube size specimens. The pullout data obtained is listed in Table 6-7 and discussed in a subsequent paragraph.

Joint strength is based on evaluating the data from a recorded load-deflection curve. The maximum force achieved is typically not used, opting instead for a value corresponding to a [^{a,c,e}]
The other variables affecting joints in operating SGs include tubesheet bending (causing the tubesheet hole to dilate and/or contract depending on the distance of a certain point below the tubesheet top), the thermal growth mismatch effect (owing to the greater thermal growth of the Alloy 600TT tube relative to the carbon steel tubesheet, and the “differential pressure tightening” of the tube within the tubesheet. The force resisting tube pullout from the tubesheet in the plant, acting on a length of a tube between elevations h_1 and h_2 , reckoned from a convenient elevation such as the tubesheet secondary side face, is shown in Section 7.2 of this report.

Mechanical loading, or pullout, tests on samples of the tube joints were run [

] ^{a,c,e}

[

] ^{a,c,e}

6.2 Leak Rate Testing Programs

The purpose of the testing programs was to provide quantified data with which to determine the [

] ^{a,c,e} As discussed in detail in Section 9.2, the analytical model for the leak rate is referred to as the Darcy or Hagen-Poiseuille formulation. The volumetric flow is a function of the pressure potential, the inverse of the crevice length, the inverse of the fluid viscosity, and the inverse of an

resistance term characteristic of the geometry of the tube-to-tubesheet joint and referred to as the loss coefficient. Thus, the purpose of the testing programs is to obtain data with which to determine the loss coefficient. Data were available from leak rate test programs that independently addressed the Model F and the Model D5 tube-to-tubesheet joints:

- a. The Model F tube joint leakage resistance program involved tests at [

] ^{a,c,e}

- b. The Model D5 tube joint leakage resistance program involved tests at [

] ^{a,c,e}

The Model F program and results are described in Section 6.2.1, followed by the description and results of the Model D5 program in Section 6.2.2.

6.2.1 Model F Tube Joint Leakage Resistance Program

A total of [

] ^{a,c,e} The leakage resistance data were calculated for the test conditions listed in Table 6-1.

6.2.1.1 Model F Test Specimen Configuration

The intent of the test samples was to model key features of the Model F tube-to-tubesheet joint for leakage tests. The following hardware was used:

A Model F tubesheet simulating collar which mimicked the radial stiffness of a Model F tubesheet unit cell with an outside diameter of approximately [] ^{a,c,e}. The length of the test collars was [] ^{a,c,e} thickness of the steam generator tubesheet. This allowed for the introduction and collection of leakage in unexpanded sections of the tube, while retaining conservative or typical hydraulic expansion lengths. The collars were drilled to the nominal design value inside diameters with the surface finish based on drawing tolerances. In addition, the run-out tolerance for the collar drilling operation was held to within ± 0.002 inch of the tubesheet nominal hole diameter.

The collars were fabricated from [

] ^{a,c,e}.

Model F A600TT tubing with a yield strength approximately the same as that of the tubes in the operating plants, which ranges from [] ^{a,c,e}. The used was from a certified heat and lot conforming to ASME SB163, Section III Class 1 and was maintained in a Quality Systems-controlled storeroom prior to use.

The intent of the leakage portion of the test program was to determine the leakage resistance of simulated Model F tube-to-tubesheet joints, disregarding the effect of the tube-to-tubesheet weld and the [

] ^{a,c,e}, see Figure 6-1. The welds were a feature of the test specimen design and made no contribution to the hydraulic resistance.

6.2.1.2 Model F Test Sample Assembly

The SG factory tube installation drawing specifies a [

] ^{a,c,e}, to facilitate the tube weld to the cladding on the tubesheet face and it was omitted from the test. Following welding of the tube to the tubesheet, a full-length hydraulic expansion of the tube into the tubesheet is performed. The hydraulic expansion pressure range for the Model F SGs was approximately [] ^{a,c,e}. The majority of the test samples were expanded using a specified

pressure of []^{a,c,e} to conservatively bound the lower expansion pressure limit used for SG fabrication.

The tube expansion tool used in the factory consisted of a pair of seals, spaced by a tie rod between them. The hydraulically expanded zone was positioned relative to the lower surface of the tubesheet, overlapping the upper end of the tack expanded region. It extended to within a short distance of the upper surface of the tubesheet. This produced a hydraulically expanded length of approximately []^{a,c,e} inch nominal tubesheet thickness. The majority of the test specimens were fabricated using [

[]^{a,c,e} Previous test programs which employed a segmented approach to expansion confirmed the expectation that uniform results from one segment to the next would result. This approach produced the desired expansion pressures for a conservative length of []^{a,c,e} inch-expanded length being simulated. The remaining length of tube was expanded to the pressure at which the expansion bladder failed, usually between []^{a,c,e}. These samples are described as “Segmented Expansion” types. A tube expansion schematic is shown on Figure 6-2.

Data were also available from a small group of the test samples that had been previously fabricated using a []^{a,c,e} tool which had been fabricated expressly for such tests. These samples were described as “Full Depth Expansion” types. The expansion method with regard to the segmented or full length aspect does not have a bearing on the test results.

6.2.2 Model F Leakage Resistance Tests

The testing reported herein was performed according to a test procedure which outlined two types of leak tests as follows:

- 1) Model F elevated temperature primary-to-secondary leak tests were performed using an [

[]^{a,c,e} These tests were performed following the room temperature primary-to-secondary side leak tests on the chosen samples. The test results showed a [

[]^{a,c,e}.

- 2) Model F room temperature primary-to-secondary side leak tests were performed on all test samples, [

] ^{a,c,e}. These tests

were performed following the elevated temperature primary-to-secondary side leak tests on the chosen samples.

6.2.2.1 Model F Leak Test Results

The leak tests on segmented expansion collars averaged [

] ^{a,c,e}. (As a point of reference, there are approximately 75,000 drops in one gallon.) Leakage data were also recorded at room temperature conditions to provide input for the low contact pressure portion of the flow loss coefficient-versus-contact pressure correlation.

6.2.3 Model D5 Tube Joint Leakage Resistance Program

A total of [

] ^{a,c,e}

The lower bound leakage resistance distribution for the collars with the nominal tubesheet hole diameter was used in the present leakage evaluation. This lower bound leakage resistance was made using data for the test conditions shown in the Table 6-2 below combined with the Model F leak test results discussed in Section 6.2.1.

6.2.3.1 Model D5 Test Specimen Configuration

The intent of the test samples was to model key features of the Model D5 tube-to-tubesheet joint for leakage tests. The following hardware was used:

- 1) A Model D5 tubesheet simulating collar matching the radial stiffness of a Model D5 tubesheet unit cell, utilizing an appropriate outside diameter of approximately [] ^{a,c,e} inches. The length of the test collars allowed the introduction of leakage in an unexpanded section of the tube. The surface finish and run-out tolerances of the tubesheet unit cell simulants were based on factory tolerances specified for the tubesheet drilling operation.

The collars were drilled to the nominal design value inside diameters. Collars were fabricated from [

$J^{a,c,e}$ which approximates that of the actual tubesheet material). It is of primary importance to approximate the flexural rigidity of the steel tubesheet, and because the [
 $J^{a,c,e}$.

- 2) Model D5 Tubing with an average yield strength for the SG Alloy 600 tubing in the Model D plants is [$J^{a,c,e}$. The Alloy 600 tubing used for these tests was from heats conforming to ASME SB163, Section III Class 1. It was obtained from a Quality Systems-controlled Storeroom

The intent of the leakage portion of the test program was to determine the leakage resistance of simulated Model D5 tube-to-tubesheet joints, disregarding the effect of the [
 $J^{a,c,e}$.

Tube-to-tubesheet stimulant samples of the Model D5 configuration were designed and fabricated. The steam generator factory tubing drawing specifies a [
 $J^{a,c,e}$.

The hydraulic expansion pressure range for the Model D5 steam generators was [
 $J^{a,c,e}$. This value conservatively bounds the lower expansion pressure limit used for the Model D5 steam generators. Refer to Figure 6-3 for the details of the configuration for the leak test. The test equipment consisted of a make-up tank (MUT), primary water autoclave (AC1) and a secondary autoclave (AC2) connected by insulated pressure tubing. Two specimens were installed into the secondary autoclave to minimize setup time and variability across test runs. AC1 was run with deoxygenated primary water containing specified amounts of boron, lithium and dissolved hydrogen. The primary chemistry conditions were controlled in the MUT and a pump and backpressure system allowed the primary water to re-circulate from the MUT to the AC1. The primary autoclave had the normal controls for heating, monitoring pressure and safety systems including rupture discs. Figure 6-4 shows the entire test system with key valves and pressure transducers identified. In addition to the normal controls for heating, monitoring pressure and maintaining safety, the secondary autoclave was outfitted water cooled condensers that converted any steam escaping from the specimens into room temperature water. The pressure in the secondary side (in the main body of AC2, was monitored by pressure transducers. For most tests, the leakage was collected in a graduated cylinder on a digital balance connected to a computer so that the amount of water could be recorded as a function of time. For some normal operating tests, the leakage was calculated based on changes in the secondary side pressure. All relevant autoclave temperatures and pressures were recorded with an automatic data acquisition system at regular time intervals.

6.2.3.2 Model D5 Test Sample Assembly

The assumption that pull-out resistance is distributed uniformly through the axial extent of the joint is an adequate technical approach. The pullout resistance is asymptotic to some large value, the form of the relation is one minus an exponential to a negative multiple of the length of

engagement. For short engagement lengths, say up to 5 to 8 inches, the linear approximation is sufficient. Extrapolations to higher pullout resistance for longer lengths could be non-conservative except for the fact that the pullout strength of the shorter lengths exceed the structural performance criteria.

6.2.4 Model D5 Leakage Resistance Tests

For the Model D5 testing, primary-to-secondary leak tests were performed on all test samples, using simulated primary water as a pressurizing medium. Refer to Figure 6-3 [

] ^{a,c,e}, to simulate a perforation of the tube wall due to corrosion cracking. All of the elevated temperature primary-to-secondary side leak tests were performed using an [^{a,c,e}] as the pressurizing/leakage medium. In the case of 800 psi back pressure tests, the leakage was collected in the autoclave as it issued from the tube-to-collar crevice. In the remainder of the autoclave tests, the leakage was collected in the autoclave as it issued from the tube-to-collar crevice but it was piped to a condenser/cooler and weighed on an instrumented scale.

6.2.4.1 Model D5 Leak Test Results

The leakage rates for the Model D5 600°F normal operating and accident pressure differential conditions were similar to the respective Model F values. Leakage ranged from [

] ^{a,c,e} Leakage data were also recorded at room temperature conditions to provide input for the low contact pressure portion of the flow loss coefficient-versus-contact pressure correlation.

6.3 Loss Coefficient on Contact Pressure Regression

In order to produce a plot of loss coefficient, K , versus contact pressure, P_c , that would be applicable for the analysis of the Model F SGs, loss coefficient values were calculated using the Darcy flow model discussed later in Section 9.2 and the Model F and D5 test data which was produced internally by Westinghouse and discussed in earlier elements of this section. Since the Model F and Model D5 steam generators have similar geometry along the crevice path, Model D5

loss coefficients can be used in the evaluation of Model F SGs if the data are adjusted to account for the change in resistance associated with tube size. The Model D5 SG tubes have an outer diameter of 0.750 inch while the Model F steam generator tubes have an outer diameter of 0.688 inch, and by its definition, the loss coefficient inherently includes the circumference of the annular leak path that is normal to the flow. Therefore, the Model D5 loss coefficients must be multiplied the ratio of the Model D5 to the Model F circumference in order to apply the Model D5 loss coefficients to the Model F SGs. By applying the scaling factor to the Model D5 loss coefficients, the results obtained are considered to be the loss coefficients that would have been obtained during the Model D5 testing if the Model D5 SGs had tubes with an outer diameter of 0.688 instead of 0.750 inch.

A logarithmic-linear (log-linear) regression and an uncertainty analysis were performed for the combined Model F and D5 SG data. Figure 6-6 provides a plot of the loss coefficient versus contact pressure with the linear regression trendline for the combined data represented as a thick, solid black line. The regression trendline is represented by the log-linear relation,

$$\ln(K) = b_0 + b_1 P_c \quad (6-1)$$

where b_0 = the $\ln(K)$ intercept of the log-linear regression trendline, and,
 b_1 = the slope of the log-linear regression trendline.

The values obtained for the intercept and slope coefficients were []^{a,c,e} for Model D5 computations respectively. The []^{a,c,e} A []

^{a,c,e} In conclusion, the log-linear fit to the combined Model F and Model D5 loss coefficient data follow a relation of the form,

$$K = e^{b_0 + b_1 P_c}, \quad (6-2)$$

where the Model D5 data were adjusted to correspond to the diameter of an installed Model F tube. The absolute leak rates *per se* are not used in the determination of B* and the confidence curve on the charts is provided for information only. Results of sensitivity studies using confidence limit values for the coefficients are discussed in Section 9.5. Since the B* value is based on the ratio of the SLB leak rate to the NOP leak rate it is not significantly sensitive to changes in the correlation slope or intercept.

Table 6-1. Model F Leak Test Program Matrix

a,c,e

Table 6-5. Model F Small Displacement Pullout Test Data

a,c,e

Table 6-6. Model F 0.25 Inch Displacement Data at 600°F

a,c,e

Table 6-7. Model D5 0.25 Inch Displacement Pullout Test Data

a,c,e

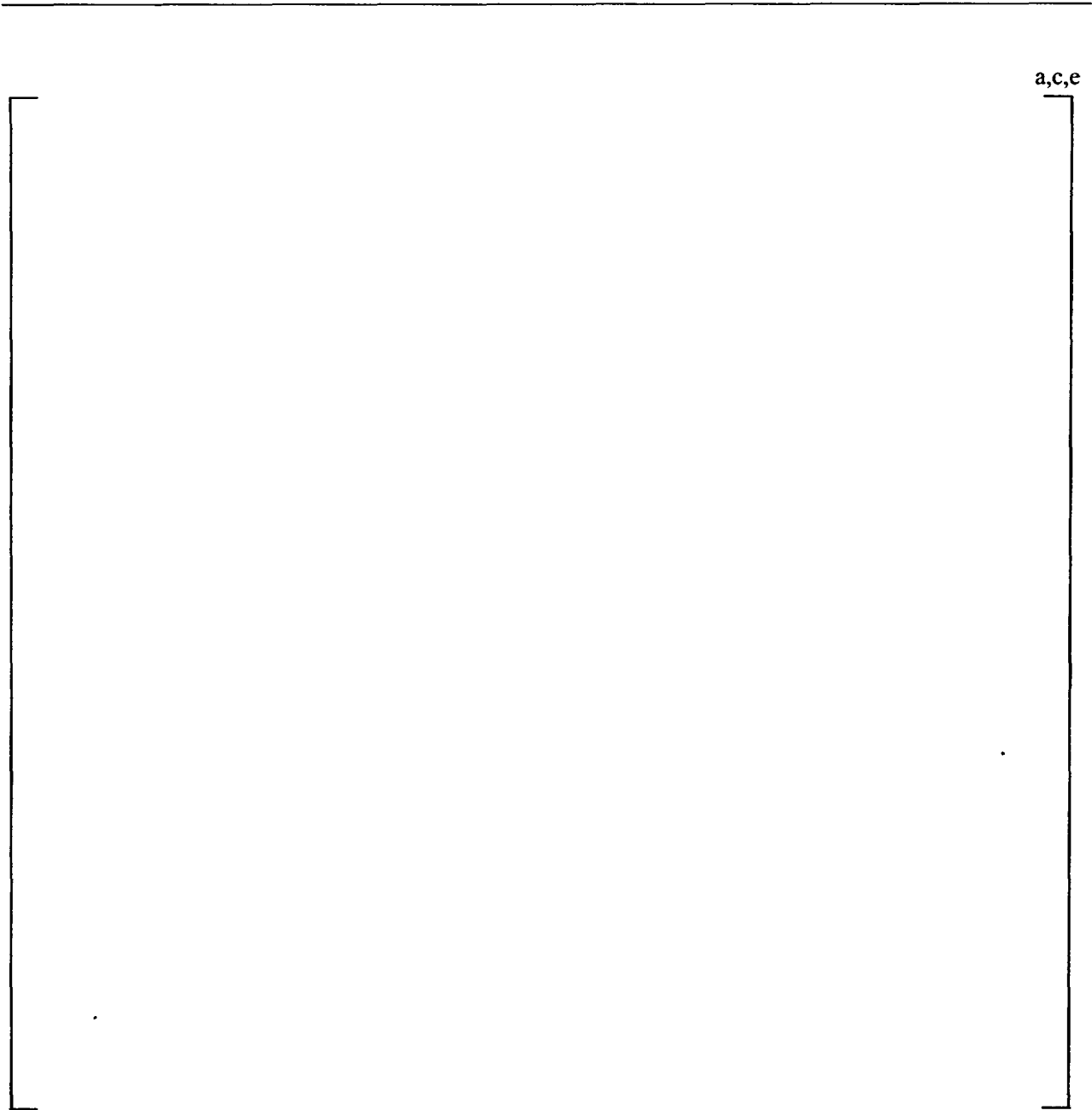


Figure 6-1. Example Leakage Test Schematic

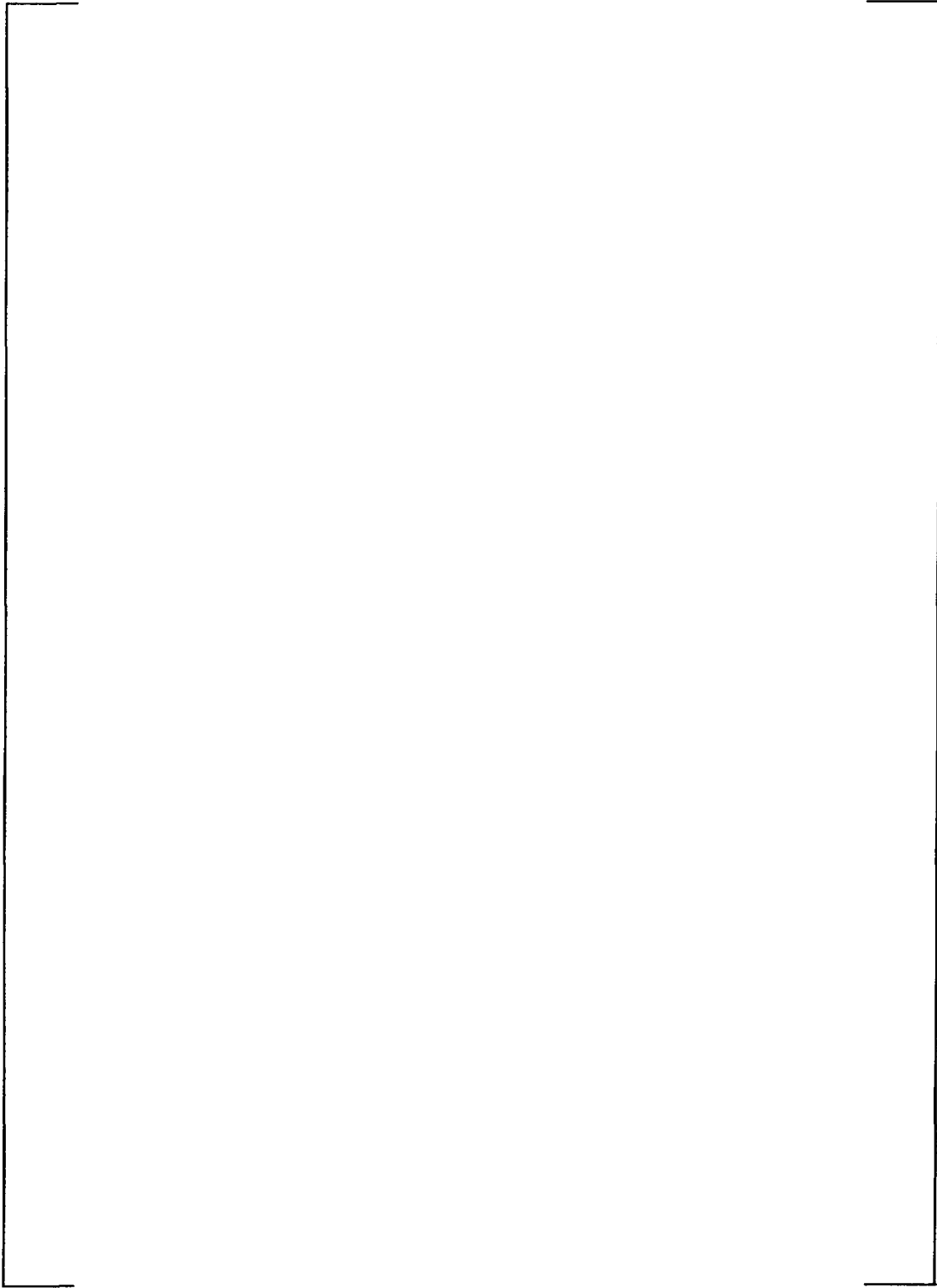


Figure 6-2. Example Tube Hydraulic Expansion Process Schematic

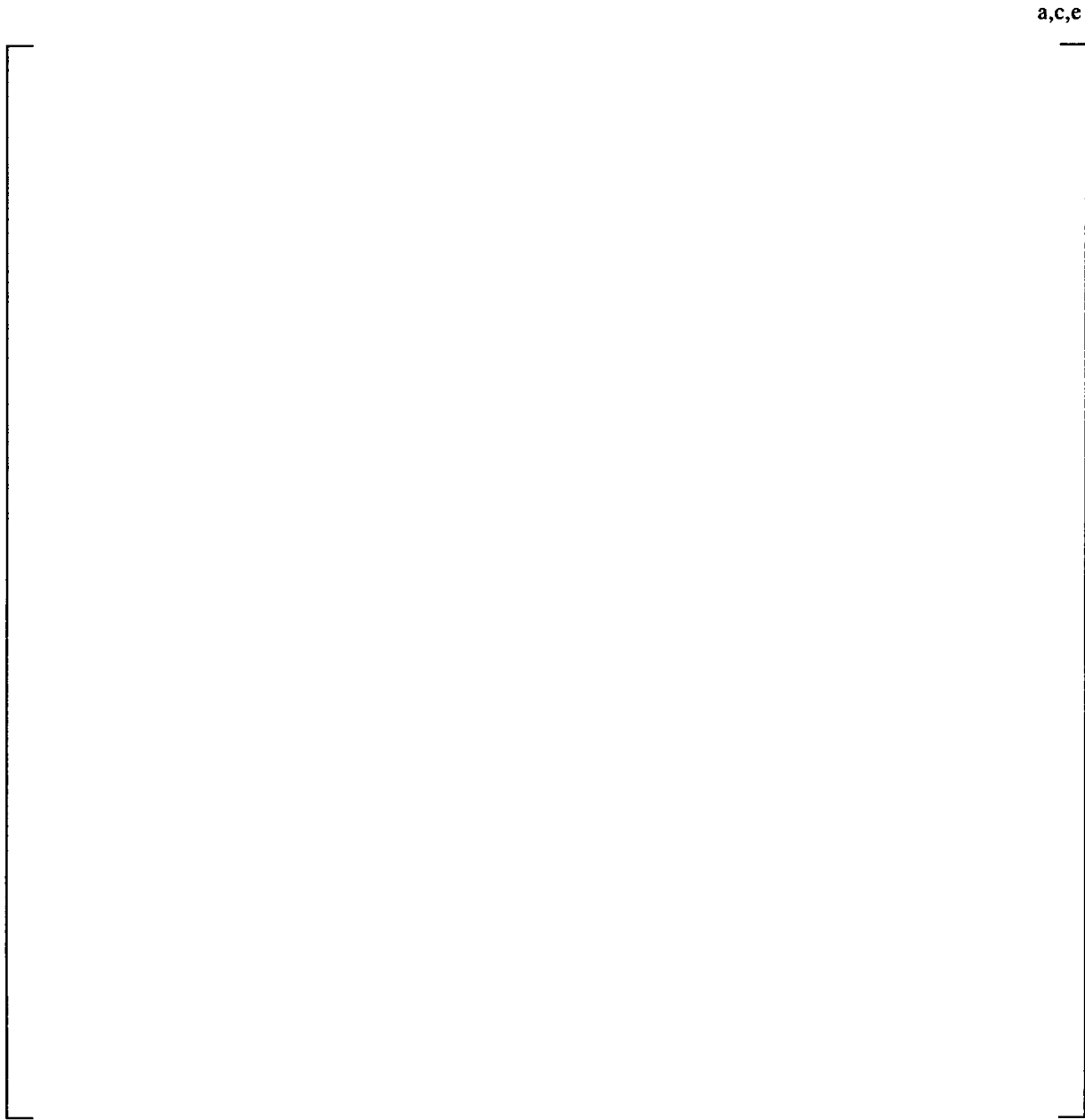


Figure 6-3. Example Tube Joint Leakage Test Configuration

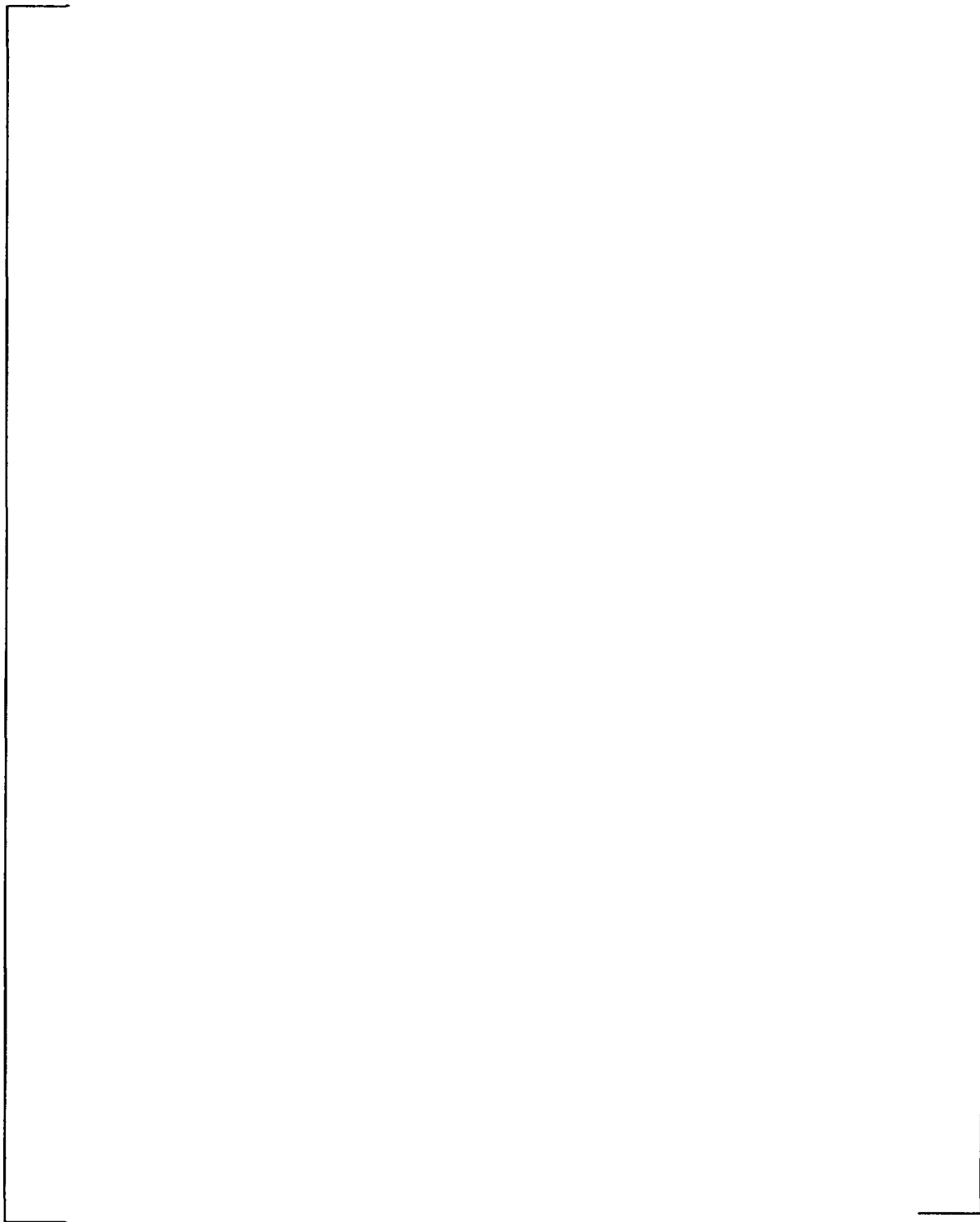


Figure 6-4. Schematic for the Test Autoclave Systems for Leak Rate Testing

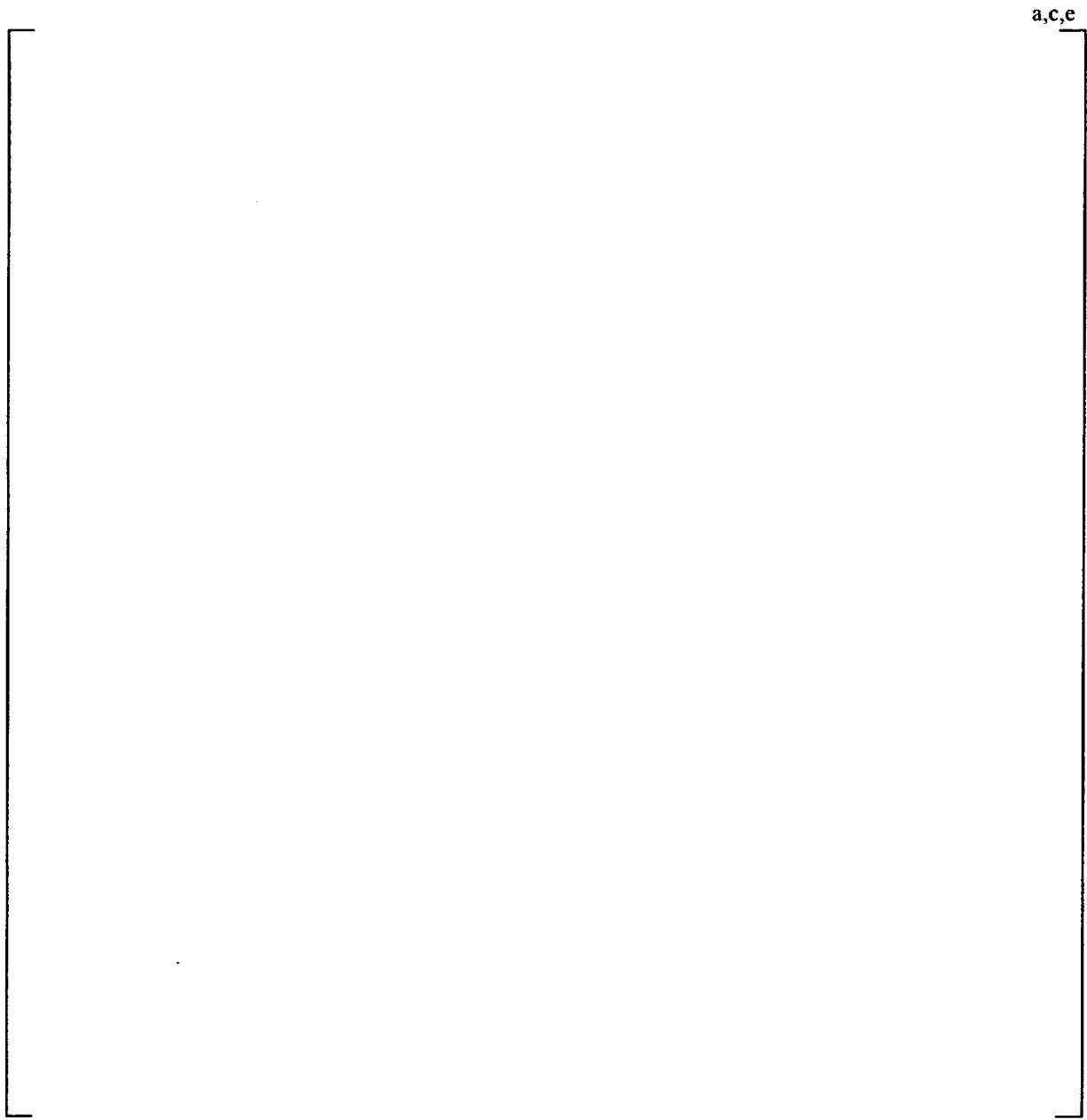


Figure 6-5. Example Tube Joint Sample Pullout Test Configuration



Figure 6-6. Loss Coefficient Values for Model F & D5 Leak Rate Analysis

7.0 Structural Analysis of Tube-to-Tubesheet Joint

This section summarizes the structural aspects and analysis of the entire tube-to-tubesheet joint region. The tube end weld was originally designed as a pressure boundary structural element in accordance with the requirements of Section III of the ASME (American Society of Mechanical Engineers) Boiler and Pressure Vessel Code, Reference 6. The construction code for the Catawba 2 SGs was the 1971 edition with the Winter 1972 and some paragraphs of the Winter 1974 addenda. This means that there were no strength considerations made with regard to the expansion joint between the tube and the tubesheet, including the tack expansion regardless of whether it was achieved by rolling or Poisson expansion of a urethane plug.

An extensive empirical and analytical evaluation of the structural capability of the as-installed tube-to-tubesheet joints based on considering the weld to be absent was performed specifically for the Catawba 2 Model D5 SGs and the results are reported below. Typical Model D5 hydraulic expansion joints with lengths comparable to those being proposed in what follows for limiting specialized probe examination were tested for pullout resistance strength at temperatures ranging from 70 to 600°F. The results of the tests coupled with those from finite element evaluations of the effects of temperature and primary-to-secondary pressure on the tube-to-tubesheet interface loads have been used to demonstrate that engagement lengths of approximately 3.45 to 8.61 inches (regardless of tube leg) were sufficient to equilibrate the axial loads resulting from consideration of 3 times the normal operating and 1.4 times the limiting accident condition pressure differences. The variation in required engagement length is a function of tube location, i.e., row and column, and decreases away from the center of the SG where the maximum value applies. The tubesheet bows, i.e., deforms, upward from the primary-to-secondary pressure difference and results in the tube holes becoming dilated above the neutral plane of the tubesheet, which is a little below the mid-plane because of the effect of the tensile membrane stress from the pressure loading. The amount of dilation is a maximum very near the radial center of the tubesheet (restricted by the divider plate) and diminishes with increasing radius outward. Moreover, the tube-to-tubesheet joint becomes tighter below the neutral axis and is a maximum at the bottom of the tubesheet⁵. In conclusion, the need for the weld is obviated by the interference fit between the tube and the tubesheet. Axial loads are not transmitted to the portion of the tube below the H* distance during operation or faulted conditions, by factors of safety of at least 3 and 1.4 respectively, including postulated loss of coolant accidents (LOCA), and inspection of the tube below the H* distance including the tube-to-tubesheet weld is not technically necessary. Also, if the expansion joint were not present, there would be no effect on the strength of the weld from axial cracks, and tubes with circumferential cracks up to about 180° by 100% deep would have sufficient strength to meet the nominal ASME Code structural requirements, based on the margins of safety reported in Reference 15.

An examination of Table 7-7 through Table 7-11 illustrates that the holding power of the tube-to-tubesheet joint in the vicinity of a depth of 11 inches is much greater than at the top of the

tubesheet in the range of H^* as listed in Table 7-12. Note that the radii reported in these tables were picked to conservatively represent the entire radial zones of consideration as defined on Figure 7-1. For example, Zone C has a maximum radius of 34.4 inches. However, in order to establish H^* values that were conservative throughout the zone, the tube location for which the analysis results were most severe above the neutral axis were reported, i.e., those values calculated for a tube at a radius of 4.08 inches. The values are everywhere conservative above the neutral surface of the tubesheet for tubes in Zone C. Likewise for tubes in Zone B under the heading 49.035 inches where the basis for the calculation was a tube at a radius of 34.4 inches. The purpose of this discussion is to illustrate the extreme conservatism associated with the holding power of the joint below the neutral surface of the tubesheet, and to identify the proper tube radii for consideration. In the center of the tubesheet the incremental holding strength in the 2.5 inch range from 8 to 10.5 inches below the top of the tubesheet is about 916 lbf per inch during normal operation. The performance criterion for $3 \cdot \Delta P$ is met by the first 2.2 inches of engagement above 11 inches. At a radius of 59 inches the corresponding length of engagement needed is about 1.9 inches. The corresponding values for steam line break conditions are 1.70 and 1.40 inches at radii of 4.08 and 58.8 inches respectively. In other words, while a HL value of 8.13 inches was determined for H^* from the top of the tubesheet, a length of 2.2 to 2.1 inches would be sufficient at the bottom of the inspection length, where the latter value corresponds to a radius of 34.4 inches from the center of the tubesheet, the maximum extent of Zone C.

7.1 Evaluation of Tubesheet Deflection Effects for Tube-to-Tubesheet Contact Pressure

A finite element model was developed for the Model D5 tubesheet, channel head, and shell region to determine the tubesheet hole dilations in the Catawba steam generators. [

] ^{a,c,e}

loads in the tube.

7.1.1 Material Properties and Tubesheet Equivalent Properties

The tubes in the Catawba 2 SGs were fabricated of A600TT material. Summaries of the applicable mechanical and thermal properties for the tube material are provided in Table 7-1. The tubesheets were fabricated from SA-508, Class 2a, material for which the properties are listed in Table 7-2. The shell material is SA-533 Grade A Class 2, and its properties are in Table 7-3. Finally, the channel head material is SA-216 Grade WCC, and its properties are in Table 7-4. The material properties are from Reference 29, and match the properties listed in the ASME Code.

⁵ There is a small reversal of the bending stress beyond a radius of about 55 inches because the support ring prevents rotation and the hole dilation is at the bottom of the tubesheet.

The perforated tubesheet in the Model D5 channel head assembly is treated as an equivalent solid plate in the global finite element analysis. An accurate model of the overall plate behavior was achieved by using the concept of an equivalent elastic material with anisotropic properties. For square tubesheet hole patterns, the equivalent material properties depend on the orientation of loading with respect to the symmetry axes of the pattern. An accurate approximation was developed [Reference 30], where energy principles were used to derive effective average isotropic elasticity matrix coefficients for the in-plane loading. The average isotropic stiffness formulation gives results that are consistent with those using the Minimum Potential Energy Theorem, and the elasticity problem thus becomes axisymmetric. The solution for strains is sufficiently accurate for design purposes, except in the case of very small ligament efficiencies, which are not of issue for the evaluation of the SG tubesheet.

The stress-strain relations for the axisymmetric perforated part of the tubesheet are given by:

$$\begin{bmatrix} \sigma_R^* \\ \sigma_\theta^* \\ \sigma_Z^* \\ \tau_{RZ}^* \end{bmatrix} = \begin{bmatrix} D_{11} & D_{12} & D_{13} & 0 \\ D_{21} & D_{22} & D_{23} & 0 \\ D_{31} & D_{32} & D_{33} & 0 \\ 0 & 0 & 0 & D_{44} \end{bmatrix} \begin{bmatrix} \epsilon_R^* \\ \epsilon_\theta^* \\ \epsilon_Z^* \\ \gamma_{RZ}^* \end{bmatrix}$$

with the elasticity coefficients are calculated as:

$$\begin{aligned} D_{11} = D_{22} &= \frac{\bar{E}_p^*}{f(1+\bar{\nu}_p^*)} \left[1 - \frac{\bar{E}_p^*}{E_Z^*} \nu^2 \right] + \frac{1}{2} \left[\bar{G}_p^* - \frac{\bar{E}_p^*}{2(1+\bar{\nu}_p^*)} \right] \\ D_{21} = D_{12} &= \frac{\bar{E}_p^*}{f(1+\bar{\nu}_p^*)} \left[\bar{\nu}_p^* + \frac{\bar{E}_p^*}{E_Z^*} \nu^2 \right] - \frac{1}{2} \left[\bar{G}_p^* - \frac{\bar{E}_p^*}{2(1+\bar{\nu}_p^*)} \right] \\ D_{13} = D_{23} = D_{31} = D_{32} &= \frac{\bar{E}_p^* \nu}{f} \\ D_{33} &= \frac{E_Z^*(1-\bar{\nu}_p^*)}{f} \text{ and } D_{44} = \bar{G}_z^* \\ \text{where } f &= 1 - \bar{\nu}_p^* - 2 \frac{\bar{E}_p^*}{E_Z^*} \nu^2 \text{ and } \bar{G}_p^* = \frac{\bar{E}_d^*}{2(1+\bar{\nu}_d^*)}. \end{aligned}$$

Here,

- \bar{E}_p^* = Effective elastic modulus for in-plane loading in the pitch direction,
- E_Z^* = Effective elastic modulus for loading in the thickness direction,
- $\bar{\nu}_p^*$ = Effective Poisson's ratio for in-plane loading in the pitch direction,
- \bar{G}_p^* = Effective shear modulus for in-plane loading in the pitch direction,
- \bar{G}_z^* = Effective modulus for transverse shear loading,
- \bar{E}_d^* = Effective elastic modulus for in-plane loading in the diagonal direction,
- $\bar{\nu}_d^*$ = Effective Poisson's ratio for in-plane loading in the diagonal direction, and,
- ν = Poisson's ratio for the solid material.

The tubesheet is a thick plate and the application of the pressure load results in a generalized plane strain condition. The pitch of the square, perforated hole pattern is 1.0625 inches and nominal hole diameters are 0.764 inch. The ID of the tube after expansion into the tubesheet is taken to be 0.67886 inch based on an assumption of 1% thinning during installation. Equivalent properties of the tubesheet are calculated without taking credit for the stiffening effect of the tubes.

$$\text{Ligament Efficiency, } \eta = \frac{h_{\text{nominal}}}{P_{\text{nominal}}}$$

where: $h_{\text{nominal}} = P_{\text{nominal}} - d_{\text{maximum}}$
 $P_{\text{nominal}} = 1.0625$ inches, the pitch of the square hole pattern
 $d_{\text{maximum}} = .764$ inches, the tube hole diameter

Therefore, $h_{\text{nominal}} = 0.2985$ inches (1.0625-0.764), and $\eta = 0.2809$ when the tubes are not included. From Slot, Reference 31, the in-plane mechanical properties for Poisson's ratio of 0.3 are:

Property	Value
\bar{E}_p^* / E	= 0.3992
$\bar{\nu}_p^*$	= 0.1636
\bar{G}_p^* / G	= 0.1674
E_z^* / E	= 0.5935
G_z^* / G	= 0.4189

where the subscripts p and d refer to the pitch and diagonal directions, respectively. These values are substituted into the expressions for the anisotropic elasticity coefficients given previously. In the global model, the X-axis corresponds to the radial direction, the Y-axis to the vertical or tubesheet thickness direction, and the Z-axis to the hoop direction. The directions assumed in the derivation of the elasticity coefficients were X- and Y-axes in the plane of the tubesheet and the Z-axis through the thickness. In addition, the order of the stress components in the WECAN/Plus (Reference 32) elements used for the global model is σ_{xx} , σ_{yy} , τ_{xy} , and σ_{zz} . The mapping between the Reference 30 equations and WECAN/+ is therefore:

Coordinate Mapping	
Reference 30	WECAN/+
1	1
2	4
3	2
4	3

Table 7-2 gives the modulus of elasticity, E, of the tubesheet material at various temperatures. Using the equivalent property ratios calculated above in the equations presented at the beginning of this section gives the elasticity coefficients for the equivalent solid plate in the perforated region of the tubesheet. These are listed in Table 7-5 for the tubesheet, without accounting for the effect of the tubes. The values for 600°F were used for the finite element unit load runs. The material properties of the tubes are not utilized in the finite element model, but are listed in Table 7-1 for use in the calculations of the tube/tubesheet contact pressures.

7.1.2 Finite Element Model

The analysis of the contact pressures utilizes conventional (thick shell equations) and finite element analysis techniques. A finite element model was developed for the Model D5 SG channel head/ tubesheet/ shell region (which includes the Catawba steam generator) in order to determine the tubesheet rotations. The elements used for the models of the channel head/ tubesheet/ shell region were the quadratic version of the 2-D axisymmetric isoparametric elements STIF53 and STIF56 of WECAN-Plus (Reference 32). The model for the D5 steam generator is shown on Figure 7-2.

The unit loads applied to this model are listed below:

Unit Load	Magnitude
Primary Side Pressure	1000 psi
Secondary Side Pressure	1000 psi
Tubesheet Thermal Expansion	500°F
Shell Thermal Expansion	500°F
Channel Head Thermal Expansion	500°F

The three temperature loadings consist of applying a uniform thermal expansion to each of the three component members, one at a time, while the other two remain at ambient conditions. The boundary conditions imposed for all five cases are: UX=0 at all nodes on the centerline, and UY=0 at one node on the lower surface of the tubesheet support ring. In addition, an end cap load is applied to the top of the secondary side shell for the secondary side pressure unit load equal to:

$$P_{endcap} = - \left[\frac{R_i^2}{R_o^2 - R_i^2} \right] P = -9708.43 \text{ psi}$$

where, R_i = Inside radius of secondary shell in finite element model = 64.69 in.
 R_o = Outside radius of secondary shell in finite element model = 67.94 in.
 P = Secondary pressure unit load = 1000 psi.

This yielded displacements throughout the tubesheet for the unit loads.

		a.c.e

The data were fit to the following polynomial equation:

$$[\quad]^{a.c.e}$$

The hole expansion calculation as determined from the finite element results includes the effects of tubesheet rotations and deformations caused by the system pressures and temperatures. It does not include the local effects produced by the interactions between the tube and tubesheet hole. Standard thick shell equations, including accountability for the end cap axial loads in the tube (Reference 33), in combination with the hole expansions from above are used to calculate the contact pressures between the tube and the tubesheet.

The unrestrained radial expansion of the tube OD due to thermal expansion is calculated as:

$$\Delta R_i^{th} = c \alpha_t (T_i - 70)$$

and from pressure acting on the inside and outside of the tube as,

$$\Delta R_{to}^{pr} = \frac{P_i c}{E_t} \left[\frac{(2 - \nu) b^2}{c^2 - b^2} \right] - \frac{P_o c}{E_t} \left[\frac{(1 - 2\nu) c^2 + (1 + \nu) b^2}{c^2 - b^2} \right],$$

- where:
- P_i = Internal primary side pressure, P_{pri} psi
 - P_o = External secondary side pressure, P_{sec} psi
 - b = Inside radius of tube = 0.33943 in.
 - c = Outside radius of tube = 0.382 in.
 - α_t = Coefficient of thermal expansion of tube, in/in/°F
 - E_t = Modulus of Elasticity of tube, psi
 - T_i = Temperature of tube, °F, and,
 - ν = Poisson's Ratio of the material.

The thermal expansion of the hole ID is included in the finite element results and does not have to be expressly considered in the algebra, however, the expansion of the hole ID produced by pressure is given by:

$$\Delta R_{TS}^{pr} = \frac{P_i c}{E_{TS}} \left[\frac{d^2 + c^2}{d^2 - c^2} + \nu \right],$$

where: E_{TS} = Modulus of Elasticity of tubesheet, psi
 d = Outside radius of cylinder which provides the same radial stiffness as the tubesheet, that is, []^{a,c,e}.

If the unrestrained expansion of the tube OD is greater than the expansion of the tubesheet hole, then the tube and the tubesheet are in contact. The inward radial displacement of the outside surface of the tube produced by the contact pressure is given by: (Note: The use of the term δ in this section is unrelated its potential use elsewhere in this report.)

$$\delta_t = \frac{P_2 c}{E_t} \left[\frac{c^2 + b^2}{c^2 - b^2} - \nu \right]$$

The radial displacement of the inside surface of the tubesheet hole produced by the contact pressure between the tube and hole is given by:

$$\delta_{TS} = \frac{P_2 c}{E_{TS}} \left[\frac{d^2 + c^2}{d^2 - c^2} + \nu \right]$$

The equation for the contact pressure P_2 is obtained from:

$$\delta_t + \delta_{TS} = \Delta R_{to} - \Delta R_{TS} - \Delta R_{ROT}$$

where ΔR_{ROT} is the hole expansion produced by tubesheet rotations obtained from finite element results. The ΔR 's are:

$$\Delta R_{to} = c\alpha_1(T_i - 70) + \frac{P_{pri}c}{E_t} \left[\frac{(2 - \nu)b^2}{c^2 - b^2} \right] - \frac{P_{sec}c}{E_t} \left[\frac{(1 - 2\nu)c^2 + (1 + \nu)b^2}{c^2 - b^2} \right]$$

$$\Delta R_{TS} = \frac{P_{sec}c}{E_{TS}} \left[\frac{d^2 + c^2}{d^2 - c^2} + \nu \right]$$

The resulting equation is:

$$\left[\right]^{a,c,e}$$

For a given set of primary and secondary side pressures and temperatures, the above equation is solved for selected elevations in the tubesheet to obtain the contact pressures between the tube and tubesheet as a function of radius. The elevations selected ranged from the top to the bottom of the tubesheet. Negative "contact pressure" indicates a gap condition.

The OD of the tubesheet cylinder is equal to that of the cylindrical (simulate) collars (1.80 inches) designed to provide the same radial stiffness as the tubesheet, which was determined from a finite element analysis of a section of the tubesheet (References 34 and 25).

The tube inside and outside radii within the tubesheet are obtained by assuming a nominal diameter for the hole in the tubesheet (0.764 inch) and wall thinning in the tube equal to the average of that measured during hydraulic expansion tests. That thickness is 0.04257 inch for the tube. The following table lists the values used in the equations above, with the material properties evaluated at 600°F. (Note that the properties in the following sections are evaluated at the primary fluid temperature).

Thick Cylinder Equations Parameter	Value
b , inside tube radius, in.	0.33943
c , outside tube radius, in.	0.382
d , outside radius of cylinder w/ same radial stiffness as TS, in.	[] ^{a,c,e}
α_t , coefficient of thermal expansion of tube, in/in °F	$7.83 \cdot 10^{-6}$
E_t , modulus of elasticity of tube, psi	$28.7 \cdot 10^6$
α_{TS} , coefficient of thermal expansion of tubesheet, in/in °F	$7.42 \cdot 10^{-6}$
E_{TS} , modulus of elasticity of tubesheet, psi	$26.4 \cdot 10^6$

7.1.4 Catawba 2 Contact Pressures

7.1.4.1 Normal Operating Conditions

The loadings considered in the analysis are based on an umbrella set of conditions as defined in References 30, 31 and 35. The current operating parameters from Reference 24 are used. The temperatures and pressures for normal operating conditions at Catawba Unit 2 are bracketed by the following two cases:

Loading	$T_{min}^{(1)}$	$T_{max}^{(2)}$
Primary Pressure	2235 psig	2235 psig
Secondary Pressure	800 psig	771 psig
Primary Fluid Temperature (T_{hot})	603.4°F	603.4°F
Secondary Fluid Temperature	520.3°F	516.2°F
⁽¹⁾ T_{ave} Coast down with 0% Tube Plugging case in Reference 24.		
⁽²⁾ T_{ave} Coast down with 10% Tube Plugging case in Reference 24.		

The primary pressure [

] ^{a,c,e}.

7.1.4.2 Faulted Conditions

Of the faulted conditions, Feedline Break (FLB) and Steamline Break (SLB) are the most limiting. FLB has a higher ΔP across the tubesheet, while the lower temperature of SLB results in less thermal tightening. Both cases are considered in this section.

Previous analyses have shown that FLB and SLB are the limiting faulted conditions, with tube lengths required to resist push out during a postulated loss of coolant accident (LOCA) typically less than one-fourth of the tube lengths required to resist pull out during FLB and SLB (References 33, 34 and 36). Therefore LOCA was not considered in this analysis.

7.1.4.3 Feedline Break

The temperatures and pressures for Feedline Break at Catawba Unit 2 are bracketed by the following two cases:

Loading	$T_{ave}^{(1)}$	$T_{ave}^{(2)}$
Primary Pressure	2835 psig	2835 psig
Secondary Pressure	0 psig	0 psig
Primary Fluid Temperature (T_{hot})	603.4°F	603.4°F
Secondary Fluid Temperature	520.3°F	516.2°F
⁽¹⁾ T_{ave} Coast down with 0% Tube Plugging case in Reference 24.		
⁽²⁾ T_{ave} Coast down with 10% Tube Plugging case in Reference 24.		

The Feedline Break condition [

] ^{a,c,e}.

7.1.4.4 Steam Line Break

As a result of SLB, the faulted SG will rapidly blow down to atmospheric pressure, resulting in a large ΔP across the tubes and tubesheet. The entire flow capacity of the auxiliary feedwater system

would be delivered to the dry, hot shell side of the faulted SG. The primary side re-pressurizes to the pressurizer safety valve set pressure. The hot leg temperature decreases throughout the transient, reaching a minimum temperature of 297°F at 2000 seconds for four loop plants. The pertinent parameters are listed below. The combination of parameters yielding the most limiting results is used.

Primary Pressure	=	2560 psig
Secondary Pressure	=	0 psig
Primary Fluid Temperature (T_{hot})	=	297°F
Secondary Fluid Temperature	=	212°F

For this set of primary and secondary side pressures and temperatures, the equations derived in Section 7.2 below are solved for the selected elevations in the tubesheet to obtain the contact pressures between the tube and tubesheet as a function of tubesheet radius for the hot leg.

7.1.4.5 Summary of FEA Results for Tube-to-Tubesheet Contact Pressures

For Catawba 2, the contact pressures between the tube and tubesheet for various plant conditions are listed in Table 7-6 and plotted versus radius on Figure 7-3 through Figure 7-7. The application of these values to the determination of the required engagement length is discussed in Section 7.2.

7.2 Determination of Required Engagement Length of the Tube in the Tubesheet

The elimination of a portion of the tube within the tubesheet from the in-service inspection requirement constitutes a change in the pressure boundary. This is the case regardless of whether or not the inspection is being eliminated in its entirety or if specialized probe examination is being eliminated when the potential for the existence of circumferential cracks is determined to be necessary for consideration. The elimination of the lower portion of the tube from examination is an H* partial-length specialized probe justification in the sense of Reference 5 and relies on knowledge of the tube-to-tubesheet interfacial, mechanical interference fit contact pressure at all elevations in the tube joint. In order to maintain consistency with other reports on this subject, the required length of engagement of the tube in the tubesheet to resist performance criteria tube end cap loads is designated by the variable H*. This length is based on structural requirements only and does not include any connotation associated with leak rate, except perhaps in a supporting role with regard to the leak rate expectations relative to normal operating conditions. Since the H* length is usually some distance from the top of the tubesheet, this is especially in the upper half of the tube joint. The contact pressure is used for estimating the magnitude of the anchorage of the tube in the tubesheet over the H* length. It is also used in estimating the impact of changes in the contact pressure on potential primary-to-secondary leak rate during postulated accident conditions.

To take advantage of the tube-to-tubesheet joint anchorage, it is necessary to demonstrate that the [

] ^{a,c,e} The residual contact pressure from the

tube installation was evaluated semi-empirically. It was determined by test for the as-fabricated condition and then analytically projected to the pertinent plant conditions. The tests involved pullout testing of tube-in-tubesheet specimens using thick collars to simulate the tubesheet as described in Section 6.1.1 for the Model F tubes.

The end cap loads for Normal and Faulted conditions are:

$$\begin{aligned}\text{Normal (maximum):} & \pi \cdot (2235-796) \cdot (0.764)^2 / 4 = 671.15 \text{ lbs.} \\ \text{Faulted (FLB):} & \pi \cdot 2835 \cdot (0.764)^2 / 4 = 1299.66 \text{ lbs.} \\ \text{Faulted (SLB):} & \pi \cdot 2560 \cdot (0.764)^2 / 4 = 1173.59 \text{ lbs.}\end{aligned}$$

Seismic loads have also been considered, but they are not significant in the tube joint region of the tubes.

A key element in estimating the strength of the tube-to-tubesheet joint during operation or postulated accident conditions is the residual strength of the joint stemming from the expansion preload due to the manufacturing process, i.e., hydraulic expansion. During operation the preload increases because the thermal expansion of the tube is greater than that of the tubesheet and because a portion of the internal pressure in the tube is transmitted to the interface between the tube and the tubesheet. However, the tubesheet bows upward leading to a dilation of the tubesheet holes at the top of the tubesheet and a contraction at the bottom of the tubesheet when the primary-to-secondary pressure difference is positive. The dilation of the holes acts to reduce the contact pressure between the tubes and the tubesheet. The H^* lengths are based on the pullout resistance associated with the net contact pressure during normal or accident conditions. The calculation of the residual strength involves a conservative approximation that the strength is uniformly distributed along the entire length of the tube. This leads to a lower bound estimate of the strength and relegates the contribution of the preload to having a second order effect on the determination of H^* .

A series of tests were performed to determine the residual strength of the joint. The data from this series of pullout tests are listed in Table 6-7. Three (3) each of the tests were performed at room temperature, 400°F, and 600°F. (Note: Three other tests were performed with internal pressure in the tube. However, in these tests, the resistance to pullout was so great that the tube yielded, furnishing only input information of joint lower bound strength. These data were not used.) [

] ^{a,c,e}.

calculated values do include the axial resistance from the residual installation pressure. The above equation is also used to find the minimum contact lengths needed to meet the pullout force requirements. In Zone C, the length calculated was 7.03 inches for the 3 times the normal operating pressure performance criterion which corresponds to a pullout force of 1979 lbf in the Hot Leg.

The top part of Table 7-9 lists the contact pressures through the thickness at each of the radial sections for Faulted (SLB) condition. The last row, " $h(0)$," of this part of the table lists the maximum tubesheet elevation at which the contact pressure is greater than or equal to zero. The above equation is used to accumulate the force resisting pull out from the top of the tubesheet to each of the elevations listed in the lower part of Table 7-9. In Zone C, the respective length for the hot and cold legs is 8.1 and 8.6 inches for the 1.4 times the accident pressure performance criterion which corresponds to a pullout force of 1643 lbs in the Hot Leg for the SLB condition. The minimum contact length needed to meet the pullout force requirement of 1819 lb. for the FLB (feed line break) condition is less as is shown in Table 7-10 and Table 7-11. The H^* calculations for each loading condition at each of the radii considered are summarized in Table 7-12. The H^* results for each zone are summarized in Table 7-13.

Therefore, the bounding condition for the determination of the H^* length is the SLB performance criterion. The minimum contact length for the SLB faulted condition is 8.13 or 8.61 inches in Zone C depending on tube leg. It is noted that the HL value reported in Reference 25 for example is slightly higher owing to the use of a margin factor of 1.43 instead of the currently allowable value of 1.4.

In Zone B, The SLB performance criterion is controlling and the minimum contact length is 5.39 and 6.25 inches respectively for the hot and cold legs. In Zone A, however, the normal operating condition is controlling and the corresponding minimum contact lengths are calculated to be 2.33 and 3.45 inches.

The conditions on the cold leg lead to conclusions similar to those for the hot leg of the SG. There are competing effects that influence the determination of the required engagement length. During normal operation:

- (1) The tube and tubesheet temperature are less which leads to a reduction in the thermal expansion contribution to the total contact pressure.
- (2) The internal pressure in the tube is also less, leading to a reduction its contribution to the total contact pressure.
- (3) This latter effect also leads to a reduction in the differential pressure induced end-cap load acting to pull and push a postulated severed tube out of the tubesheet.
- (4) Finally, the magnitude of the bowing deformation of the tubesheet is reduced, meaning that the reduction of the contact pressure associated with tubesheet deflection is also diminished.

The net effect is an increase in the calculated value of H^* during normal operation of about 1.1 inches at the maximum location, and an increase of about 0.5 inch near the periphery. The values obtained near the center of the TS are determined by NOp conditions and the values outboard of about 34 inches are determined by the SLB conditions.

Table 7-1. Summary of Material Properties Alloy 600 Tube Material							
Property	Temperature (°F)						
	70	200	300	400	500	600	700
Young's Modulus (psi·10 ⁶)	31.00	30.20	29.90	29.50	29.00	28.70	28.20
Thermal Expansion (in/in/°F·10 ⁻⁶)	6.90	7.20	7.40	7.57	7.70	7.82	7.94
Density (lb-sec ² /in ⁴ ·10 ⁻⁴)	7.94	7.92	7.90	7.89	7.87	7.85	7.83
Thermal Conductivity (Btu/sec-in-°F·10 ⁻⁴)	2.01	2.11	2.22	2.34	2.45	2.57	2.68
Specific Heat (Btu-in/lb-sec ² -°F)	41.2	42.6	43.9	44.9	45.6	47.0	47.9

Table 7-2. Summary of Material Properties for SA-508 Class 2a Tubesheet Material							
Property	Temperature (°F)						
	70	200	300	400	500	600	700
Young's Modulus (psi·10 ⁶)	29.20	28.50	28.00	27.40	27.00	26.40	25.30
Thermal Expansion (in/in/°F·10 ⁻⁶)	6.50	6.67	6.87	7.07	7.25	7.42	7.59
Density (lb-sec ² /in ⁴ ·10 ⁻⁴)	7.32	7.30	7.29	7.27	7.26	7.24	7.22
Thermal Conductivity (Btu/sec-in-°F·10 ⁻⁴)	5.49	5.56	5.53	5.46	5.35	5.19	5.02
Specific Heat (Btu-in/lb-sec ² -°F)	41.9	44.5	46.8	48.8	50.8	52.8	55.1

Table 7-3. Summary of Material Properties SA-533 Grade A Class 2 Shell Material							
Property	Temperature (°F)						
	70	200	300	400	500	600	700
Young's Modulus (psi·10 ⁶)	29.20	28.50	28.00	27.40	27.00	26.40	25.30
Thermal Expansion (in/in/°F·10 ⁻⁶)	7.06	7.25	7.43	7.58	7.70	7.83	7.94
Density (lb-sec ² /in ⁴ ·10 ⁻⁴)	7.32	7.30	7.283	7.265	7.248	7.23	7.211

Table 7-12. Summary of H* Calculations for Catawba Unit 2

a,c,e

Table 7-13. H* Summary Table

Zone	Limiting Loading Condition	Engagement from TTS (inches)
A	3.0 NO ΔP ^(1,2)	HL 2.33 ⁽³⁾ CL 3.45
B	1.4 SLB ΔP ^(1,2)	HL 5.39 CL 6.25
C	1.4 SLB ΔP ^(1,2)	HL 8.13 CL 8.61

Notes:

1. Seismic loads have been considered and are not significant in the tube joint region (Reference 38).
2. The scenario of tubes locked at support plates is not considered to be a credible event in Model D5 SGs as they are manufactured with stainless steel support plates. However, conservatively assuming that the tubes become locked at 100% power conditions, the maximum force induced in an active tube as the SG cools to room temperature is []^{a,c,e}
3. 0.3 inches added to the maximum calculated H* for Zone A to account for the hydraulic expansion transition region at the top of the tubesheet.

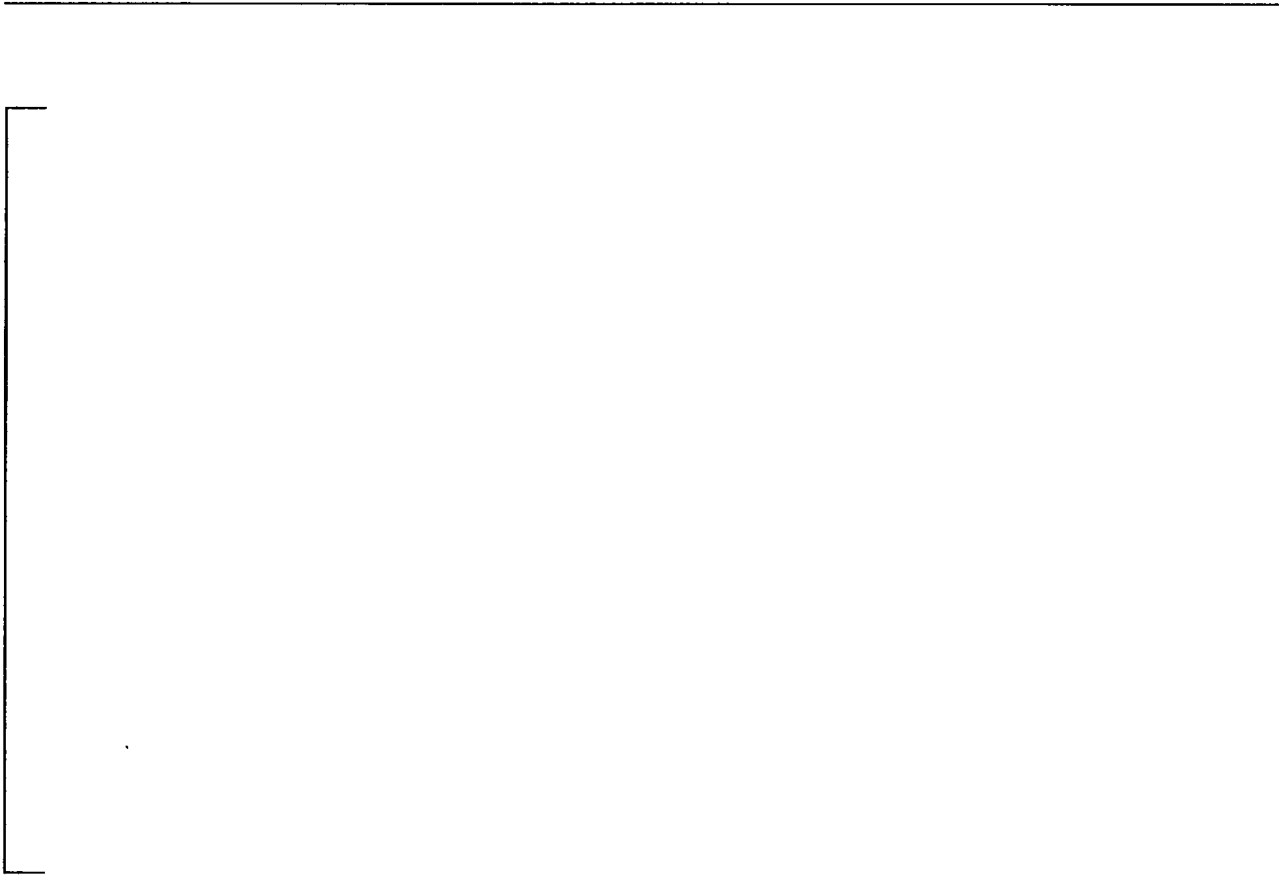


Figure 7-1. Definition of H* Zones

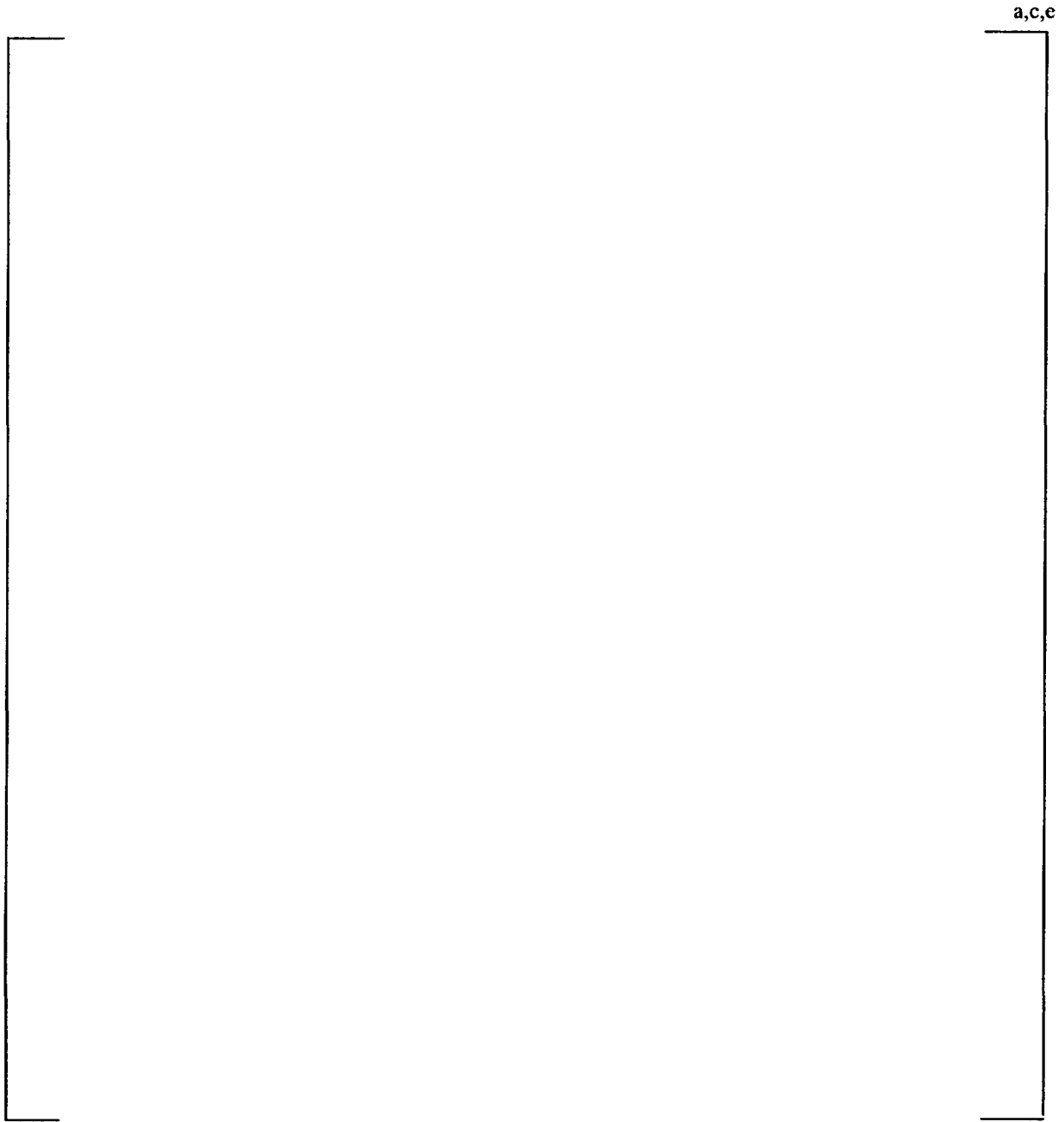


Figure 7-2. Finite Element Model of Model D5-3 Tubesheet Region

a,c,e



Figure 7-3. Contact Pressures for Normal Condition (10% SGTP) at Catawba 2

a.c.e



Figure 7-4. Contact Pressures for Normal Condition (0% SGTP) at Catawba Unit 2

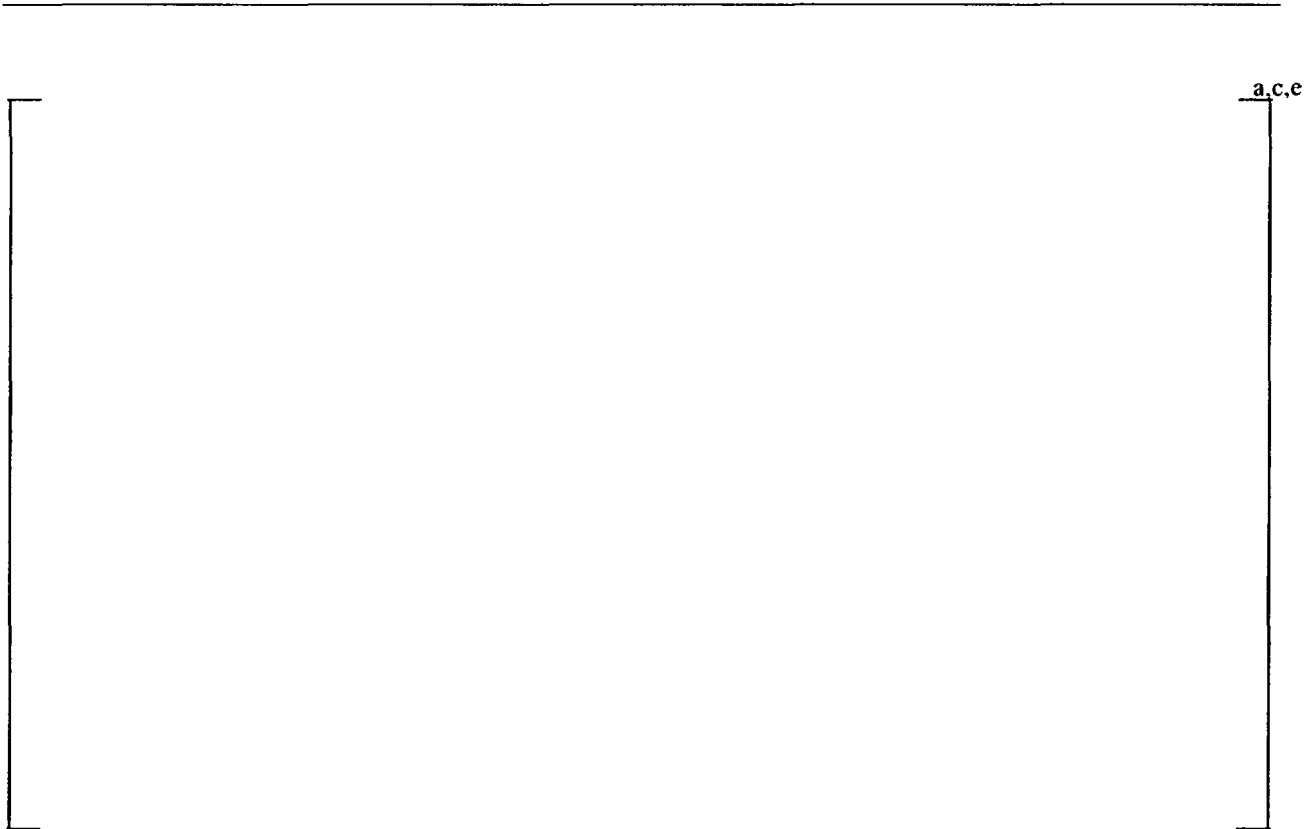


Figure 7-5. Contact Pressures for SLB Faulted Condition at Catawba 2



Figure 7-6. Contact Pressures for FLB Condition at Catawba 2 T_{ave} Coastdown 0% Plugging

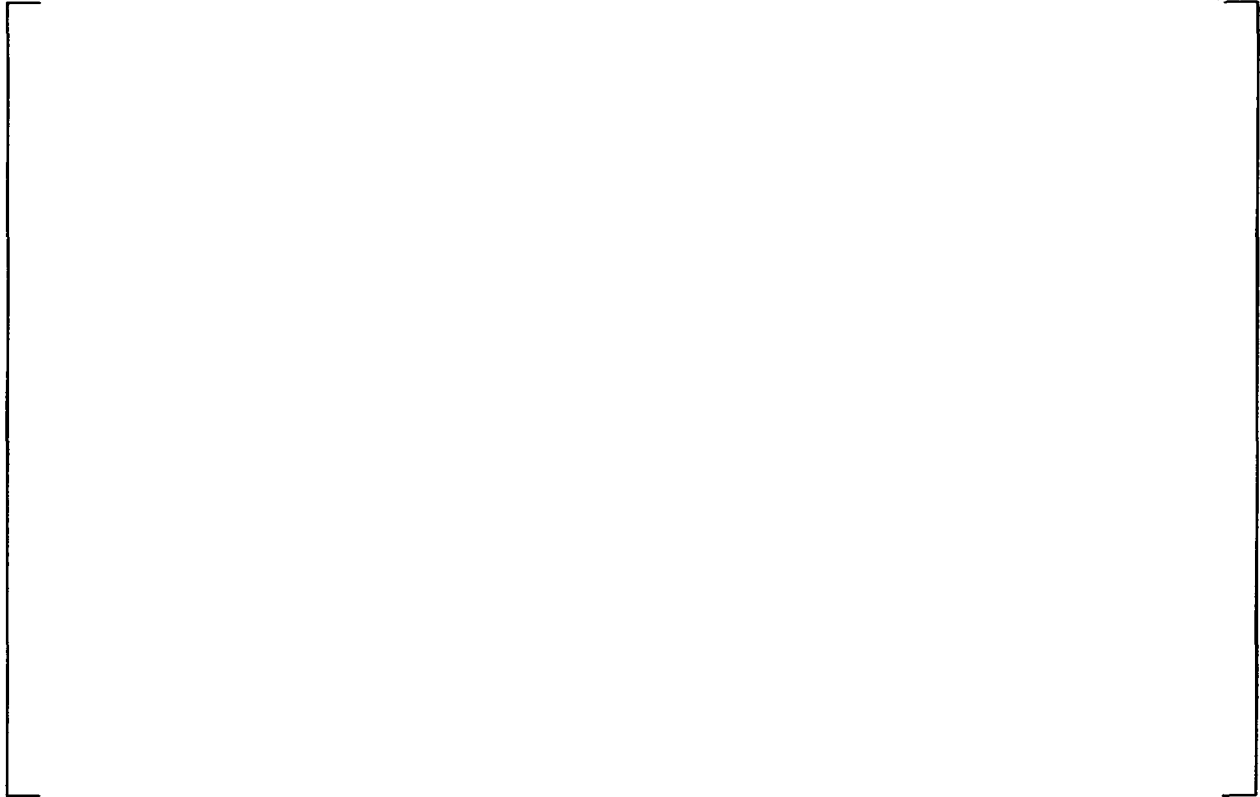


Figure 7-7. Contact Pressures for FLB Condition at Catawba 2 T_{ave} Coastdown 10% Plugging

8.0 Leak Rate Analysis of Cracked Tube-to-Tubesheet Joints

This section of the report presents a discussion of the leak rate expectations from axial and circumferential cracking confined to the tube-to-tubesheet joint region, including the tack expansion region, the tube-to-tubesheet welds and areas where degradation could potentially occur due to bulges and overexpansions within the tube at a distance at or below 10 inches from the top of the tubesheet. Although the welds are not part of the tube per the technical specifications, consideration is given in deference to the discussions of the NRC staff in References 2 and 8. It is noted that the methods discussed below support a permanent change to the Catawba 2 Technical Specification. With regard to the inherent conservatism embodied in the application of any predictive methods it is noted that the presence of cracking was not confirmed because removal of a tube section was not performed at Catawba 2 or Vogtle 1.

8.1 The Bellwether Principle for Normal Operation to Steam Line Break Leak Rates

From an engineering expectation standpoint, if there is no meaningful primary-to-secondary leakage during normal operation, there should likewise be no meaningful leakage during postulated accident conditions from indications located approximately below the mid-plane of the tubesheet. The rationale for this is based on consideration of the deflection of the tubesheet with attendant dilation and diminution (expansion and contraction) of the tubesheet holes. In effect, the leakage flow area depends on the contact pressure between the tube and tubesheet and would be expected to decrease during postulated accident conditions below some distance from the top of the tubesheet. The primary-to-secondary pressure difference during normal operation is on the order of 1200 to 1500 psi, while that during a postulated accident, e.g., steam line and feed line break, is on the order of 2560 to 2650 psi.⁶ Above the neutral plane of the tubesheet the tube holes tend to experience a dilation due to pressure induced bow of the tubesheet. This means that the contact pressure between the tubes and the tubesheet would diminish above the neutral plane in the central region of the tubesheet at the same time as the driving potential would increase. Therefore, if there was leakage through the tube-to-tubesheet crevice during normal operation from a through-wall tube indication, that leak rate could be expected to increase during postulated accident conditions. Based on early NRC staff queries regarding the leak rate modeling code associated with calculating the expected leak rate, see Reference 5 for example, it was expected that efforts to license criteria based on estimating the actual leak rate as a function of the contact pressure during faulted conditions on a generic basis would be problematic.

As noted, the tube holes diminish in size below the neutral plane of the tubesheet because of the upward bending and the contact pressure between the tube and the tubesheet increases. When the differential pressure increases during a postulated faulted event the increased bow of the tubesheet leads to an increase in the tube-to-tubesheet contact pressure, increasing the resistance to flow. Thus, while the dilation of the tube holes above the neutral plane of the tubesheet presents additional analytic problems in estimating the leak rate for indications above the neutral plane, the

⁶ The differential pressure could be on the order of 2405 psi if it is demonstrated that the power operated relief valves will be functional.

diminution of the holes below the neutral plane presents definitive statements to be made with regard to the trend of the leak rate, hence, the bellwether principle. Independent consideration of the effect of the tube-to-tubesheet contact pressure leads to similar conclusions with regard to the opening area of the cracks in the tubes, thus further restricting the leak rate beyond that through the interface between the tube and the tubesheet.

In order to accept the concept of normal operation being a bellwether for the postulated accident leak rate for indications above the neutral plane of the tubesheet, the change in leak rate had to be quantified using a somewhat complex, physically sound model of the thermal-hydraulics of the leak rate phenomenon. This is not necessarily the case for cracks considered to be present below the neutral plane of the tubesheet. This is because a diminution of the holes takes place during postulated accident conditions below the neutral plane relative to normal operation. For example, at a radius of approximately 34 inches from the center of the SG, the contact pressure during normal operation is calculated to be about 2180 to 2225 psi⁷, see the last contact pressure entry in the center columns of Table 7-8 and Table 7-7 respectively, while the contact pressure during a postulated steam line break would be on the order of 3320 psi at the bottom of the tubesheet, Table 7-9, and during a postulated feed line break would be on the order of 4240 psi at the bottom of the tubesheet, Table 7-10 and Table 7-11 are close to the same number.

Note: The radii specified in the heading of the tables are the maximum values for the respective zones analyzed, hence the contact pressures in the center column correspond to the radius specified for the left column, etc. The leftmost column lists the contact pressure values for a radius of 4.08 inches. Also, the values tabulated do not include the calculated residual preload from the tube installation, which is not necessary for this comparison.

The analytical model for the flow through the crevice, the Darcy equation for flow through porous media, indicates that flow would be expected to be proportional to the differential pressure. Thus, a doubling of the leak rate could be predicted if the change in contact pressure between the tube and the tubesheet were ignored. Examination of the nominal correlation on Figure 6-6 indicates that the crevice resistance to flow per unit length (the loss coefficient) would increase during a postulated SLB event.

The leak rate from a crack located within the tubesheet is governed by the crack opening area, the resistance to flow through the crack, and the resistance to flow provided by the tube-to-tubesheet joint. The path through the tube-to-tubesheet joint is also frequently referred to as a crevice, but is not to be confused with the crevice left at the top of the tubesheet from the expansion process. The presence of the joint makes the flow from cracks within the tubesheet much different from the flow to be expected from cracks outside of the tubesheet. The tubesheet prevents outward deflection of the flanks of cracks, a more significant effect for axial than for circumferential cracks, which is a significant contributor to the opening area presented to the flow. In addition, the restriction provided by the tubesheet greatly restrains crack opening in the direction perpendicular

⁷ The change occurs as a result of considering various hot and cold leg operating temperatures.

to the flanks regardless of the orientation of the cracks. The net effect is a large, almost complete restriction of the leak rate when the tube cracks are within the tubesheet.

The leak path through the crack and the crevice is very tortuous. The flow must go through many turns within the crack in order to pass through the tube wall, even though the tube wall thickness is relatively small. The flow within the crevice must constantly change direction in order to follow a path that is formed between the points of hard contact between the tube and the tubesheet as a result of the differential thermal expansion and the internal pressure in the tube. There is both mechanical dispersion and molecular diffusion taking place. The net result is that the flow is best described as primary-to-secondary weepage. At its base, the expression used to predict the leak rate from tube cracks through the tube-to-tubesheet crevice is the Darcy expression for flow rate, Q , through porous media, i.e.,

$$Q = \frac{1}{K\mu} \frac{dP}{dz} \quad (3)$$

where μ is the viscosity of the fluid, P is the driving pressure, z is the physical dimension in the direction of the flow, and K is the “loss coefficient” which can also be termed the flow resistance if the other terms are taken together as the driving potential. The loss coefficient is found from a series of experimental tests involving the geometry of the particular tube-to-tubesheet crevice being analyzed, including factors such as surface finish, and then applied to the cracked tube situation.

If the leak rate during normal operation was 0.05 gpm (about 75 gpd), the postulated accident condition leak rate would be on the order of 0.1 gpm if only the change in differential pressure were considered, however, the estimate would be reduced when the increase in contact pressure between the tube and the tubesheet was included during a postulated steam line break event. An examination of the contact pressures as a function of depth in the tubesheet from the finite element analyses of the tubesheet as reported in Table 7-7 through Table 7-11 shows that the bellwether principle applies to a significant extent to all indications below the neutral plane of the tubesheet, and may apply to somewhat higher elevations. At the central plane of the tubesheet, the increase in contact pressure shown on Figure 8-4 is more on the order of 300 psi relative to that during normal operation for all tubes regardless of radius. Still, the fact that the contact pressure increases means that the leak rate would be expected to be bounded by a factor of two relative to normal operation. At a depth of 17 inches from the top of the tubesheet the contact pressure increases by about 1600 to 1700 psi relative to that during normal operation. The flow resistance would be expected to increase by about 60%, thus the increase in driving pressure would be mostly offset by the increase in the resistance of the joint.

The numerical results from the finite element analyses are presented on Figure 8-1 at the bottom of the tubesheet. A comparison of the contact pressure during postulated SLB conditions relative to that during NOp is also provided for depths of 16.9, 12.6, 10.5 and 8.25 inches below the top of the tubesheet. The observations are discussed in the following.

-
- At the bottom of the tubesheet, Figure 8-1, the contact pressure increases by 1665 psi near the center of the tubesheet, exhibits no change at a radius of about 55 inches, and diminishes by 365 psi at the extreme periphery, a little less than 61 inches from the center.
 - At 16.9 inches below the top of the tubesheet (a little over 4.1 inches from the bottom) the tubesheet the contact pressure increases by about 1085 psi at the center to a minimum of about 125 psi at a radius of 57 inches, Figure 8-2. The contact pressure during a SLB is everywhere greater than that during NOp. The influence of the channelhead and shell at the periphery causes the deformation to become non-uniform near the periphery.
 - At a depth of 12.6 inches, Figure 8-3, the contact pressure increase ranges from a maximum of about 520 psi near the center of the tubesheet to 265 psi at a radius of 55 inches as shown on Figure 8-3.
 - At roughly the neutral surface, about 10.5 inches, Figure 8-4, the contact pressure during SLB is uniformly greater than that during normal operation by about 250 psi (ranging from 245 to 280 psi traversing outward).
 - At a depth of 8.25 inches from the TTS, Figure 8-5, the contact pressure decreases by about 55 psi near the center of the TS to (Row 2) a maximum increase of 260 psi near the periphery.
 - At a depth of about 6 inches from the TTS, Figure 8-6, the contact pressure decreases by about 365 psi at the center of the TS, is invariant at a radius of about 42 inches and increases by about 240 psi near the periphery.

The absolute value of the contact pressure is not as important as the change in contact pressure because the parameter of interest in applying the B* criteria is the relative leak rate between NOp and SLB conditions. The analysis results indicate that there is a location within the tubesheet as a function of radius from the center where the contact pressure is invariant between NOp and SLB. The analysis results discussed in the next section include a plot of the invariant elevation of the Catawba 2 SGs. The change in the distribution of the contact pressure would result in a decrease in contact pressure near the top of the tubesheet in the central region. Thus, it would not be sufficient to simply use the depth of 8.25 inches and suppose that the leak rate would be relatively unchanged even if the pressure potential difference were the same without further analysis. However, the fact that the contact pressure generally increases below that elevation indicates that the leak rate would be relatively unaffected for indications a little deeper into the tubesheet.

The leak rate from any indication is determined by the total resistance of the crevice from the elevation of the indication to the top of the tubesheet in series with the crack itself, which is also expected to increase with contact pressure.⁸ A comparison of the curves on Figure 8-5 relative to

⁸ The effect of hoop compression on axial cracks would overwhelm the effect of the fluid pressure on the flanks.

those on Figure 8-4 indicates that the contact pressure generally increases for a length of at least 2 inches upward from the mid-plane for all tubes.

The trend is consistent, at radii where the contact pressure decreases or the increase is not as great near the bottom of the tubesheet, the increase at higher elevations would be expected to compensate. For example, the contact pressures on Figure 8-4 at the bottom of the tubesheet show a decrease beyond a radius of 55 inches, however, the increase at 8.4 inches above the bottom, Figure 8-2 is significant. For the outboard tubes the increase in contact pressure extends all the way to the top of the tubesheet.

A comparison of the curves at the various elevations leads to the conclusion that for a length of 8 inches upward from an elevation of 4.26 inches above the bottom of the tubesheet there is always an increase in the contact pressure in going from normal operation conditions to postulated SLB conditions. Hence, it is reasonable to omit any consideration of inspection of bulges or other artifacts below a depth of 10 inches from the top of the tubesheet. Therefore, applying a very conservative inspection sampling length of 10 inches downward from the top of the tubesheet during the Catawba 2 outages provides a high level of confidence that the potential leak rate from indications below the lower bound inspection elevation during a postulated SLB event will be bounded by twice the normal operation primary-to-secondary leak rate.

Noting that the density of the number of tubes populating the tubesheet increases with the square of the radius, the number of tubes for which the contact pressure is greater during a SLB than during NOp at a depth of 6 inches from the TTS is far greater than the number for which the contact pressure decreases, i.e., 75% of the tubes are at a radius greater than 30 inches from the center of the tubesheet.

8.2 Ligament Tearing Discussion

One of the concerns that must be addressed in dealing with cracks in SG tubes is the potential for ligament tearing to occur during a postulated accident when the differential pressure is significantly greater than during normal operation. While this is accounted for in the strength evaluations that demonstrate a resistance to pullout in excess of $3 \cdot \Delta P$ for normal operation and $1.4 \cdot \Delta P$ for postulated accident conditions, the potential for ligament tearing to significantly affect the leak rate predictions needs to be accounted for.

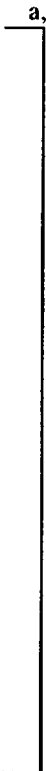
Ligament tearing considerations for circumferential tube cracks that are located below the H^* depths within the tubesheet are significantly different from those for potential cracks at other locations. The reason for this is that H^* has been determined using a factor of safety of three relative to the normal operating pressure differential and 1.4 relative to the most severe accident condition pressure differential. Therefore, the internal pressure end cap loads which normally lead to an axial stress in the tube are not transmitted below about $2/3$ of the H^* depth. This means that the only source of stress acting to extend the crack is the primary pressure acting on the flanks of the crack. Since the tube is captured within the tubesheet, there are additional forces acting to resist opening of the crack. The contact pressure between the tube and tubesheet results in a friction induced shear stress acting opposite to the direction of crack opening, and the pressure on

the flanks is compressive on the material adjacent to the plane of the crack, hence a Poisson's ratio radial expansion of the tube material in the immediate vicinity of the crack plane is induced which also acts to restrain the opening of the crack. In addition, the differential thermal expansion of the tube is greater than that of the carbon steel tubesheet, thereby inducing a compressive stress in the tube below the H* length.

A scoping evaluation of the [

]a,c,e.

In summary, considering the worst-case scenario, the likelihood of ligament tearing from radial circumferential cracks resulting from an accident pressure increase is small since at most, only 9% of the cross-sectional area is needed to maintain tube integrity. Also, since the crack face area will be less than the total cross-sectional area used above, the difference in the force applied as a result of normal operating and accident condition pressures will be less than the 58 lbs associated with the above numbers. Therefore, the potential for ligament tearing is considered to be a secondary effect of essentially negligible probability and should not affect the results and conclusions reported for the H* evaluation. The leak rate model does not include provisions for predicting ligament tearing and subsequent leakage, and increasing the complexity of the model to attempt to account for ligament tearing has been demonstrated to be not necessary (Reference 39).



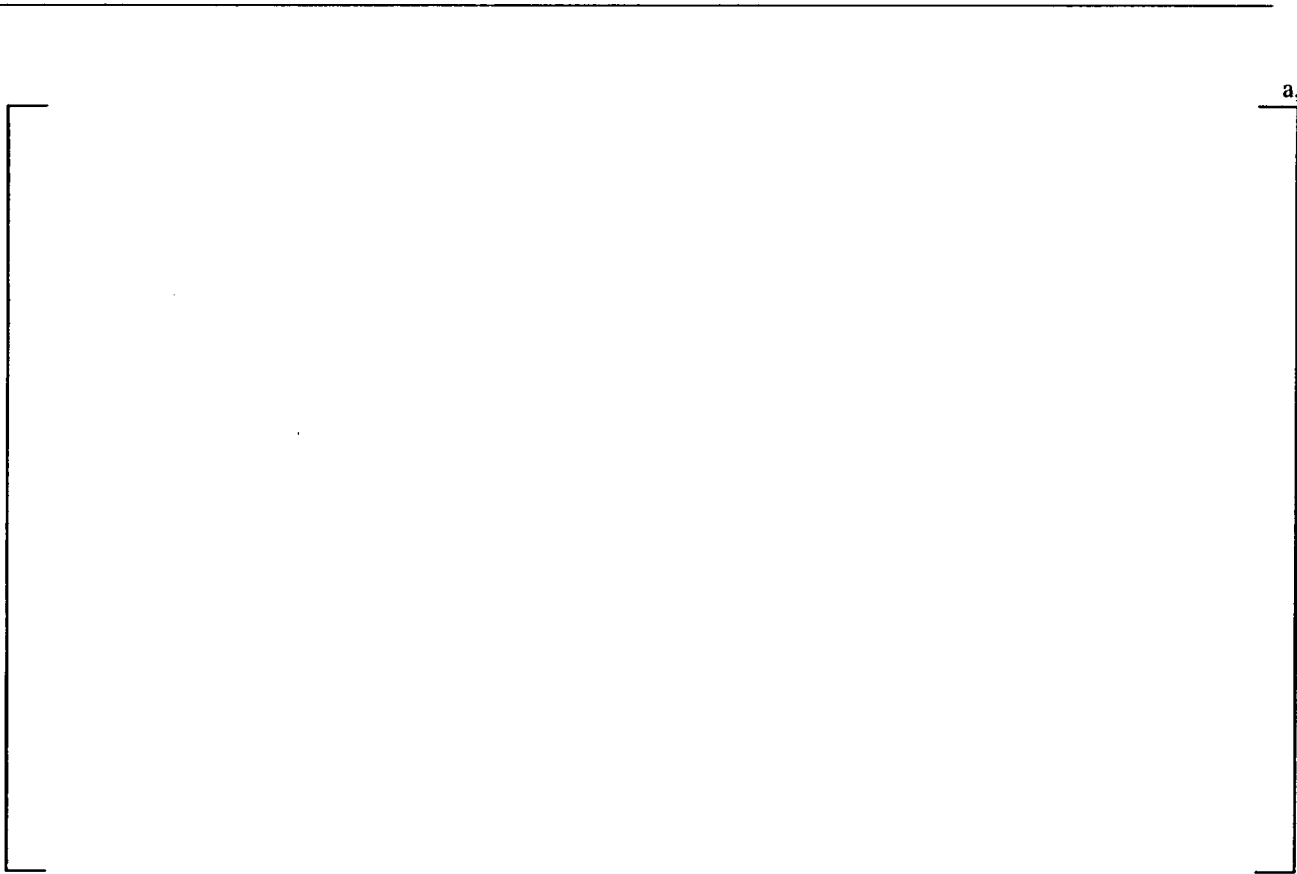
a,c,e

Figure 8-1. Change in contact pressure at 21.0 inches below the TTS



a,c,e

Figure 8-2. Change in contact pressure at 16.9 inches below the TTS



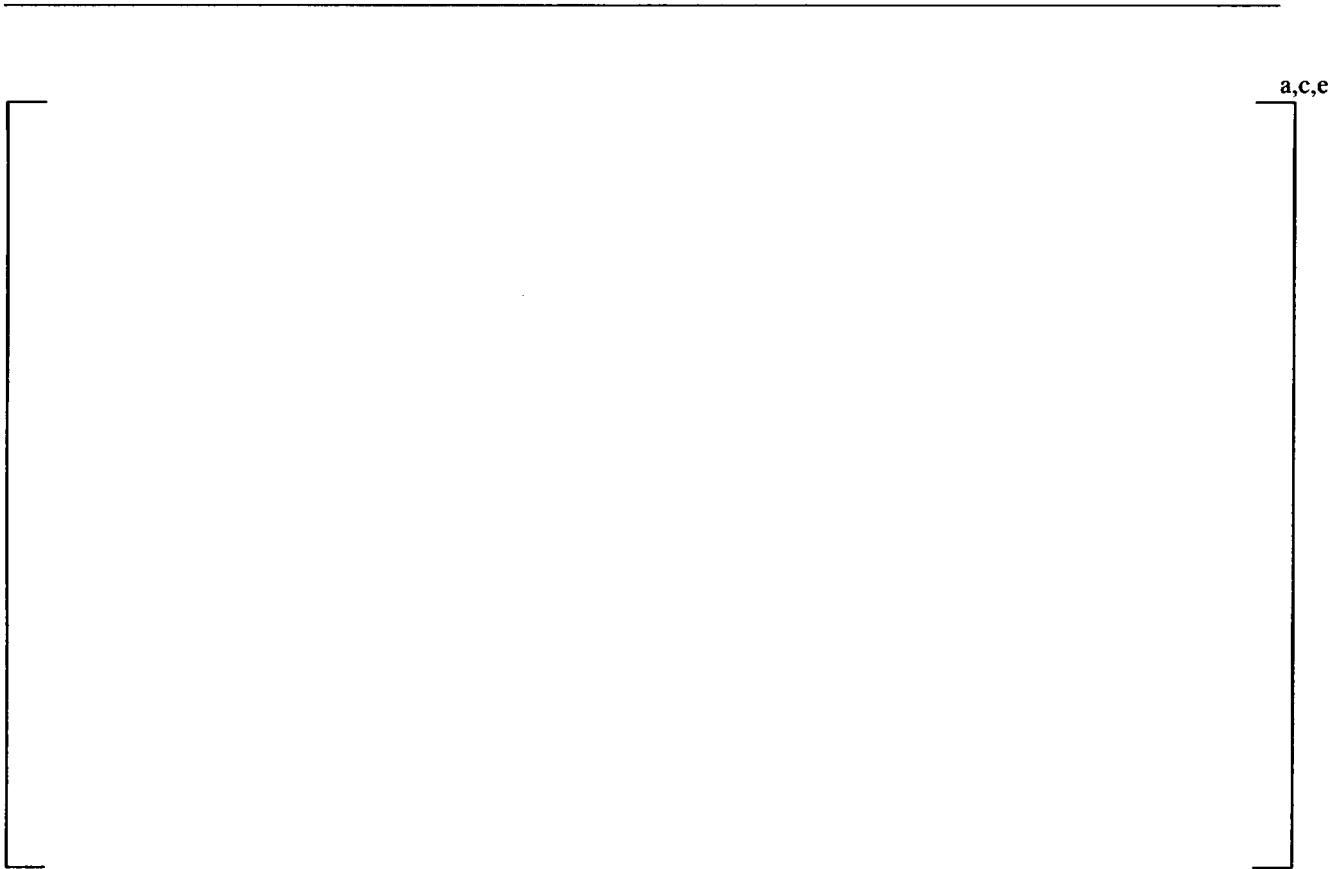
a,c,e

Figure 8-3. Change in contact pressure at 12.6 inches below the TTS



a,c,e

Figure 8-4. Change in contact pressure at 10.5 inches below the TTS



a,c,e

Figure 8-5. Change in contact pressure at 8.25 inches below the TTS



a,c,e

Figure 8-6. Change in contact pressure at 6.0 inches below the TTS

9.0 Determination of the B* Distance

B* is the length of engagement in the tubesheet needed for the leak rate during a postulated steam line break (SLB) event to be bounded by a specified multiple of the leak rate during normal operation (NOp). The rationale for the determination of B* is that there are changes during a SLB relative to NOp that lead to the expectation of an increase in the leak rate and other changes that lead to the expectation of a higher resistance to leakage. The determination of B* is based on analyzing the contributing factors and making an estimate of the change in leak rate that would be expected. The factors that lead to an expectation of an increase in the leak rate are as follows:

- 1) An increase in the primary-to-secondary differential pressure force on the water inside a postulated tube crack and the tube-to-tubesheet interface. For Catawba 2 this is a factor of about 1.75 to 1.78.
- 2) A decrease in the tube-to-tubesheet contact pressure above the neutral plane of the tubesheet resulting from dilation of the tubesheet holes in response to an increase in the bending deformation from the primary-to-secondary pressure difference increase. This does not apply to the periphery of the tubesheet where the opposite effect occurs.
- 3) A decrease in the tube-to-tubesheet contact pressure associated with the higher coefficient of thermal expansion of the tube material relative to that of the tubesheet if the temperature of the tubesheet decreases.

The factors that lead to an expectation of a decrease in the leak rate are:

- 1) The increase in primary pressure within the tube expands the tube into tighter contact with the tubesheet, resulting in an increase of the resistance of the material interface to flow between the tube and the tubesheet.
- 2) An increase in the tube-to-tubesheet contact pressure below the neutral plane of the tubesheet resulting from diminution of the tubesheet holes in response to the increase in the bending deformation from the primary-to-secondary pressure difference increase. Again, the effect is opposite for tubes on the periphery of the tubesheet.
- 3) An increase in the resistance to flow associated with an increase in the viscosity of the water in the crevice if the temperature of the tubesheet decreases.

The basis for the determination of B* is the consideration of each of the above effects using results from finite element analyses of the tubesheet and results from leak rate testing of the tube-to-tubesheet interface. The analyses and testing are described in other sections of this report. In summary, the leak rate is characterized by the Darcy equation for flow through a porous medium, an equation of the same form as the Hagen-Poiseuille equation for fully developed flow. The resistance to flow was developed from test data as a function of the contact pressure between the tube and the tubesheet. The finite element analysis results provide calculated results for the contact pressure as a function of tube location and depth into the tubesheet based on the NOp and postulated SLB pressure and temperature conditions of the plant.

The following are discussed, background information giving a qualitative overview supporting the development of B^* , flow through a crevice formulation, tube-to-tubesheet contact pressure variation, the determination of the B^* distance, and conclusions regarding the B^* values.

9.1 Background Information

A natural question regarding the development and application of the B^* criterion is whether or not numerical studies were performed to verify that the reduction in leak rate resistance above the neutral surface of the tubesheet associated with tubesheet bowing was adequately bounded by the increase in resistance below the neutral surface. The following discussion is intended to provide technical insight into the behavior of the leak rate from throughwall tube indications within the tubesheet by presenting:

- 1) the theoretical detail that is the basis for the observations from the test data and extrapolation of the test data for leak rate as function of joint length as expressed as the flow loss coefficient, and,
- 2) the explanation as to why the leak rate at normal operating conditions provides a bellwether for and can be used to establish a bounding value for the leak rate during steam line break conditions.

For most of the tube locations in the tubesheet the bow is concave downwards, like a dome. The tube-to-tubesheet contact pressure is an increasing linear function of the depth from the top of the tubesheet. Thus, for any specified location within the tubesheet the contact pressure increases below that location and decreases above that location. The resistance to leakage through the tube-to-tubesheet interface is an increasing function of the contact pressure between the tube and the tubesheet. The bellwether principle is based on considering the leak rate during a postulated steam line break (SLB) event relative to that during normal operating conditions (NOp). The differential pressure during a SLB event is greater than that during NOp so that bowing of the tubesheet increases with an associated change in the slope of the contact pressure versus depth relation as a function of tube location. For all tubes, except for the small percentage of tubes that are located on the periphery, the slope increases. For tubes on the periphery the slope increases in an absolute sense since there is an inflection point near the periphery. The evaluation applies regardless because increasing the contact pressure has a greater influence on the leak rate than decreasing the contact pressure.

Numerical studies were not initially performed because the subject was considered to be adequately addressed based on a qualitative evaluation using first principles considerations as follows:

- 1) In the limiting case of no dependence of the leak rate loss coefficient, i.e., the resistance per unit length, on the contact pressure, the leak rate during NOp and postulated SLB would be a function of the length of the crevice and pressure difference only. Using the Darcy equation, the leak rate is a direct function of the differential pressure and the inverse of the crevice length. Since the length remains the same and the driving pressure increases by a factor of

about 1.75, about 1435 psi to 2560 psi, the leak rate change is bounded by a similar factor. Any other theoretical dependence of leak rate on pressure difference, e.g., the square root of the pressure difference à la the Bernoulli equation, results in a reduction of the bounding factor relative to the result obtained using the Darcy equation.

- 2) The test data have demonstrated that the resistance per unit length is a monotonically increasing, non-linear function of the contact pressure with a positive second derivative. The deflection of the TS in combination with the increase in internal pressure results in the change in the contact pressure being zero between NOp and SLB at some depth below the TTS that is above the neutral surface of the tubesheet. The net contact pressure decreases above and increases below that depth, which is a function of location within the tube bundle. Using this elevation as a reference, the increase in resistance per unit length below the zero-change location must always be more than the absolute value of the decrease in resistance per unit length above the zero-change elevation. Thus, the average resistance in going from NOp to SLB must increase and the average leak rate must decrease. This is independent of the individual leak rates involved and only depends on the trend. The latter observation is apparent by inspection of the Figure relating loss coefficient to contact pressure in all submittals on the subject of leak rate through tube-to-tubesheet crevices.

There are alternate approaches to proving the above statements from the observations regarding the leak rate from test specimens.

9.2 Flow Through a Crevice (Darcy's Equation)

The equation that is solved for flow through a crevice is Darcy's model for flow through a porous media, that is, the volumetric flow, Q , is a function of the differential driving pressure, ΔP , and the respective inverse values of the viscosity, μ , the loss coefficient, K , and the length of the path, L , as,

$$Q = \frac{1}{\mu K} \frac{\Delta P}{L} \quad (4)$$

The driving pressure is based on the upstream minus the downstream values, else a negative sign would be needed in front of the equation. The viscosity is a function of the pressure and temperature of the fluid. The Darcy equation is also of the same form as the Hagen-Poiseuille flow equation for fully developed, laminar, axial flow in an annular gap, i.e.,

$$Q = \frac{1}{\mu} \frac{\Delta P}{\frac{6}{\pi R a^3} L} \quad (5)$$

Here, R is the average radius of the gap and a is a characteristic or effective gap dimension for the rough tube-to-tubesheet interface, expected to be very small, on the order of $4 \cdot 10^{-5}$ inch. Thus, the loss coefficient would be expected to be proportional to the inverse of the cube of the effective gap. The Hagen-Poiseuille form of the leak rate equation gives insight into the relationship

between the average resistance, characterized by the loss coefficient, K , and the contact pressure, i.e.,

$$K = \frac{6}{\pi R \alpha^3} \quad (6)$$

If the characteristic gap were proportional to the contact pressure between the tube and the tubesheet, doubling the pressure would increase the leak resistance by a factor of 8, although this is not expected to be the case because of the complex nature of the interface. In addition, it would not be unexpected that a plot of the $\ln(K)$ versus the contact pressure would approximate a straight line. For the rough tube-to-tubesheet interface, the length of the torturous path can also be considered to be characterized as being effective because the flow does not necessarily have a straight path to follow to the TTS (top of the tubesheet). Approximation of the path as the legs of an equilateral triangle would essentially double the distance traveled from the throughwall location to the TTS. Hence, the use of the loss coefficient integrates the accounting of the effective gap and effective length.

The electrical analogy for the flow considers Q as the current flow and ΔP as the potential, hence the quantity $\mu K L$ is the resistance to flow, R . Since K is a function of the contact pressure, P_c , the resistance is a function of the location within the tubesheet. The total resistance can be found as the average value of the quantity μK , the resistance per unit length, multiplied by L or by integrating the incremental resistance, $dR = \mu K dL$ over the length L , i.e.,

$$R = \mu \bar{K} (L_2 - L_1) = \int_{L_1}^{L_2} \mu K dL, \quad (7)$$

where both μ and K could be functions of location L . The viscosity is a very weak function of the pressure of the water in the crevice and can be considered to be constant for a given plant condition with negligible error, Figure 9-13, References 40 and 41. The viscosity is also a strong function of the temperature of the water in the crevice, Figure 9-14, and the tubesheet temperature for the condition being analyzed must be considered.

9.3 Tube-to-Tubesheet Contact Pressure Variation

Six tubesheet radial locations for which the contact pressure as a function of depth was determined were used in calculating the length of sound tubing below the TTS required to resist the NOp and SLB axial loads, i.e., the H^* depth. The intercept, b_0 , and slope, b_1 , parameters for the calculation of the contact pressure as a function of length, L , into the tubesheet for the six radial locations are listed in . The relationships are always in linear first order form,

$$P_c = b_0 + b_1 L \quad (8)$$

where the coefficients b_0 and b_1 vary as a function of the radial location of the tube in the tubesheet. This is simply a consequence of the fact that the linear elastic stress analysis, no yielding occurs. A comparison of the FEA results with first order, linear representations is

provided on Figure 9-5 for NOP and SLB conditions at a radius of 34 inches from the center of the tubesheet.

Further calculations examined the relationship between the intercept and slope of the prediction equations as a function of tube location radius. It was found that second order polynomial expressions can be used to describe the parameters almost exactly, i.e., with negligible error. A plot of the total contact pressures, which does not include the residual contact pressure from the hydraulic expansion process is provided on Figure 9-6 for each location during NOP and Figure 9-7 provides similar information during the postulated SLB event. The polynomial coefficients that were used to determine the values of the intercept and slope, i.e., b_0 and b_1 , for any given radius, R (not to be confused with the designation for resistance in the previous section), from the center of the tubesheet for NOP conditions are illustrated on Figure 9-8. Here, the following relationships are depicted where the g and h values were determined from the regression analyses,

$$\begin{aligned}
 \text{Normal Operation} \quad b_0 &= g_0 + g_1R + g_2R^2 && \text{(Intercept)} \\
 b_1 &= h_0 + h_1R + h_2R^2 && \text{(Slope)}
 \end{aligned} \tag{9}$$

The coefficients, u and v , of a similar set of expressions were calculated for determining the contact pressure at all locations within the tubesheet during a SLB event, i.e.,

$$\begin{aligned}
 \text{SLB Conditions} \quad b_0 &= u_0 + u_1R + u_2R^2 && \text{(Intercept)} \\
 b_1 &= v_0 + v_1R + v_2R^2 && \text{(Slope)}
 \end{aligned} \tag{10}$$

The polynomial coefficients that were used to determine the values of the intercept and slope for use in calculating the contact pressure during a SLB are illustrated on Figure 9-9. A comparison of the coefficients for the two conditions is provided on Figure 9-10.

9.4 Determination of the B* Distance

The results from multiple leak rate testing programs indicate that the logarithm of the loss coefficient is a linear function of the contact pressure, i.e.,

$$\ln K = a_0 + a_1P_c, \tag{11}$$

where the coefficients, a_0 and a_1 of the linear relation are found from a regression analysis of the test data; both coefficients are greater than zero. Simply put, the loss coefficient is greater than zero at the point where the contact pressure is zero and the loss coefficient increases with increasing contact pressure. Thus,

$$K = e^{a_0+a_1P_c}, \tag{12}$$

and the loss coefficient is an exponential function of the contact pressure. Combining Equation 12 for the loss coefficient as a function of the contact pressure with Equation 8 for the contact

pressure as a function of length yields,

$$K = e^{a_0 + a_1(b_0 + b_1 L)} = e^{c_0 + c_1 L} \quad (13)$$

here L is reckoned downward from the lower of the top of the tubesheet or the bottom of the expansion transition and the joined coefficients are given by $c_0 = a_0 + a_1 b_0$ and $c_1 = a_1 b_1$. Away from the periphery of the tubesheet, b_1 is greater than zero, hence c_1 is also greater than zero and the loss coefficient increases with depth into the tubesheet. Alternatively, the relation also means that near the periphery of the tubesheet the resistance to flow increases above any depth when the tubesheet bows upward. Since the B^* distance into the tubesheet is based on finding the depth for which the resistance to leak during SLB is the same as that during NOP, the meaningful radial region of the tubesheet is away from the periphery, that is, where the resistance to leakage decreases near the top of the tubesheet. Another point to note from the above expression is that in the region of interest the second derivative of the loss coefficient with respect to depth is positive. This means that the resistance per unit length is increasing with depth into the tubesheet. One consequence of the relation is that the decrease in resistance for a specified distance above any reference point is balanced by the increase in resistance over a shorter distance below that reference point. The coefficients for the contact pressure as a function of location are given by Equations 9 and 10 for NOP and SLB respectively.

The B^* distance is designated by L_B in the following equations and is the depth at which the resistance to leak during SLB is the same as that during NOP. Note that the product of the viscosity and the loss coefficient is the resistance per unit length for any location in the tubesheet. The resistance to leak, R , as a function of the viscosity, μ , average loss coefficient, \bar{K} , and length of the leak path from some uppermost location, L_0 , to L_B for any condition is given by,

$$R = \mu \bar{K} (L_B - L_0) = \int_{L_0}^{L_B} e^{c_0 + c_1 L} dL. \quad (14)$$

The limits of the integration define the range over which there is a contact pressure between the tube and the tubesheet that is greater than zero, i.e., ignoring any resistance to flow above that elevation. The lower limit is the lower of the TTS, the BET, or the point where the contact pressure is zero. Carrying out the integration,

$$R = \mu \frac{e^{c_0}}{c_1} [e^{c_1 L_B} - e^{c_1 L_0}]. \quad (15)$$

The equation can be used directly when the point of zero contact pressure between the tube and the tubesheet is at or below the TTS or BET, whichever is lower.

In order to account for the condition wherein L_0 is < 0 , i.e., at or above the TTS or BET, whichever is lower, the equation is written as,

$$R = \mu \frac{e^{c_0}}{c_1} [e^{c_1 L_B} - \text{if}(L_0 > 0, e^{c_1 L_0}, 1)]. \quad (16)$$

Here, the first argument of the “if” statement is the condition to be tested, the second argument is the value used if the condition is true, and the third argument is used if the condition is false. When zero contact pressure is predicted above the TTS or BET. For normal operation the resistance to leakage is given by,

$$R_N = \mu_N \frac{e^{c_{1,N}}}{c_{1,N}} \left[e^{c_{1,N}L_B} - \text{if}(L_{0,N} > 0, e^{c_{1,N}L_{0,N}}, 1) \right], \quad (17)$$

and for SLB by,

$$R_S = \mu_S \frac{e^{c_{1,S}}}{c_{1,S}} \left[e^{c_{1,S}L_B} - \text{if}(L_{0,S} > 0, e^{c_{1,S}L_{0,S}}, 1) \right]. \quad (18)$$

The B* distance is such that the resistance during SLB is the same as than during NOP, thus the solution is obtained for the value of L_B that makes $R_S = R_N$.

For the Catawba 2 SGs the value of B* varies from a maximum of 8.0 inches at a radius of 2 inches, about row 1 at the center of the bundle, to 4.5 inches at a radius of 36 inches, about row 33 between columns 57 and 58, and 3 inches at a radius of 38 inches. Thereafter, the leak resistance is always greater during a SLB event than during NOP. A plot of the calculated B* values is provided on Figure 9-15. Here, any values less than 1 inch were truncated to 1 inch. For example, the top of the tubes at the extreme periphery of the tubesheet are in compression during NOP because of contraction of the tube holes due to convex downward bending. The level of compression increases during a SLB event because the magnitude of the convex bending increases. Thus, any leak rate during NOP would bound the leak rate during SLB. While the driving pressure would increase by a factor of up to 1.8, the contact pressure between the tube and the tubesheet would increase toward the top of the tubesheet.

9.5 Sensitivity of the B* Calculation

Two approaches were taken to examine the sensitivity of the determination of the B* distance to the parameters of the analysis. The first was to vary the loss coefficient versus contact pressure parameters based on the confidence values from the regression calculations. The value of the largest B* depth changed by about 0.15 inch in going from an upper to a lower 95% confidence bound on the slope. Changes in the intercept coefficient did not have as significant an effect. Regardless, the most conservative values were used for the reported analysis results.

As an alternative approach, the depths for which the integration of the product of the viscosity with the contact pressure remained constant were also calculated. Compared to the previous section this is simply a pseudo-resistance, R_P , that is found as,

$$R_P = \int_{L_0}^{L_B} \mu P_c dL = \int_{L_0}^{L_B} \mu (b_0 + b_1 L) dL \quad (19)$$

so,

$$R_P = \mu \left[b_0 (L_B - L_0) + \frac{1}{2} b_1 (L_B^2 - L_0^2) \right] \quad (20)$$

Setting $R_{PN} = R_{PS}$ at a radius of 2 inches leads to a value of L_B of 7.3 inches. A value of 7.0 inches results from the same calculation at a radius of 8 inches. At radii of 20, 30 and 33 inches the depths for equal values of R_P during NOp and SLB conditions were found to be 6.8, 2.8 and 1.1 inches respectively. The integrated resistance is greater for all depths for radii greater than 34 inches. The result for a radius of 8 inches is illustrated on Figure 9-18 to be a depth of 7.0 inches. The results are comparable to those of the previous section and diminish more rapidly with radius than the approach that accounts for the loss coefficient from the testing program. For radii greater than about 50 inches the value of R_P is always greater during NOp than during SLB regardless of the depth into the tubesheet. The inherent assumption here is that the resistance is proportional to the contact pressure. This is not an unreasonable assumption in light of the dependence on the inverse third power of the effective gap thickness as implied by the Hagen-Poiseuille equation. Therefore, the results from the B* analysis based on the consideration of the slope of the loss coefficient are considered to be effectively confirmed, i.e., validated.

The B* evaluations were performed utilizing the same operating parameters that were used for the determination of the depths required to meet the structural performance criteria, that is, conservative values for the operating temperature. An increase in the hot leg temperature of about 15°F to 618°F results in an increase of the largest B* value of 0.33 inch. For a uniform inspection depth of 11 inches, the leak rate from indications near the center of the tubesheet would increase by about 3% relative to normal operation, about 2% less at 12 inches, 12% less at 32 inches, 20% less at 45 inches, and about 35% less at the periphery.

9.6 Conclusions Relative to B*

The resistance equations above can be used to show that the resistance is always bounded by the region through the thickness of the tubesheet where the contact pressure increases relative to the region where the contact pressure decreases. This simply means that the leak rate resistance increases during a SLB event relative to that during normal operation for similar lengths about a reference depth from the TTS, for example, B*. The resistance equations were used to calculate B* as the distance from the TTS for which the resistance during a postulated SLB event is the same as that during NOp. This means that the leak rate during SLB from any and all indications below B* will be bounded by a multiple of the leak rate during NOp based on the relative driving pressure for the two conditions. The differential pressure during a SLB at Catawba 2 is 1.75 to 1.78 times that during NOp depending on the operating conditions considered, e.g., differences in plugging level. Hence, the leak rate during a postulated SLB event would be expected to be no more than 1.8 times the leak rate being experienced during normal operation. Moreover, the B* analysis did not take into consideration the effect of the increase in the contact pressure below the B* elevation on the leak rate through postulated tube cracks within the tubesheet. For axial cracks the flanks would be compressed and the leak rate through the cracks themselves would be

expected to decrease. For circumferential cracks the resistance to flank displacement in the axial direction would be expected to negate the effect of the slight increase in pressure on the crack flanks. In conclusion, the use of a factor of 2 would be expected to be conservative.

The results reported were from analyses performed with regard to the contact pressures applicable to the hot leg of the SG. The contact pressures on the hot leg of the SG are greater during normal operation because of the higher temperature, and are, therefore, more restrictive to leak. In addition, the differential pressure on the cold leg is less than that on the hot leg and both the driving pressure and the tubesheet bow loosening would be diminished. The results of Section 7.2 indicate that slightly more engagement is needed during normal operation to meet the structural performance criteria, indicating that the loss of contact pressure governs the pullout resistance result. The attendant implication is that the leak resistance on the cold leg is also slightly reduced. The contact pressures on the cold leg during postulated accident conditions can be expected to be similar to those on the hot leg because of the length of time assumed to have elapsed without the cooling function of the secondary side fluid. Thus, the resistance to leak would be expected to be similar for both legs during a postulated SLB event. The net effect is that the ratio of the leak rate during SLB from throughwall tube indications on the cold leg would be expected to be less than that from corresponding indications on the hot leg. Calculations performed similar to those for the H* structural performance evaluation indicate that the required engagement length decreases slightly to result in the same leak rate resistance, confirming the expectation that the resistance ratio would be greater on the cold leg.

Table 9-1. First Order Equation Coefficients for the Variation of Contact Pressures Through Tubesheet

	a.c.e			

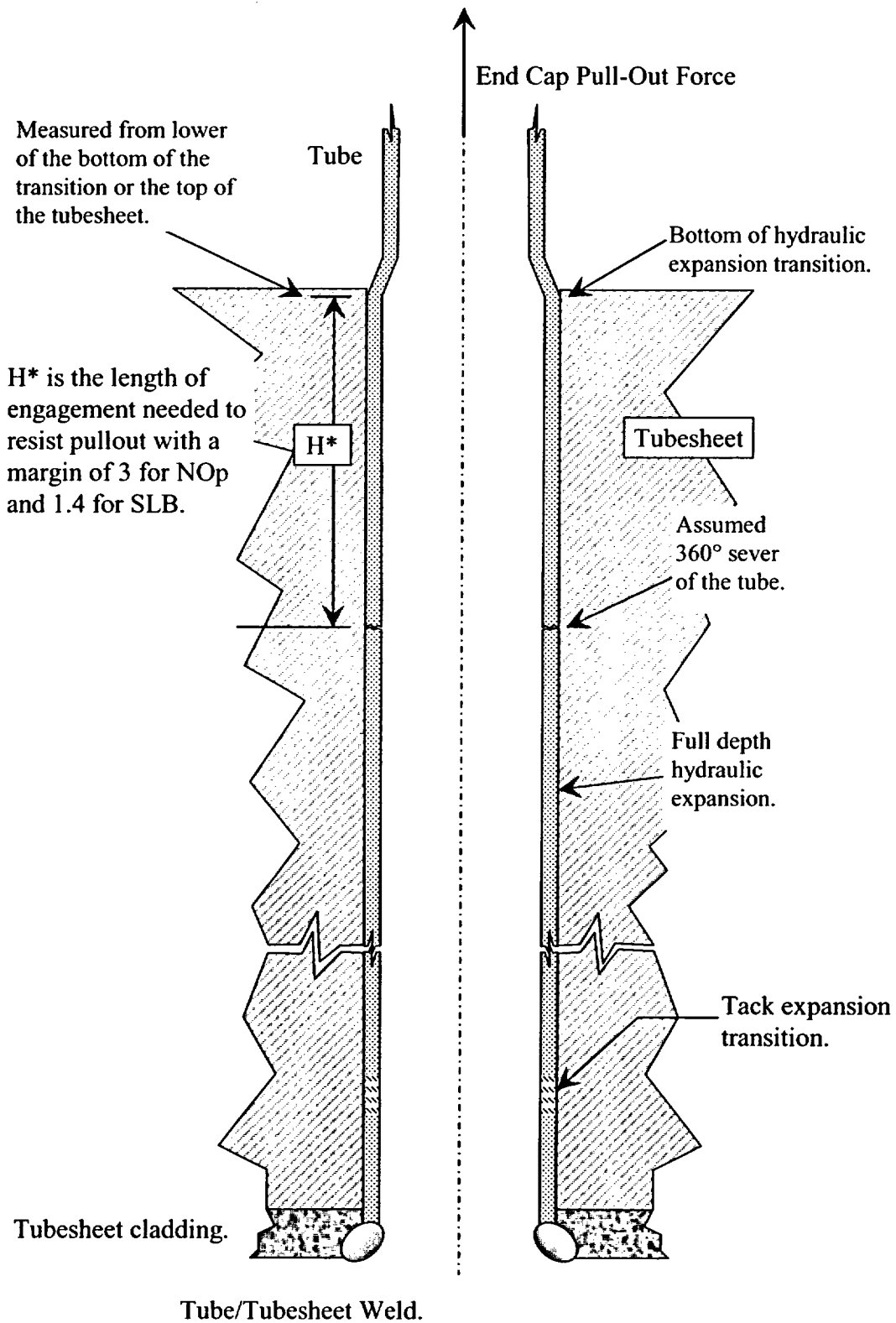


Figure 9-1. Determination of H^*

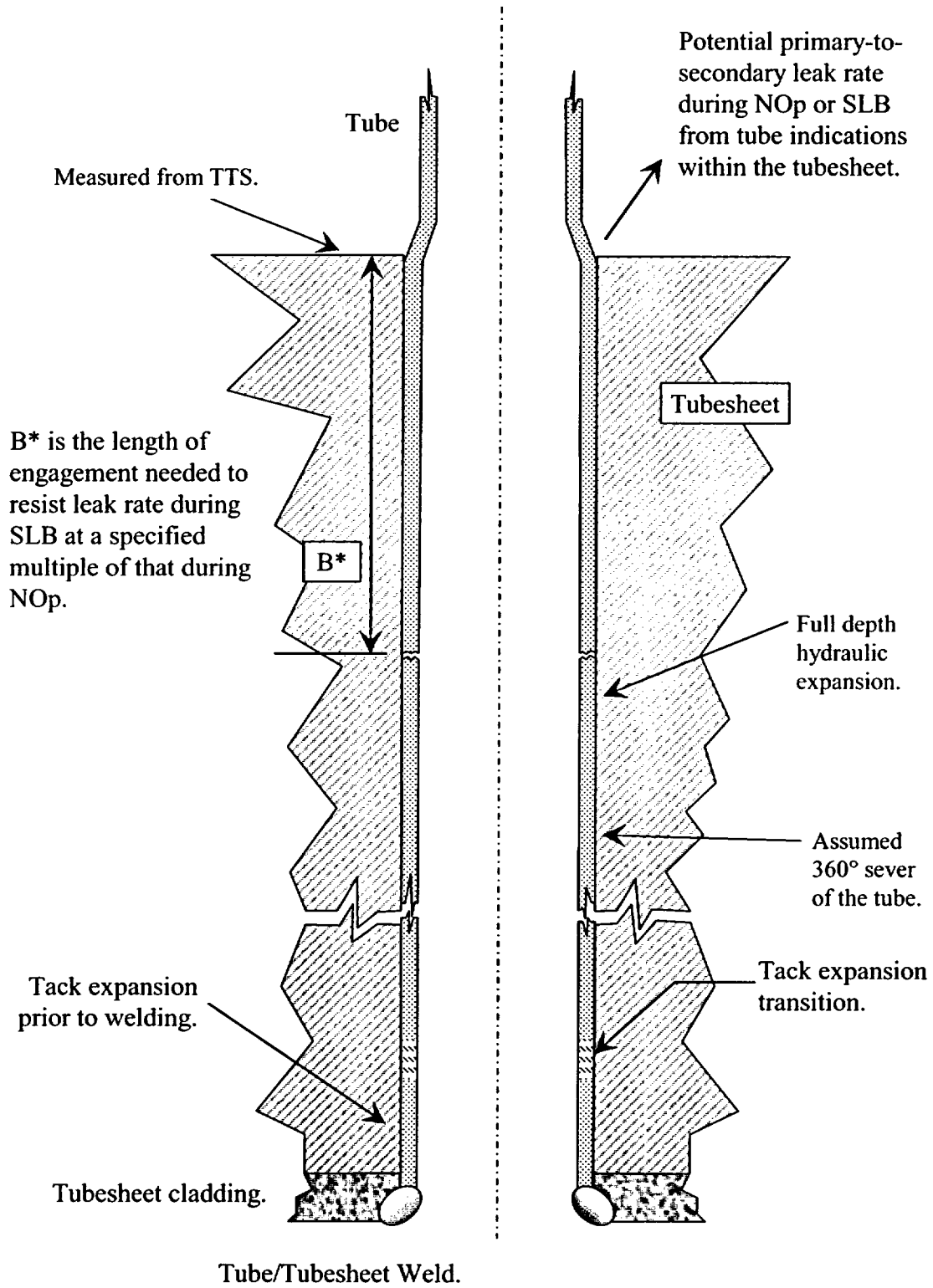


Figure 9-2. Determination of B^*

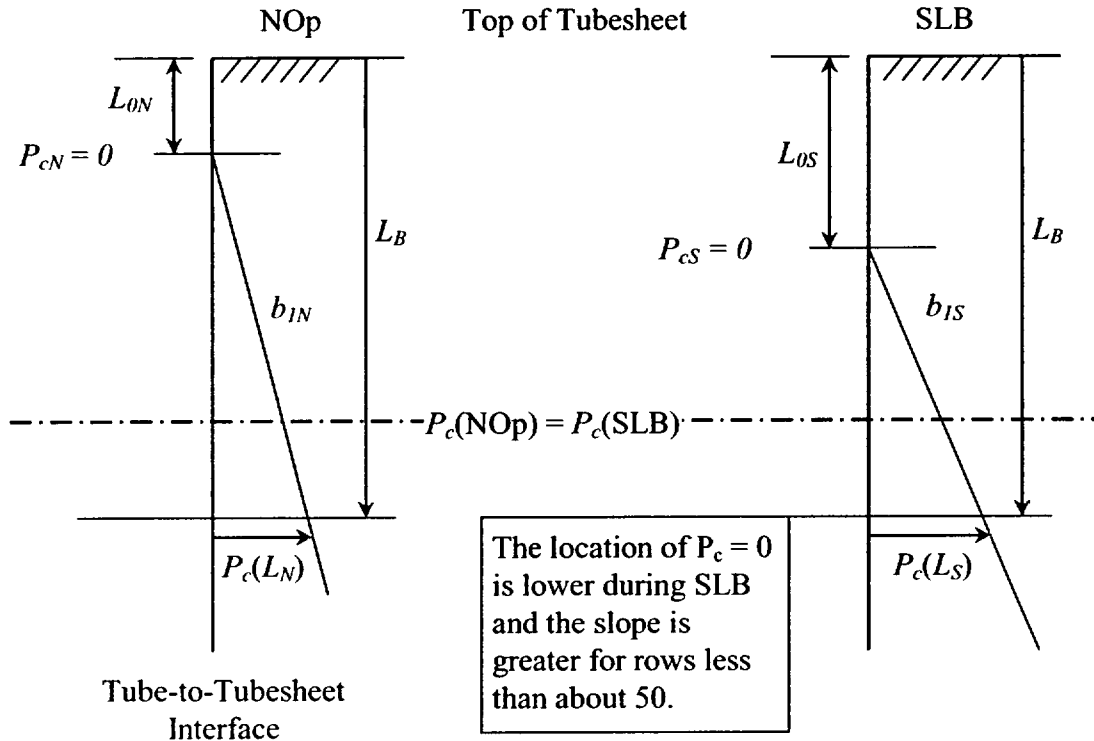


Figure 9-3. Concepts for the Determination of B*

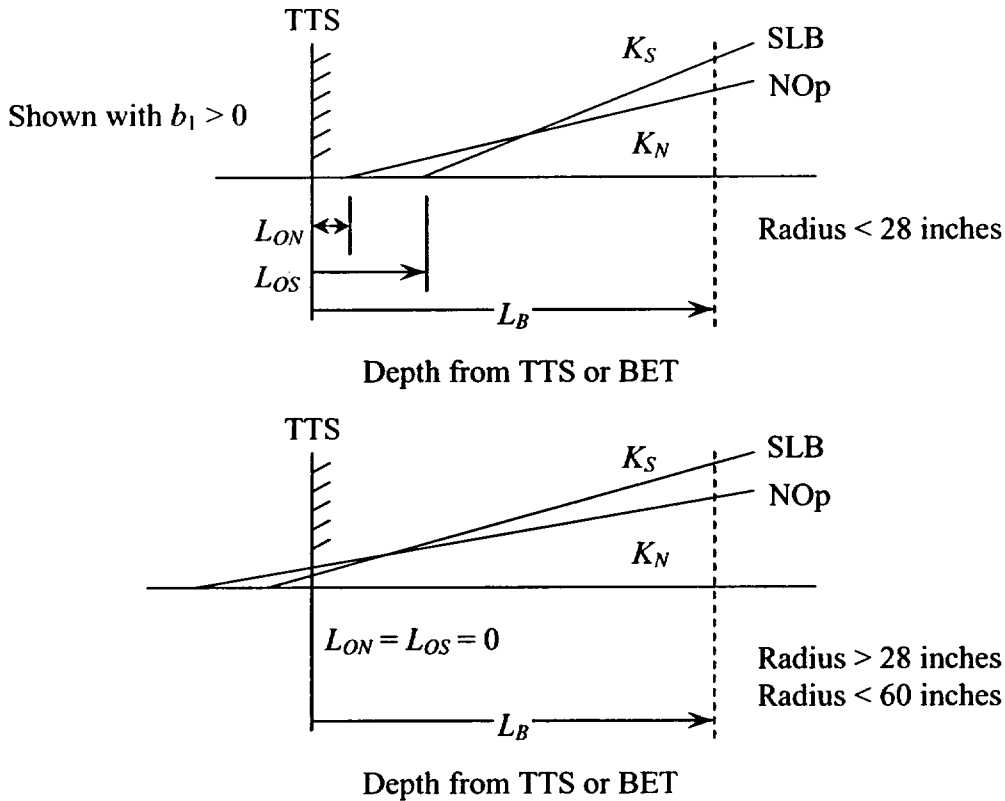


Figure 9-4. Determination of B* Parameters

a,c,e



Figure 9-5. First Order Linear Representation of Contact Pressure

a,c,e



Figure 9-6. Contact Pressure During Normal Operation

a,c,e



Figure 9-7. Contact Pressure During SLB, 2560 psi at 297°F

a,c,e



Figure 9-8. NOp Contact Pressure vs. Depth Coefficients by Radius

a,c,e



Figure 9-9. SLB Contact Pressure vs. Depth Coefficients by Radius

a,c,e



Figure 9-10. Contact Pressure Coefficients for NOp & SLB

a,c,e



Figure 9-11. Elevation Below the TTS for Invariant Contact Pressure

a,c,e



Figure 9-12. TTS Pc for NOP & SLB Conditions

a,c,e



Figure 9-13. Viscosity of Water as a Function of Pressure

a,c,e

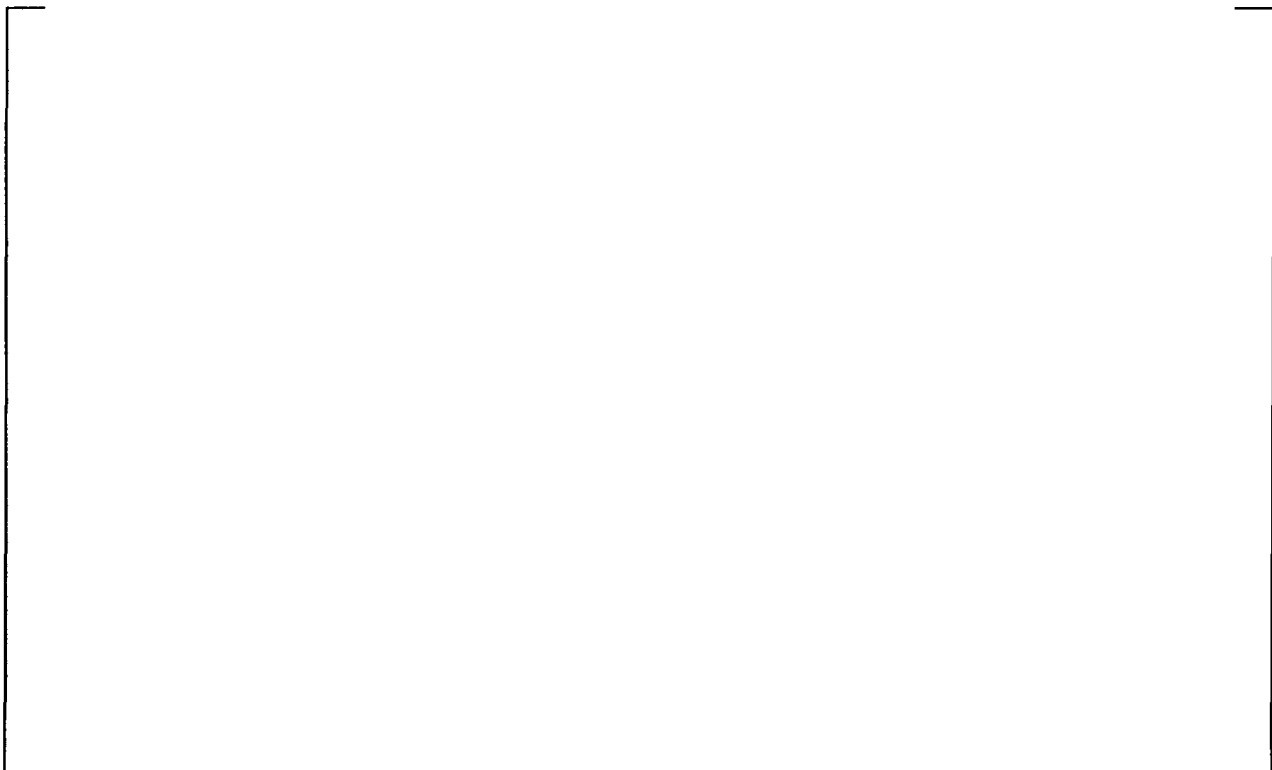


Figure 9-14. Viscosity of Water at 2560 psi as a Function of Temperature

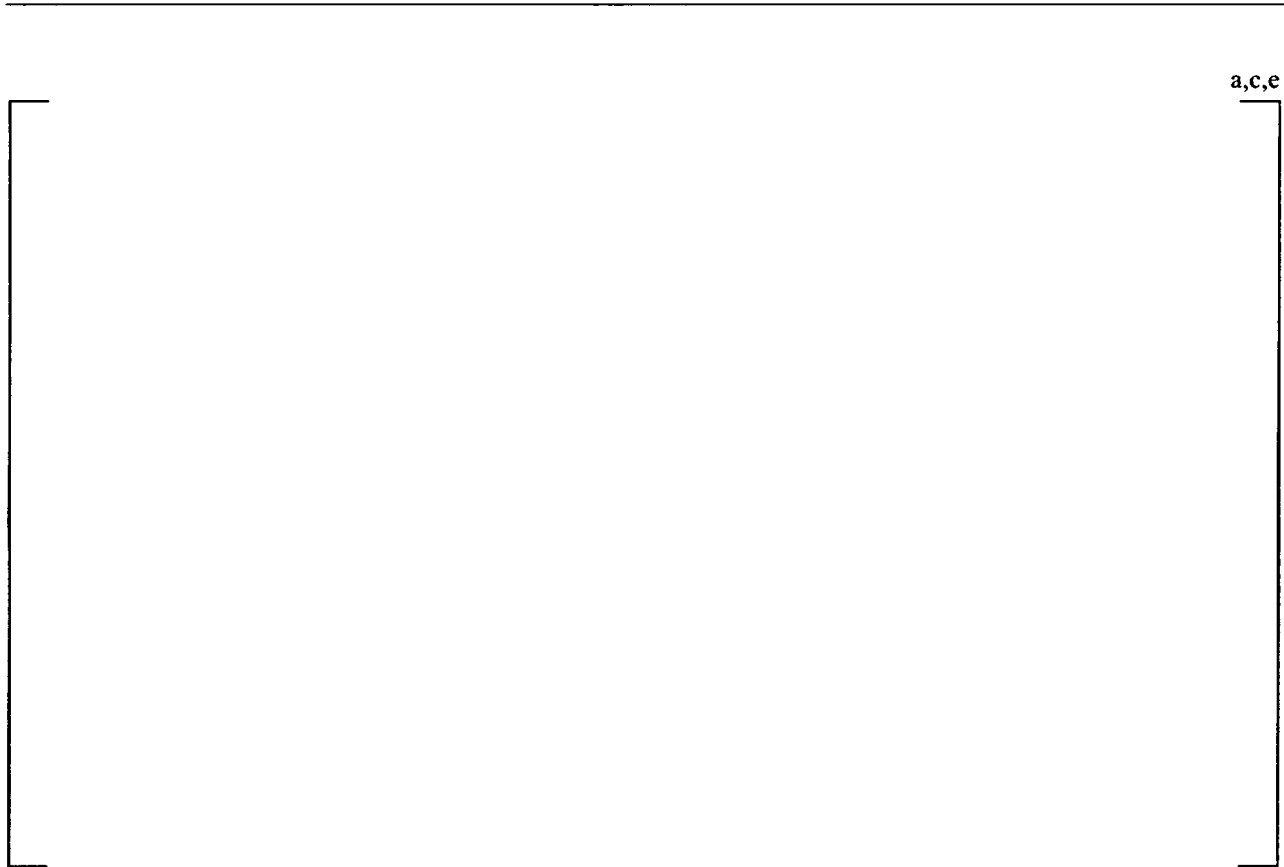


Figure 9-15. B* Depths for No Change in Resistance



Figure 9-16. B* Depths for Catawba 2 SGs for No Change in Leak Rate

a,c,e

Figure 9-17. Graphical Determination of B* Depth from Flow Resistance

a,c,e

Figure 9-18. Approximate Determination of B* Depth from Contact Pressure

10.0 Discussion of NRC Staff One Cycle Approval B* Braidwood Unit 2

10.1 Joint Structural Integrity Discussion

As noted in Section 4.1, “Joint Structural Integrity” of Reference 9 and Section 3.1 of Reference 10, the NRC staff stated that the Westinghouse analyses that concluded that the required hot leg engagement distances that vary from 2.33 to 8.13 (was 2.99 to 8.57) inches were not reviewed in detail and more qualitative arguments were used by the NRC staff for one time approval of the 17 inch tube joint inspection length. The qualitative arguments are stated below.

- Pullout tests demonstrate that the radial contact pressure produced by the hydraulic expansion alone is such as to require an engagement distance of 6 inches to ensure adequate safety margins against pullout. This estimate is a mean minus one standard deviation based on nine pullout tests. The estimate ignores that effect on needed engagement distance from differential thermal expansion, and tubesheet bore dilations associated with tubesheet bow.
- Radial differential thermal expansion between the tube and the tubesheet under hot operating conditions will act to further tighten the joint (i.e., increase radial contact pressure) and to reduce the necessary engagement distance relative to room temperature conditions. The radial differential thermal expansion arises from the fact that Alloy 600 tubing has a slightly higher (by 6 percent) coefficient of thermal expansion than does the SA-508 Class 2a tubesheet material and that tubes are a little hotter than the tubesheet.
- The internal primary pressure inside the tube under normal operating and accident conditions also acts to tighten the joint relative to unpressurized conditions, thus reducing the necessary engagement distance.
- Tubesheet bore dilations caused by the tubesheet bow under primary to secondary pressure can increase or decrease contact pressure depending on tube location within the bundle and the location along the length of the tube in the tubesheet region. Basically, the tubesheet acts as a flat, circular plate under an upward acting net pressure load. The tubesheet is supported axially around its periphery with a partial restraint against tubesheet rotation provided by the steam generator shell and the channel head. The SG divider plate provides a spring support against upward displacement along a diametral mid-line. Over most of the tubesheet away from the periphery, the bending moment from the resulting from the applied primary to secondary pressure load can be expected to put the tubesheet in tension at the top and compression at the bottom. Thus, the resulting distortion of the tubesheet bore (tubesheet bore dilation) tends to be such as to loosen the tube to tubesheet joint at the top of the tubesheet and to tighten the joint at the bottom of the tubesheet. The amount of dilation and resulting change in joint contact pressure would be expected to vary in a linear fashion from the top to the bottom of a tubesheet. Given the neutral axial to be at approximately the mid-point of the tubesheet thickness (i.e., 10.5 inches below the TTS to 17 inches below the TTS), tubesheet bore dilation effects would be expected to further tighten the joint from 10 inches below the TTS to 17 inches below the TTS which would be the lower limit of the proposed tubesheet region inspection

zone. Combined with the effects of the tube joint tightening associated with the radial differential thermal expansion and primary pressure inside the tube, contact pressure over at least a 6.5 inch distance should be considerably higher than the contact pressure simulated in the above mentioned pullout tests. A similar logic applied to the periphery of the tubesheet leads the staff to conclude that at the top 10.5 inches of the tubesheet region, contact pressure over at least a 6.5 inch distance should be considerably higher than the contact pressure simulated in the above mentioned pull out tests. Thus, the staff concludes that the proposed 17-inch engagement distance (or inspection zone) is acceptable to ensure the structural integrity of the tubesheet joint.

The NRC qualitative arguments are further supported on a more quantitative basis based on a study completed for the Model F steam generators for another plant (Reference 43). Moreover, similar statements were made in Reference 10 in approving a similar amendment for a plant with Model F SGs.

10.1.1 Discussion of Interference Loads

There are four source terms that must be considered relative to the determination of the interface pressure between the tube and the tubesheet. These are,

1. the initial preload from the installation of the tube,
2. internal pressure in the tube that is transmitted from the ID to the OD,
3. thermal expansion of the tube relative to the tubesheet, and
4. bowing of the tubesheet that results in dilation of the tubesheet holes.

The initial preload results from the plastic deformation of the tube material relative to that of the tubesheet. The material on the inside diameter experiences more plastic deformation than the material on the outside and thus has a deformed diameter which is incrementally greater. Equilibrium of the hoop forces and moments in the tube means that the OD is maintained in a state of hoop tension at a diameter greater than a stress free state. The model for the determination of the initial contact pressure between the tube and the tubesheet, P_c , is illustrated on Figure 10-2. Both the tube and the tubesheet behave as elastic springs after the expansion process is applied. The normal stress on the tube must be equal in magnitude to the normal stress on the tubesheet and the sum of the elastic springback values experienced by each must sum to the total interference.

As long as the tube and the tubesheet remain in contact the radial normal stresses must be in equilibrium. Thus, the problem of solving for the location of the interface and the contact pressure is determinate. The elements considered in the analysis are illustrated on Figure 9-3 for all operating and postulated accident conditions; the centerline of the tube and tubesheet hole are to the left in the figure. Each source of deformation of the tube outside surface starting from the installed equilibrium condition can be visualized starting from the top left side of the figure. The sources of deformation of the tubesheet inside surface can be visualized starting from the lower left side of the figure. As illustrated, although not to scale, the tube material has a coefficient of

thermal expansion that is greater than that of the tubesheet. The radial flexibility⁹, f , of the tube relative to that of the tubesheet determines how much of the pressure is actually transmitted to the interface between the tube and the tubesheet. Positive radial deformation of the tube in response to an internal pressure is found as the product of the pressure, P_p , and the tube flexibility associated with an internal pressure, discussed in the next section. Thus, the tube gets tighter in the tubesheet hole as the temperature of the tube and tubesheet increase. The deformation of the tube in response to an external pressure, P_s , is the product of the pressure times the flexibility associated with an external pressure. The normal operation contact pressure, P_N , is found from compatibility and equilibrium considerations. The deformation of the tubesheet hole in response to an internal pressure, P_s , is found as the product of the pressure and the flexibility of the tubesheet associated with an internal pressure. The opening or closing of the tubesheet hole, δr_i , resulting from bow induced by the primary-to-secondary pressure difference is in addition to the deformations associated with temperature and internal pressure. Once the tube has been installed, the deformations of the tube and tubesheet associated thermal expansion, internal pressure, and tubesheet bow remain linearly elastic.

Because of the potential for a crack to be present and the potential for the joint to be leaking, the pressure in the crevice is assumed to vary linearly from the primary pressure at the crack elevation to the secondary pressure at the top of the tubesheet. If the joint is not leaking, it would be expected that there was no significant fluid pressure in the crevice. The pressure assumption is considered to be conservative because it ignores the pressure drop through the crack, and the leak path is through the crevice will not normally be around the entire circumference of the tube. In addition, the leak path is believed to be between contacting microscopic asperities between the tube and the tubesheet, thus the pressure in the crevice would not be acting over the entire surface area of the tube and tubesheet. In any event, pressure in the crevice is always assumed to be present for the analysis.

There is no bow induced increase in the diameter of the holes during normal operation or postulated accident conditions below the mid span elevation within the tubesheet, hence most analyses concentrate on locations near the top of the tubesheet. The tubesheet bow deformation under postulated accident conditions will increase because of the larger pressure difference between the bottom and top of the tubesheet. The components remain elastic and the compatibility and equilibrium equations from the theory of elasticity remain applicable. Below the mid span elevation within the tubesheet the tubesheet holes will contract. The edges of the tubesheet are not totally free to rotate and there is some suppression of the contraction near the outside radius. This also means that the dilation at the top of the tubesheet is also suppressed near the outside radius of the tubesheet. The maximum hole dilations occur near the center of the tubesheet.

The application of the theory of elasticity means that the individual elements of the analysis can be treated as interchangeable if appropriate considerations are made. The thermal expansion of the tube can be thought of as the result of some equivalent internal pressure by ignoring Poisson

⁹ Flexibility is the ratio of deformation to load and is the inverse of the stiffness.

effects, or that tubesheet bow could be analytically treated as an increase in temperature of the tubesheet while ignoring associated changes in material properties.

10.1.2 Flexibility Discussion

Recall flexibility, f , is defined as the ratio of deflection relative to applied force. It is the inverse of stiffness which commonly used to relate force to deformation. There are four flexibility terms associated with the radial deformation of a cylindrical member depending on the surface to which the loading is applied and the surface for which the deformation is being calculated, e.g., for transmitted internal pressure one is interested in the radial deformation of the OD of the tube and the ID of the tubesheet. The deformation of the OD of the tube in response to external pressure is also of interest. The geometry of the tube-to-tubesheet interface is illustrated on Figure 9-1. The flexibility of the tubesheet, designated herein by the subscript c , in response to an internal pressure, P_{ci} , is found as,

$$\left[\begin{array}{l} \text{Inside Radius,} \\ \text{Internal Pressure} \end{array} \right]^{a,c,e} \quad \left[\right] \quad \text{Tubesheet (1)}$$

where, r_{ci} = inside radius of the tubesheet and outside radius of the tube,
 r_{co} = outside radius of the tubesheet hole unit cell,
 E_c = the elastic modulus of the carbon steel tubesheet material, and
 ν = Poisson's ratio for the tubesheet material.

Here, the subscripts on the flexibility stand for the component, c for tubesheet (and later t of tube), the surface being considered, i for inside or o for outside, and the surface being loaded, again, i for inside and o for outside. The superscript designates whether the cylinder is open, o , or closed, c , of interest in dealing with the end cap load from pressure in the tube. The former case is a state of plane stress and the latter is not since a closed cylinder has an end cap load. The flexibility of the tube in response to the application of an external pressure, P_{ro} , e.g., the contact pressure within the tubesheet, is,

$$\left[\begin{array}{l} \text{Outside Radius,} \\ \text{Outside Pressure} \end{array} \right]^{a,c,e} \quad \left[\right] \quad \text{Open Tube (2)}$$

Poisson's ratio is the same for the tube and the tubesheet. When the external pressure can act on the end of the tube,

$$\left[\begin{array}{l} \text{Outside Radius,} \\ \text{Outside Pressure} \end{array} \right]^{a,c,e} \quad \left[\right] \quad \text{Closed Tube (3)}$$

where E_t is the elastic modulus of the tube material. The flexibility of the tube in response to an external pressure is different when the secondary side pressure is present because that pressure also acts to compress the tube in the axial direction giving rise to a Poisson expansion effect, resisting the radial compression due to the pressure.

Finally, the flexibility of the outside radius of the tube in response to an internal pressure, P_{ti} , is,

$$\left[\begin{array}{l} \text{Outside Radius,} \\ \text{Inside Pressure} \end{array} \right]^{a,c,e} \quad \left[\begin{array}{l} \\ \\ \end{array} \right] \quad \text{Closed Tube (4)}$$

where r_{ti} is the internal radius of the tube and the tube is assumed to be closed. For an open tube the term in parentheses in the numerator is simply 2. A closed tube expands less due to Poisson contraction associated with the end cap load from the internal pressure. A summary of the applicable flexibilities is provided in Table 10-1. Note that during normal operation there is an end cap load on the tube from the secondary pressure but not from that associated with the fluid in the crevice if the joint is leaking. Both flexibilities would then be involved in calculating the radial deformation of the outside of the tube. Only the open tube flexibility is used with the pressure in the crevice for postulated accident conditions.

When the inside of the tube is pressurized, P_{ti} , some of the pressure is absorbed by the deformation of the tube within the tubesheet and some of the pressure is transmitted to the OD of the tube, P_{to} , as a contact pressure with the ID of the tubesheet. The magnitude of the transmitted pressure is found by considering the relative flexibilities of the tube and the tubesheet as,

$$\left[\begin{array}{l} \\ \\ \text{Transmitted Pressure} \end{array} \right]^{a,c,e} \quad \left[\begin{array}{l} \\ \\ \end{array} \right] \quad (5)$$

Note that the tube flexibility in response to the contact pressure is for an open tube because there is no end cap load associated with the contact pressure. The denominator of the fraction is also referred to as the interaction coefficient between the tube and the tubesheet. About 85 to 90% of the pressure internal to the tube is transmitted through the tube in Westinghouse designed SGs. However, the contact pressure is not increased by that amount because the TS acts as a spring and the interface moves radially outward in response to the increase in pressure. The net increase in contact pressure is on the order of 56.4% of the increase in the internal pressure. For example, the contact pressure between the tube and the tubesheet is increased by about 1970 psi during normal operation relative to ambient conditions. Likewise, the increase in contact pressure associated with SLB conditions is about 2250 psi relative to ambient conditions.

When the temperature increases from ambient conditions to operating conditions the differential thermal expansion of the tube relative to the tubesheet increases the contact pressure between the tube and the tubesheet. The mismatch in expansion between the tube and the tubesheet, δ , is given

by,

$$\delta = (\alpha_t \Delta T_t - \alpha_c \Delta T_c) r_{to} \quad \text{Thermal Mismatch} \quad (6)$$

where: α_t, α_c = thermal expansion coefficient for the tube and tubesheet respectively,
 $\Delta T_t, \Delta T_c$ = the change in temperature from ambient conditions for the tube and tubesheet respectively.

During normal operation the temperature of the tube and tubesheet are effectively identical to within a very short distance from the top of the tubesheet and the individual changes in temperature can usually be replaced by ΔT_t , thus,

$$\delta = (\alpha_t - \alpha_c) \Delta T_t r_{to}. \quad (7)$$

The change in contact pressure due to the increase in temperature relative to ambient conditions, P_T , is given by,

$$\left[\begin{array}{l} \text{Thermal Expansion} \\ \text{Contact Pressure} \end{array} \right] \cdot \overset{\text{a.c.e}}{\left[\right]} \quad (8)$$

Likewise, the same equation can be used to calculate the reduction in contact pressure resulting from a postulated reduction the temperature of the tube during a postulated SLB event.

The net contact pressure, P_C , between the tube and the tubesheet during operation or accident conditions is given by,

$$\text{Net Contact Pressure} \quad P_C = P_0 + P_P + P_T - P_B \quad (9)$$

where P_B is the loss of contact pressure due to dilation of the tubesheet holes, P_0 is the installation preload, P_P is the pressure induced load, and P_T is the thermal induced contact load. There is one additional term that could be considered as increasing the contact pressure. When the temperature increases the tube expands more in the axial direction than the tubesheet. This is resisted by the frictional interface between the tube and the tubesheet and a compressive stress is induced in the tube. This in turn results in a Poisson expansion of the tube radius, increasing the interface pressure. The effect is not considered to be significant and is essentially ignored by the analysis.

10.1.3 Analysis

From the preceding discussions it is apparent that the contact pressure during normal operation can be found by equating the total deformation of the outside radius of the tube, r_{to} , to the total deformation of the inside radius of the tubesheet hole, r_{ci} , where the net deformation of the outside of the tube, δ_{to} , is given by,

$$\text{Tube Deformation} \quad \delta_{to} = \alpha_t \Delta T_t r_{to} + P_p f_{toi}^c + P_s f_{too}^c + P_N f_{too}^o \quad (10)$$

and the net deformation of the tubesheet hole, δ_{ci} , is given by,

$$\text{TS Deformation} \quad \delta_{ci} = \alpha_c \Delta T_c r_{ci} + P_s f_{ccl}^o + \delta r_i + P_N f_{ccl}^o. \quad (11)$$

The inclusion of the P_N terms assures compatibility and the two net deformations must be equal. It can usually be assumed that the secondary fluid pressure does not penetrate the tubesheet hole and the terms involving P_s may be ignored. All of the terms except for the final contact pressure, P_N , are known and the tubesheet bow term, δr_i , is found from the finite element model analysis of the tubesheet. The total contact pressure during operation is then found as P_N plus P_c , the installation contact pressure. For postulated SLB conditions the solution is obtained from,

$$\alpha_t \Delta T_t r_{to} + P_p f_{toi}^c + P_N f_{too}^o = \alpha_c \Delta T_c r_{ci} + \delta r_i + P_N f_{ccl}^o, \quad (12)$$

or, the total contact pressure during a postulated SLB event is given by,

$$\text{SLB Contact Pres.} \quad P_T = P_c + \frac{\alpha_t \Delta T_t r_{to} - \alpha_c \Delta T_c r_{ci} + P_p f_{toi}^c - \delta r_i}{f_{ccl}^o - f_{too}^o}, \quad (13)$$

where $r_{to} = r_{ci}$. A similar expression with more terms is used to obtain the contact pressure during normal operation. The denominator of the above equation is referred to as the tube-to-tubesheet influence coefficient because it related deformations associated with the interfacing components to the interface pressure. The influence coefficient for Westinghouse Model F SG tubes is calculated using the information tabulated in Table 10-1 as $3.33 \cdot 10^{-6}$ psi/inch.

By taking partial derivatives with respect to the various terms on the right the rate of change of the contact pressure as a function of changes in those parameters can be easily calculated. For example, the rate of change of the contact pressure with the internal pressure in the tube is simply,

$$\frac{\Delta P_N}{\Delta P_p} = \frac{f_{toi}^c}{f_{ccl}^o - f_{too}^o}. \quad (14)$$

Thus, the rate of change of contact pressure with internal pressure in the tube is 0.564 psi/psi. Likewise, the rate of change of the contact pressure with change in the tube temperature or tubesheet temperature is given by,

$$\frac{\Delta P_N}{\Delta T_t} = \frac{\alpha_t r_{to}}{f_{ccl}^o - f_{too}^o} \quad \text{and} \quad \frac{\Delta P_N}{\Delta T_c} = - \frac{\alpha_c r_{ci}}{f_{ccl}^o - f_{too}^o}, \quad (15)$$

respectively. Again using the values in Table 10-1, the rate of change of contact pressure with tube temperature is 22.25 psi/°F with no increase in tubesheet temperature. Likewise, an increase in tubesheet temperature without an increase in tube temperature results in a 21.11 psi/°F decrease in the contact pressure. Therefore, there is a net change in the contact pressure of 1.14 psi/°F for uniform tube and tubesheet temperature changes.

Finally, the rate of change of contact pressure with tubesheet bow is calculated as,

$$\frac{\Delta \mathcal{F}_N}{\Delta \delta r_{ci}} = \frac{1}{f_{cii}^o - f_{100}^o} \quad (16)$$

The effect of the dilation associated with the tubesheet bow can be calculated using the information tabulated in Table 10-1. For each 0.1 mil of diameter dilation the interface pressure is reduced on the order of 380 psi. A summary of all of the contact pressure influence factors is provided in Table 10-1. A summary of tubesheet bow induced hole dilation values is provided in Table 10-2.

10.1.4 Conclusions

Although the study was completed for a Model F SG, the results listed in Table 10-2 indicate that the effect of tubesheet bow can result in a significant average decrease in the contact pressure during postulated accident conditions above the neutral plane. However, for the most severe case in one plant, in tube R18C77, the diametral change at the worst case location is less than 0.2 mils at the H* depth during postulated accident conditions. This same type of result would be expected to be the case for the Model D-5 steam generators in Catawba 2. Below the neutral plane, tubesheet bow is shown not to result in any tube dilation thus supporting the NRC staff conclusion that:

“Given the neutral axis to be at approximately the mid-point of the tubesheet thickness (i.e., 10.5 inches below the TTS to 17 inches below the TTS), tubesheet bore dilation effects would be expected to further tighten the joint from 10 inches below the TTS to 17 inches below the TTS which would be the lower limit of the proposed tubesheet region inspection zone. Combined with the effects of the tube joint tightening associated with the radial differential thermal expansion and primary pressure inside the tube, contact pressure over at least a 6.5 inch distance should be considerably higher than the contact pressure simulated in the above mentioned pullout tests.”

10.2 Joint Leakage Integrity Discussion

As noted in Section 4.2, “Joint Leakage Integrity,” of Reference 9, the NRC staff reviewed the qualitative arguments developed by Westinghouse regarding the conservatism of the conclusion that a minimum 17 inch engagement length ensures that leakage during a main steam line break (MSLB) will not exceed two times the observed leakage during normal operation, but the NRC staff’s depth of review did not permit it to credit Westinghouse’s insights from leak test data that leak flow resistance is more sensitive to changes in joint contact pressure as contact pressure increases due to the log normal nature of the relationship. The staff was still able to conclude that there should be no significant reduction in leakage resistance when going from normal operating to accident conditions.

The basis for the Westinghouse conclusion that flow resistance varies as a log normal linear function of joint contact pressure is provided in detail below. The data from the worst case tube in

a comparative study analytically supports the determination that there is at least an eight inch zone in the upper 17 inches of the tubesheet where there is an increase in joint contact pressure due to a higher primary pressure inside the tube and changes in tubesheet bore dilation along the length of the tubes. The NRC concurs (Reference 21) that the factor of 2 increase in leak rate as an upper bound by Westinghouse is reasonable given the stated premise that the flow resistance between the tube and the tubesheet remains unchanged between normal operating and accident pressure differential. The NRC staff notes in Reference 9 that the assumed linear relationship between leak rate and differential pressure is conservative relative to alternative models such as the Bernoulli or orifice models, which assumes leak rate to be proportional to the square root of the differential pressure.

The comparative study supports the NRC staff conclusion that “considering the higher pressure loading when going from normal operating to accident conditions, Westinghouse estimates that contact pressures, and, thus, leak flow resistance, always increases over at least an 8 inch distance above 17 inches below the top of the tubesheet appears reasonable to the NRC Staff.”

Table 10-1. Radial Flexibilities Times Elastic Modulus
(in./psi)

a,c,e

Table 10-2. Example Contact Pressure Influence Factors
for Models F & D5 SG Tubes at 600°F

a,c,e

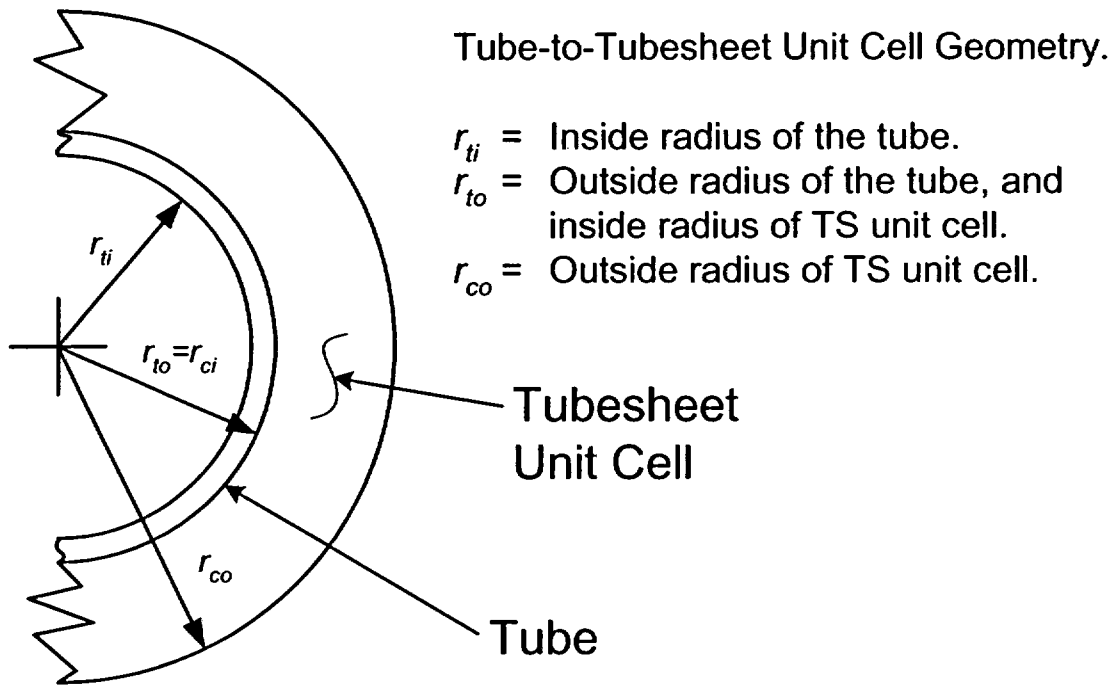


Figure 10-1. Geometry of the Tube-to-Tubesheet Interface



Figure 10-2. Model for Initial Contact Pressure



Figure 10-3. Determination of Contact Pressure, Normal or Accident Operation

(As illustrated, the bow does not result in a loss of contact, however, there are situations where the bow is sufficient to result in a loss of contact between the tube and the tubesheet at the top of the tubesheet.)

11.0 Conclusions

The evaluation of Section 7.0 of this report provides a technical basis for assuring that the structural performance criteria of NEI 97-06 are inherently met for degradation of any extent below the H* depth identified in Table 7-13, i.e., depths ranging from 2.33 to 8.61 inches below the BET or TTS whichever is lower selected to be bounding for all tubes in three particular zones. The corresponding evaluation presented in Section 9.0 provides a technical basis for bounding the potential leak rate from non-detected indications in the tube region below about 8 inches from the top of the tubesheet as no more than twice the leak rate during normal operation, see Figure 9-15. A similar analysis obtained a depth of about 11 inches based on restricting the expected leak rate to being the same as that during normal operation, Figure 9-16. The evaluation is independent on the magnitude of any degradation that might occur because it is based solely on the resistance of the interface between the tube and the tubesheet. In other words, the tube below the B* depth may be nonexistent. This conclusion is general in that the depths determined are for the most severely affected region of the tubesheet, the central region. The conclusion also applies to any postulated indications in the tack expansion region and in the tube-to-tubesheet welds, although the level of conservatism would be significantly more. As noted in the introduction to this report, the reporting of crack-like indications in the tube-to-tubesheet welds would be expected to occur inadvertently since no structural or leak rate technical reason exists for a specific examination to take place.

A graphical summary of the findings for the hot leg are presented on Figure 11-1.

- The depths associated with H*¹⁰ and B* are presented relative to the left ordinate while the leak rates are presented relative to the right ordinate as a function of radial location from the center of the tubesheet.
- The H* depths are bounding relative to a B* for equal leak rate resistance during NOp and SLB.
- The SLB and NOp leak rates at the H* depth are equal at a radius of about 40 inches, with the SLB less twice than that for NOp for all other locations.
- At a depth of 11 inches the SLB leak rate resistance the same NOp leak rate at the center of the tubesheet, decreasing almost linearly to 60% at the periphery.

A similar summary for the cold leg is presented on Figure 11-2. The conclusions to be drawn from the performed evaluations are that:

- 1) There is no structural integrity concern associated with tube or tube weld cracking of any extent provided it occurs below the H* distance as reported in Section 7.0 of this report. The pullout resistance of the tubes has been demonstrated for axial forces associated with 3 times the normal operating differential pressure and 1.4 times differential pressure associated with the most severe postulated accident.

¹⁰ The presented H* depths are depicted for individual radii from the center of the tubesheet rather than by zone for comparative purposes.

-
- 2) Contact forces during postulated LOCA events are sufficient to resist axial motion of the tube. Also, if the tube end welds are not circumferentially cracked, the resistance of the tube-to-tubesheet hydraulic joint is not necessary to resist push-out. Moreover, the geometry of any postulated circumferential cracking of the weld would result in a configuration that would resist pushout in the event of a loss of coolant accident. In other words, the crack flanks would not form the cylindrical surface necessary such that there would be no resistance to expulsion of the tube in the downward direction.
 - 3) The SLB leak rate for indications below the H* depth from the top of the tubesheet would be bounded by less than twice the leak rate that is present during NOP at the worst location in the bundle. This is initially apparent from comparison of the contact pressures from the finite element analyses over the full range of radii from the center of the tubesheet, and ignores any increase in the leak rate resistance due to the contact pressure changes and associated tightening of the crack flanks. The expectation that this would be the case was confirmed by the detailed analysis of the relative leak rates of Section 9.0. A similar analysis obtained a depth of about 11 inches based on restructuring the expected leak rate to being the same as that during normal operation.
 - 4) The B* depth of 11 inches for less than or to equal leak rates during SLB and NOP is greater than the H* depth and is bounding for the relocation of the pressure boundary. The B* evaluations were performed utilizing the same operating parameters that were used for the determination of the depths required to meet the structural performance criteria, that is, conservative values for the operating temperature. Ignoring the expected reduction in the differential pressure, an increase in the hot leg temperature to 618°F results in an increase in the leak rate from indications near the center of the tubesheet by about 3% relative to normal operation, decreasing by 2% at 12 inches and decreasing thereafter.

In conclusion, a relocation of the pressure boundary to the deeper of the H* or B* values is acceptable from both structural and leak rate considerations depending to the relative allowable leak rate during accident conditions. The prior conclusions rely on the inherent strength and leak rate resistance of the hydraulically expanded tube-to-tubesheet joint, a feature which was not considered or permitted to be considered for the original design of the SG. Thus, omission of the inspection of the weld constitutes a reassignment of the pressure boundary to the tube-to-tubesheet interface. Similar considerations for tube indications require NRC staff approval of a license amendment. Consideration of the allowable leak rate during accident conditions may necessitate locating the reassigned pressure boundary to a depth greater than that required for structural integrity, i.e., H*. Reassigning the pressure boundary to a depth of 11 inches results in the leak rate during a postulated SLB event being no more than that during NOP.

The analyses demonstrate that the evaluation of the conditions on the hot leg bound those for the cold leg with regard to leak rate performance. However, as previously noted, the structural results for the cold leg are bounding relative to the hot leg. The difference is a maximum at a radius of about 15 inches and is less than about 0.85 inch. A summary is provided in Table 7-13.

It is important to note that all of the evaluations performed considered the tube to be severed at the reassigned pressure boundary location with no resistance to flow from the leak path within the tube itself, i.e., cracks. At the specified depths the crack flanks would be restricted from opening or parting, and may be held tighter, thus reducing the accident condition leak to below that anticipated herein.

With regards to the preparation of a significant hazards determination, the results of the testing and analyses demonstrate that the relocation of the pressure boundary to a depth based on the more conservative of either H* or B* does not lead to an increase in the probability or consequences of the postulated limiting accident conditions because the margins inherent in the original design basis are maintained and the expected leak rate during the postulated accident is not expected to increase beyond the plant specific limit. In addition, the relocation of the pressure boundary does not create the potential for a new or departure from the previously evaluated accident events. Finally, since the margins inherent in the original design bases are maintained, no significant reduction in the margin of safety would be expected.

a,c,e



Figure 11-1. Comparison of Hot Leg H* and B* Results

a,c,e



Figure 11-2. Comparison of Cold Leg H* and B* Results

12.0 References

1. OE19662 (Restricted & Confidential), "Steam Generators (Catawba Nuclear Power Station)," Institute of Nuclear Power Operations (INPO), Atlanta, GA, USA, December 13, 2004.
2. IN 2005-09, "Indications in Thermally Treated Alloy 600 Steam Generator Tubes and Tube-to-Tubesheet Welds," United States Nuclear Regulatory Commission, Washington, DC, April 7, 2005.
3. SGMP-IL-05-01, "Catawba Unit 2 Tubesheet Degradation Issues," EPRI, Palo Alto, CA, March 4, 2005.
4. OE20339, "Vogtle Unit 1 Steam Generator Tube Crack Indications," Institute of Nuclear Power Operations (INPO), Atlanta, GA, USA, April 4, 2005.
5. WCAP-16153, "Justification of the Partial-Length Rotating Pancake Coil (RPC) Inspection of the Tube Joints of the Catawba Unit 2 Model D5 Steam Generators," Westinghouse Electric Company LLC, Pittsburgh, PA, December 2003.
6. ASME Boiler and Pressure Vessel Code, Section III, "Nuclear Power Plant Components," American Society of Mechanical Engineers, New York, New York, 1971, Winter 1974 Addenda.
7. WNEP-8441, "Model D5 Steam Generator Stress Report for Duke Power Company Catawba Unit 2," Westinghouse Electric Company LLC, Pittsburgh, PA, July 1984.
8. GL 2004-01, "Requirements for Steam Generator Tube Inspections," United States Nuclear Regulatory Commission, Washington, DC, August 30, 2004.
9. NRC Letter, "Braidwood Station, Units 1 and 2 – Issuance of Exigent Amendments Re: Revision of Scope of Steam Generator Inspections for Unit 2 Refueling Outage 11 – (TAC Nos. MC6686 and MC6687)," United States Nuclear Regulatory Commission, Washington, DC, April 25, 2005.
10. NRC Letter, "Vogtle Electric Generating Plant, Units 1 and 2 RE: Issuance of Amendments Regarding the Steam Generator Tube Surveillance Program (TAC Nos. MC8078 and MC8079)," United States Nuclear Regulatory Commission, Washington, DC, September 21, 2005.
11. NEI 97-06, Rev. 2, "Steam Generator Program Guidelines," Nuclear Energy Institute, Washington, DC, October 2005.
12. RG 1.121 (Draft), "Bases for Plugging Degraded PWR Steam Generator Tubes," United States Nuclear Regulatory Commission, Washington, DC, August 1976.
13. Federal Register, Part III, Nuclear Regulatory Commission, National Archives and Records Administration, Washington, DC, pp. 10298 to 10312, March 2, 2005.
14. NPD/E/PEN-99-255, "Applicable ASME Codes for the Original and Replacement Steam Generators," Westinghouse Electric Company LLC, Pittsburgh, PA, June 29, 1999.

-
15. WNET-153 (Proprietary), "Model D5 Steam Generator Stress Report Commonwealth Edison Company Byron Station 2," [Generic for Model D5 SGs] Westinghouse Electric Company LLC, Pittsburgh, PA, June 1982.
 16. ASME Boiler and Pressure Vessel Code, Section XI, "Rules for Inservice Inspection of Nuclear Power Plant Components," American Society of Mechanical Engineers, New York, New York, 1971.
 17. ASME Boiler and Pressure Vessel Code, Section XI, "Rules for Inservice Inspection of Nuclear Power Plant Components," American Society of Mechanical Engineers, New York, New York, 2004.
 18. WCAP-11224, Rev. 1, "Tubesheet Region Plugging Criterion for the Duke Power Company McGuire Nuclear Station Units 1 and 2 Steam Generators," Westinghouse Electric Company LLC, Pittsburgh, PA, October 1986.
 19. WCAP-13532, Rev. 1, "Sequoyah Units 1 and 2 W* Tube Plugging Criteria for SG Tubesheet Region of WEXTEx Expansions," Westinghouse Electric Company LLC, Pittsburgh, PA, 1992.
 20. WCAP-14797, "Generic W* Tube Plugging Criteria for 51 Series Steam Generator Tubesheet Region WEXTEx Expansions," Westinghouse Electric Company LLC, Pittsburgh, PA, 1997.
 21. "Safety Evaluation by the Office of Nuclear Reactor Regulation Related to Amendment No. 129 to Facility Operating License No. DPR-80 and Amendment No. 127 to Facility Operating License No. DPR-82 Pacific Gas and Electric Company Diablo Canyon Nuclear Power Plant, Units 1 and 2 Docket Nos. 50-275 and 50-323," United States Nuclear Regulatory Commission, Washington, DC, 1999.
 22. NSD-RFK-96-015, "Vogtle 1 Tube Integrity Evaluation, Loose Part Affected SG," Westinghouse Electric Company LLC, Pittsburgh, PA, June 9, 1996.
 23. WCAP-14871 (Proprietary), "Vogtle Electric Generating Plant (VEGP) Steam Generator Tube-to-Tubesheet Joint Evaluation," Westinghouse Electric Company LLC, Pittsburgh, PA, May 1997.
 24. Calculation Note CN-SGDA-03-85, Rev. 1 "H*/P* Input for Model D5 and Model F Steam Generators," Westinghouse Electric Company LLC, Pittsburgh, PA, September 2003 (Proprietary Report).
 25. CN-SGDA-03-87 (Proprietary), "Evaluation of the Tube/Tubesheet Contact Pressures and H* for Model D5 Steam Generators at Byron, Braidwood, Catawba and Comanche Peak," Westinghouse Electric Company LLC, Pittsburgh, PA, October 2003.
 26. CN-SGDA-03-133 (Proprietary), Rev. 0, "Evaluation of the H* Zone Boundaries for Specific Model D-5 and Model F Steam Generators," Westinghouse Electric Company LLC, Pittsburgh, PA, October 2003.
 27. Calculation Note CN-SGDA-08-87, Westinghouse Electric Company LLC, Pittsburgh, PA, October 2003 (Proprietary Report.)

-
28. Roark, R. J., and Warren C. Young, *Formulas for Stress and Strain*, Fifth Edition, McGraw-Hill, New York, New York, 1975.
 29. NSD-E-SGDA-98-3611 (Proprietary), "Transmittal of Yonggwang Unit 2 Nuclear Power Plant Steam Generator Tube-to-Tubesheet Joint Evaluation," Westinghouse Electric Company LLC, Pittsburgh, PA, November 1998.
 30. Porowski, J.S. and W. J. O'Donnell, "Elastic Design Methods for Perforated Plates," Transactions of the ASME Journal of Engineering for Power, Vol. 100, p. 356, 1978.
 31. Slot, T., "Stress Analysis of Thick Perforated Plates," PhD Thesis, Technomic Publishing Co., Westport, CN 1972.
 32. Computer Program WECAN/Plus, "User's Manual," 2nd Edition, Revision D, Westinghouse Government Services LLC, Cheswick, PA, May 2000.
 33. SM-98-102 (Proprietary), Rev. 2, "Tube/Tubesheet Contact Pressures for Yonggwang 2," Westinghouse Electric Company LLC, Pittsburgh, PA, November 1998.
 34. Nelson, L.A., "Reference for Model D Tubesheet Simulate of 1.800 Inch Diameter, electronic mail (Contained in Reference 31), Westinghouse Electric Company LLC, Pittsburgh, PA, August 2003.
 35. ASME Boiler and Pressure Vessel Code Section III, "Rules for Construction of Nuclear Power Plant Components," 1989 Edition, The American Society of Mechanical Engineers, New York, NY.
 36. CN-SGDA-02-152 (Proprietary), Rev. 1, "Evaluation of the Tube-to-Tubesheet Contact Pressures for Callaway Model F Steam Generators," Westinghouse Electric Company LLC, Pittsburgh, PA, March 2003.
 37. CN-SGDA-03-87 (Proprietary), "Evaluation of the Tube/Tubesheet Contact Pressures and H* for Model D-5 Steam Generators at Byron, Braidwood, Catawba and Comanche Peak," Westinghouse Electric Company LLC, Pittsburgh, PA, October 2003.
 38. WNET-153, Vol. 5 (Proprietary), "Model D-5 Steam Generator Stress Report: Tube Analysis," Westinghouse Electric Company LLC, Pittsburgh, PA, March 1982.
 39. CN-SGDA-03-121 (Proprietary), "H* Ligament Tearing for Models F and D5 Steam Generators," Westinghouse Electric Company LLC, Pittsburgh, PA, October 2003.
 40. VBA/Excel compatible version of the steam67.dll (dynamic link library) from Winsim.com, Internet available
 41. ChemicalLogic SteamTab Companion, "Thermodynamic and Transport Properties of Steam, Version 2.0, Based on the IAPWS-95 Formulation," ChemicalLogic Corporation, Burlington, MA, 2003.
 42. NCE-88-271 (Proprietary), "Assessment of Tube-to-Tubesheet Joint Manufacturing Processes for Sizewell B Steam Generators Using Alloy 690 Tubing," Westinghouse Electric Company LLC, Pittsburgh, PA, November 1988.

-
43. WCAP 15932-P, Revision 1, "Improved Justification of Partial-Length RPC Inspection of Tube Joints of Model F Steam Generators of Ameren-UE Callaway Plant," Westinghouse Electric Company LLC, Pittsburgh, PA May 2003.

ENCLOSURE 3

**AFFIDAVIT AND WESTINGHOUSE ELECTRIC COMPANY, LLC AUTHORIZATION
LETTER, CAW-05-2086, APPLICATION FOR WITHHOLDING PROPRIETARY
INFORMATION FROM PUBLIC DISCLOSURE**



Westinghouse Electric Company
Nuclear Services
P.O. Box 355
Pittsburgh, Pennsylvania 15230-0355
USA

U.S. Nuclear Regulatory Commission
Document Control Desk
Washington, DC 20555-0001

Direct tel: (412) 374-4419
Direct fax: (412) 374-4011
e-mail: maurerbf@westinghouse.com

Our ref: CAW-05-2086

December 16, 2005

**APPLICATION FOR WITHHOLDING PROPRIETARY
INFORMATION FROM PUBLIC DISCLOSURE**

Subject: LTR-CDME-05-180-P, Rev. 2, "Steam Generator Tube Alternate Repair Criteria for the Portion of the Tube Within the Tubesheet at Catawba 2," dated December 2005 (Proprietary)

The proprietary information for which withholding is being requested in the above-referenced report is further identified in Affidavit CAW-05-2086 signed by the owner of the proprietary information, Westinghouse Electric Company LLC. The affidavit, which accompanies this letter, sets forth the basis on which the information may be withheld from public disclosure by the Commission and addresses with specificity the considerations listed in paragraph (b)(4) of 10 CFR Section 2.390 of the Commission's regulations.

Accordingly, this letter authorizes the utilization of the accompanying affidavit by Duke Energy Corporation.

Correspondence with respect to the proprietary aspects of the application for withholding or the Westinghouse affidavit should reference this letter, CAW-05-2086, and should be addressed to B. F. Maurer, Acting Manager, Regulatory Compliance and Plant Licensing, Westinghouse Electric Company LLC, P.O. Box 355, Pittsburgh, Pennsylvania 15230-0355.

Very truly yours,

A handwritten signature in black ink, appearing to read "B. F. Maurer".

B. F. Maurer, Acting Manager
Regulatory Compliance and Plant Licensing

Enclosures

cc: B. Benney, NRC
L. Feizollahi, NRC

bcc: B. F. Maurer (ECE 4-7) 1L
R. Bastien, 1L (Nivelles, Belgium)
C. Brinkman, 1L (Westinghouse Electric Co., 12300 Twinbrook Parkway, Suite 330, Rockville, MD 20852)
RCPL Administrative Aide (ECE 4-7A) 1L, 1A (letter and affidavit only)
G. W. Whiteman, Waltz Mill
R. F. Keating, Waltz Mill
H. O. Lagally Waltz Mill
J. Gambino, ECE-557D
D. C. Beddingfield, WEC – E558B

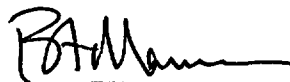
AFFIDAVIT

COMMONWEALTH OF PENNSYLVANIA:

SS

COUNTY OF ALLEGHENY:

Before me, the undersigned authority, personally appeared B. F. Maurer, who, being by me duly sworn according to law, deposes and says that he is authorized to execute this Affidavit on behalf of Westinghouse Electric Company LLC (Westinghouse), and that the averments of fact set forth in this Affidavit are true and correct to the best of his knowledge, information, and belief:

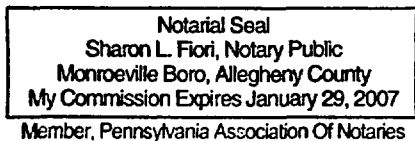


B. F. Maurer, Acting Manager
Regulatory Compliance and Plant Licensing

Sworn to and subscribed
before me this 16th day
of December, 2005



Notary Public



- (1) I am Acting Manager, Regulatory Compliance and Plant Licensing, Nuclear Services, Westinghouse Electric Company LLC (Westinghouse), and as such, I have been specifically delegated the function of reviewing the proprietary information sought to be withheld from public disclosure in connection with nuclear power plant licensing and rule making proceedings, and am authorized to apply for its withholding on behalf of Westinghouse.
- (2) I am making this Affidavit in conformance with the provisions of 10 CFR Section 2.390 of the Commission's regulations and in conjunction with the Westinghouse "Application for Withholding" accompanying this Affidavit.
- (3) I have personal knowledge of the criteria and procedures utilized by Westinghouse in designating information as a trade secret, privileged or as confidential commercial or financial information.
- (4) Pursuant to the provisions of paragraph (b)(4) of Section 2.390 of the Commission's regulations, the following is furnished for consideration by the Commission in determining whether the information sought to be withheld from public disclosure should be withheld.
 - (i) The information sought to be withheld from public disclosure is owned and has been held in confidence by Westinghouse.
 - (ii) The information is of a type customarily held in confidence by Westinghouse and not customarily disclosed to the public. Westinghouse has a rational basis for determining the types of information customarily held in confidence by it and, in that connection, utilizes a system to determine when and whether to hold certain types of information in confidence. The application of that system and the substance of that system constitutes Westinghouse policy and provides the rational basis required.

Under that system, information is held in confidence if it falls in one or more of several types, the release of which might result in the loss of an existing or potential competitive advantage, as follows:

 - (a) The information reveals the distinguishing aspects of a process (or component, structure, tool, method, etc.) where prevention of its use by any of Westinghouse's competitors without license from Westinghouse constitutes a competitive economic advantage over other companies.

- (b) It consists of supporting data, including test data, relative to a process (or component, structure, tool, method, etc.), the application of which data secures a competitive economic advantage, e.g., by optimization or improved marketability.
- (c) Its use by a competitor would reduce his expenditure of resources or improve his competitive position in the design, manufacture, shipment, installation, assurance of quality, or licensing a similar product.
- (d) It reveals cost or price information, production capacities, budget levels, or commercial strategies of Westinghouse, its customers or suppliers.
- (e) It reveals aspects of past, present, or future Westinghouse or customer funded development plans and programs of potential commercial value to Westinghouse.
- (f) It contains patentable ideas, for which patent protection may be desirable.

There are sound policy reasons behind the Westinghouse system which include the following:

- (a) The use of such information by Westinghouse gives Westinghouse a competitive advantage over its competitors. It is, therefore, withheld from disclosure to protect the Westinghouse competitive position.
- (b) It is information that is marketable in many ways. The extent to which such information is available to competitors diminishes the Westinghouse ability to sell products and services involving the use of the information.
- (c) Use by our competitor would put Westinghouse at a competitive disadvantage by reducing his expenditure of resources at our expense.
- (d) Each component of proprietary information pertinent to a particular competitive advantage is potentially as valuable as the total competitive advantage. If competitors acquire components of proprietary information, any one component may be the key to the entire puzzle, thereby depriving Westinghouse of a competitive advantage.

- (e) Unrestricted disclosure would jeopardize the position of prominence of Westinghouse in the world market, and thereby give a market advantage to the competition of those countries.
- (f) The Westinghouse capacity to invest corporate assets in research and development depends upon the success in obtaining and maintaining a competitive advantage.
- (iii) The information is being transmitted to the Commission in confidence and, under the provisions of 10 CFR Section 2.390, it is to be received in confidence by the Commission.
- (iv) The information sought to be protected is not available in public sources or available information has not been previously employed in the same original manner or method to the best of our knowledge and belief.
- (v) The proprietary information sought to be withheld in this submittal is that which is appropriately marked in LTR-CDME-05-180-P, Rev. 2, "Steam Generator Tube Alternate Repair Criteria for the Portion of the Tube Within the Tubesheet Catawba 2," dated December 2005 (Proprietary). The information is provided in support of a submittal to the Commission, being transmitted by Duke Energy Corporation and Application for Withholding Proprietary Information from Public Disclosure, to the Document Control Desk. The proprietary information as submitted for use by Westinghouse for Catawba Unit 2 is expected to be applicable to other licensee submittals in support of implementing a limited inspection of the tube joint with a rotating probe within the tubesheet region of the steam generators.

This information is part of that which will enable Westinghouse to:

- (a) Provide documentation of the analyses, methods, and testing for the implementation of alternate repair criteria for the portion of the tubes within the tubesheet of the Catawba Unit 2 steam generators.
- (b) Provide a primary-to-secondary side leakage evaluation for Catawba Unit 2 during all plant conditions.

- (c) Assist the customer to respond to NRC requests for information.

Further this information has substantial commercial value as follows:

- (a) Westinghouse plans to sell the use of similar information to its customers for purposes of meeting NRC requirements for licensing documentation.
- (b) Westinghouse can sell support and defense of this information to its customers in the licensing process.
- (c) The information requested to be withheld reveals the distinguishing aspects of a methodology which was developed by Westinghouse.

Public disclosure of this proprietary information is likely to cause substantial harm to the competitive position of Westinghouse because it would enhance the ability of competitors to provide similar licensing support documentation and licensing defense services for commercial power reactors without commensurate expenses. Also, public disclosure of the information would enable others to use the information to meet NRC requirements for licensing documentation without purchasing the right to use the information.

The development of the technology described in part by the information is the result of applying the results of many years of experience in an intensive Westinghouse effort and the expenditure of a considerable sum of money.

In order for competitors of Westinghouse to duplicate this information, similar technical programs would have to be performed and a significant manpower effort, having the requisite talent and experience, would have to be expended.

Further the deponent sayeth not.

PROPRIETARY INFORMATION NOTICE

Transmitted herewith are proprietary and/or non-proprietary versions of documents furnished to the NRC in connection with requests for generic and/or plant-specific review and approval.

In order to conform to the requirements of 10 CFR 2.390 of the Commission's regulations concerning the protection of proprietary information so submitted to the NRC, the information which is proprietary in the proprietary versions is contained within brackets, and where the proprietary information has been deleted in the non-proprietary versions, only the brackets remain (the information that was contained within the brackets in the proprietary versions having been deleted). The justification for claiming the information so designated as proprietary is indicated in both versions by means of lower case letters (a) through (f) located as a superscript immediately following the brackets enclosing each item of information being identified as proprietary or in the margin opposite such information. These lower case letters refer to the types of information Westinghouse customarily holds in confidence identified in Sections (4)(ii)(a) through (4)(ii)(f) of the affidavit accompanying this transmittal pursuant to 10 CFR 2.390(b)(1).

COPYRIGHT NOTICE

The reports transmitted herewith each bear a Westinghouse copyright notice. The NRC is permitted to make the number of copies of the information contained in these reports which are necessary for its internal use in connection with generic and plant-specific reviews and approvals as well as the issuance, denial, amendment, transfer, renewal, modification, suspension, revocation, or violation of a license, permit, order, or regulation subject to the requirements of 10 CFR 2.390 regarding restrictions on public disclosure to the extent such information has been identified as proprietary by Westinghouse, copyright protection notwithstanding. With respect to the non-proprietary versions of these reports, the NRC is permitted to make the number of copies beyond those necessary for its internal use which are necessary in order to have one copy available for public viewing in the appropriate docket files in the public document room in Washington, DC and in local public document rooms as may be required by NRC regulations if the number of copies submitted is insufficient for this purpose. Copies made by the NRC must include the copyright notice in all instances and the proprietary notice if the original was identified as proprietary.